



NTNU – Trondheim
Norwegian University of
Science and Technology

Study of Rat Olfactory Ensheathing Cells in Alginate based Matrices

Marthe Fredheim Fjelldal

Biotechnology (5 year)

Supervisor: Gudmund Skjåk-Bræk, IBT

Co-supervisor: Berit L. Strand, IBT

Norwegian University of Science and Technology
Department of Biotechnology

Preface

This work was carried out at the Department of Biotechnology and the Department of Cancer Research and Molecular Medicine at NTNU.

I would like to thank my supervisors, Berit L. Strand and Ioanna Sandvig for invaluable help, support and tireless revising of my texts.

I would also like to thank my “unofficial supervisor” Marita Westhrin for always answering my questions and correcting my thesis, even though she was not obligated to do so.

A big thanks to Kjartan W. Egeberg for teaching me about the CLSM, and to Manuela Perrotta for keeping me company as well as teaching me the most important Italian words. Grazie mille!

The helpfulness of the co-workers at IKM and NOBIPOL must also be acknowledged, as they kindly provided answers to my questions at any time.

And last, but not least I have to thank Simen for his endless patience, support and computer skills.

Marthe Fredheim Fjelldal
May 2012

Table of Contents

1. Theory	1
1.1. Alginate.....	1
1.1.1. Alginate in solution	2
1.1.2. Mannuronan C-5 epimerases	2
1.1.3. Alginate gel.....	3
1.1.4. Alginate as a biomaterial	4
1.2. Alginate derivatives.....	5
1.2.1. Covalently modified alginate.....	5
1.3. Encapsulation	7
1.4. Olfactory Ensheathing Cells and CNS repair.....	9
1.4.1. Damage in the Central nervous system (CNS).....	9
1.4.2. Cell Transplant mediated repair.....	9
1.4.3. Olfactory ensheathing cells.....	10
1.5. 3D culture	12
1.6. Molecules in the extracellular matrix (ECM)	13
1.6.1. Integrins.....	13
1.6.2. Hyaluronic acid	15
1.6.3. Proteoglycans.....	15
1.6.4. Collagen	15
1.6.5. Fibronectin.....	17
1.6.6. Laminin	18
2. Materials and methods	21
2.1. Alginate characteristics.....	21
2.2. Cell purification and culture	23
2.3. Gelling solution	24
2.4. Encapsulation of OECs.....	25
2.5. alamarBlue®.....	27
2.5.1. Method 1- OECs encapsulated in 1.8% UP-LVG alginate.....	27
2.5.2. Method 2 - OECs encapsulated in 1.0% Alg Epi RGD I	27
2.5.3. Test round - OECs encapsulated in 1.0% UP-LVG alginate.....	28
2.6. MTT assay.....	29
2.7. Live/Dead	29
2.8. Actin filament and nucleus staining using Phalloidin and DRAQ5	31
2.9. Capsule stability	32
3. Results.....	34
3.1. Different concentrations of OECs encapsulated in 1.8% UP-LVG alginate	34

3.2. Encapsulation of OECS in 1.0% LG alginate grafted with 0.2% RGD peptide...	37
3.3. Encapsulation of OECs in 1.0% UP-LVG alginate I.....	42
3.4. Encapsulation of OECs in 1.0% UP-LVG alginate II.....	46
3.5. OECs encapsulated in 1.0% UP-LVG alginate mixed with different concentrations of gelatin I.....	49
3.6. OECs encapsulated in 1.0% UP-LVG alginate mixed with different concentrations of gelatin II.....	54
3.7. OECs encapsulated in 0.9% UP-LVG mixed with different ECM molecules and sulphated alginate	57
3.8. Encapsulation of OECS in 1.0% LG alginate grafted with 0,1-0.4% RGD peptide.....	61
3.9. Actin filament and nucleus staining.....	66
3.10. Bubble formation around cell clusters.....	68
3.11. alamarBlue® and MTT assay	68
3.12. Capsule stability.....	73
4. Discussion	75
4.1. Cell viability.....	75
4.1.1. Alginate concentration	77
4.1.2. Alginate gel porosity	78
4.1.3. Structural differences between UP-LVG capsules and epimerized alginate capsules.....	79
4.1.4. RGD peptide grafted alginate I and II	80
4.2. Alginate mixed with ECM molecules.....	82
4.2.1. 1.0% UP-LVG alginate mixed with gelatin	82
4.2.2. 1.0% UP-LVG mixed with different ECM molecules, and sulphated MG alginate	83
4.3. Morphology	84
4.4. Capsule stability	85
4.5. alamarBlue®	87
4.6. Future perspectives	87
5. Conclusion.....	90
Literature	92

Appendixes

Appendix A: alamarBlue® assay.....	99
A1: Procedure of the alamarBlue assay performed in experiment 3.1.....	99
A2: Fluorescence values and calculations from experiment 3.1	101
A3: Graph of fluorescence/1000 cells from experiment 3.1	104
A4: Second experiment: The alamarBlue procedure for experiment 3.2	105
A5: Fluorescence values and calculations from experiment 3.2.....	107
A6: Graph of fluorescence value/1000 cells from experiment 3.2	111
A7: Fluorescence values and calculations for experiment 3.4.....	112
A8: Graph of fluorescence values per 1000 cells for experiment 3.4	116
A9: Fluorescence values and calculations for experiment 3.5.....	117
A10: Fluorescence values/1000 cells from experiment 3.5	121
Appendix B: MTT assay performed in comparison with the alamarBlue® assay ...	122
B1: Absorbance values and calculations from the MTT assay.	122
B2: Graph showing the MTT absorbance values for 1.5 mil/mL encapsulated in 1.0% UP-LVG.....	123
B3: Fluorescence values from the alamarBlue® assay performed on comparison with the MTT assay	124
B4: Graph showing fluorescence per cell from alamarBlue® assay performed in comparison with MTT assay.....	126
Appendix C: Excel tables for the estimated live cell percentages in chapter 3.....	127

Summary

Alginate hydrogel made from alginate and crosslinking divalent ions is a natural biomaterial that is biocompatible, has low toxicity, is relatively cheap and has mild gelation chemistry. It is a porous material that allows diffusion of small molecules. Alginate hydrogel is a polymeric network that contains 95-99% water and it does in many ways resemble the natural extracellular matrix (ECM) that surrounds cells in the body. It is also hydrophilic, which reduces friction in body fluids and minimizes protein adsorption and it is easily stored and sterilized.

Alginate is produced by both algae and bacteria, and it is initially synthesized as mannuronan (M) with 100% M-residues. Guluronic acid residues (G) are introduced in a post-polymerization step by enzymes called mannuronan C-5 epimerases that catalyze conversion of M into G without breaking the glycosidic bond. Seven different mannuronan C-5 epimerases have been sequenced, cloned and produced recombinantly, and these enzymes introduce MG-blocks, G- blocks or both in the alginate chains. With the use of these mannuronan C-5 epimerases it is now possible to engineer alginate with desired and known structure. It is also possible to covalently modify alginates with coupling of cell specific adhesion molecules to the carboxylic group in the monomers. An example is the RGD peptide (arginine-glycine-aspartic acid) that is commonly found in collagen and fibronectin in the ECM. The RGD peptide is the smallest sequence that integrin receptors can recognize and bind to.

Central nervous system (CNS) damage is still one of the major causes of both death and disability, despite intense research efforts to achieve neurogenesis and restore functional synaptic connection of CNS neurons. None of the current therapy strategies promote regeneration or regrowth of neural cells or axons. *In vitro* and *in vivo* studies has shown that CNS axons can regenerate when located in a permissive environment and it is known that on-going neurogenesis occurs in certain areas of the adult brain, such as the olfactory bulb. Olfactory ensheathing cells (OECs) are found in the olfactory mucosa and olfactory bulb and secrete neurotrophins, provide necessary ECM molecules and substrates for axon elongation and myelination. They do not activate and induce inhibitory molecules or hypertrophy in astrocytes, and are therefore believed to be a promising candidate for cell-mediated repair of the CNS.

The major aims of this study was to investigate whether encapsulation of OECs in different types of alginate matrices would improve cell viability over time and induce change of cell morphology, as a future goal is to transplant OECs into the CNS. Viability of OECs up to 14 days in 1.8% UP-LVG capsules have been reported by Kristin Karstensen (Karstensen, 2010), and similar results were achieved in an experiment in this project. Indications of cell concentration dependency on viability were observed in this experiment, with higher viability in capsules with low cell concentration (1.5 mil cells/mL alginate, 3.0 and 5.0 mil/mL).

It was decided to conduct an encapsulation of high and low OEC concentration (4.0 mil/mL and 1.0 mil/mL) in 1.0% UP-LVG $\text{Ca}^{2+}/\text{Ba}^{2+}$ alginate, with the aim of examining whether reduced alginate concentration would improve cell viability. The results were promising, with a live cell percentage of 50% in the low cell concentration batch after 51 days. The high cell concentration batch was discarded after 22 days with estimated 30% live cells. This result strengthened the hypothesis that lower cell concentration enhanced cell viability, and confirmed that lower alginate concentration improved cell viability notably. These indications were supported by the results of a second encapsulation with similar settings.

High and low concentrations (1.5 mil/mL and 5.0 mil/mL) of OECs were encapsulated in 1.0% epimerized Ca^{2+} alginate with and without 0.2 % RGD peptide graft. The experiment did not show an effect of the RGD peptide on cell viability or morphology. The viability of the cells was extended with one week and viable cells could be observed for 22 days, but in this experiment increased viability as a result of lower cell concentration was less pronounced. This experiment was therefore inconclusive in terms of improved viability connected to cell concentration, but indicated that a lower alginate concentration had a beneficial impact on cell viability.

Star shaped channels were observed inside all capsules in this experiment, and a large fraction of dead cells were found to be located inside these channels. This experiment was later repeated with another source of epimerized alginate grafted with $\approx 0.4\%$ RGD peptide with comparable results in terms of cell viability and morphology.

Two encapsulations of low cell concentration in 1.0% UP-LVG $\text{Ca}^{2+}/\text{Ba}^{2+}$ alginate mixed with three different concentrations of gelatin (0.5%, 1.0% and 2.0%) were carried out, with the aim of observing capsule stability and cell viability. In first experiment the capsule stability appeared to be inversely proportional with gelatin concentration. This was not confirmed when the experiment was repeated, as the batch with the middle gelatin concentration was perceived as most stable. The cell viability was overall high for both encapsulations.

Finally, four batches of 1.5 mil/mL OECs were encapsulated in 0.9% UP-LVG $\text{Ca}^{2+}/\text{Ba}^{2+}$ alginate gel with one type of ECM molecule mixed with the alginate per batch to yield a concentration of 1.0 mg/mL. Sulphated MG alginate was mixed with 0.9% UP-LVG $\text{Ca}^{2+}/\text{Ba}^{2+}$ alginate to a final concentration of 1.0 mg/mL, and included in the experiment. The experiment was terminated at day 28, with varying cell viabilities in the different batches. Common for all was overall lower cell viability compared with the viability observed for cells with similar concentration encapsulated in pure 1.0% UP-LVG, but the capsules proved to be relatively stable.

In conclusion, reducing the alginate concentration from 1.8% to 1.0% had notable positive effect on cell viability. High cell concentration in the alginate capsules also proved to have a negative impact on cell viability, but this effect was most evident in

the UP-LVG alginate gels. The negative effect on cell viability related to high cell concentration was not as profound in the epimerized alginate gels.

RGD peptide grafted onto alginate did not show any unambiguous effect on cell viability and no effect on cell morphology, regardless of 0.2 % peptide graft or \approx 0.4% peptide graft. The gelatin-1.0% UP-LVG alginate mixes also failed to induce morphology change in the OECs, and neither did any of the ECM molecule-1.0% UP-LVG alginate mixes or the sulphated alginate-1.0% UP-LVG alginate mix. The cells encapsulated in gelatin-alginate mix capsules displayed an overall high viability, while the cells encapsulated in ECM molecule- alginate mix and sulphated alginate-alginate mix displayed lower viability than cells encapsulated in pure UP-LVG alginate.

All capsule varieties displayed generally good stability in culture, with the exception of the gelatin-alginate mix capsules that progressively dissolved in culture.

Sammendrag (Norwegian)

Alginat hydrogel laget av alginat og kryssbindende divalente ioner er et naturlig biomaterial, som er biokompatibelt, billig, har mild gelingskjemi og lav toksisitet. Det er et porøst materiale som tillater diffusjon av små molekyler. Alginat hydrogel består av et polymerisk nettverk som inneholder 95-99% vann og minner på mange måter om ekstracellulært matriks (ECM) som omslutter cellene i kroppen. Det er også hydrofilt, hvilket reduserer friksjon i kroppsvæsker og minimerer proteinadsorpsjon. Alginatløsninger er enkle å lagre og sterilisere.

Alginat blir produsert av både alger og bakterier, og det blir først syntetisert som mannuronan (M) med 100% M innhold. Guluronsyremonomerer (G) blir introdusert i et post-polymeriseringsteg av enzymer kalt mannuronan C-5 epimeraser som katalyserer omgjøringen av M til G uten å bryte det glykosidiske båndet mellom monomerene. Syv forskjellige mannuronan C-5 epimeraser har blitt sekvensert, klonet og produsert rekombinant i *Escherichia coli*, og disse enzymene introduserer MG-blokker, G-blokker eller begge i alginatkjedene. Ved hjelp av disse mannuronan C-5 epimerasene er det nå mulig å skreddersy alginat med ønsket og kjent sammensetning. Det er også mulig å modifisere alginat ved å kovalent binde cellespesifikke adhesjonsmolekyler til karboksylgruppene på alginatkjedene. Et eksempel er RGD peptidet (arginin-glysin-aspartat) som vanligvis blir funnet i kollagen og fibronektin i ECM. RGD peptidet er den korteste peptidsekvensen et integrin kan kjenne igjen å binde seg til.

Skader i sentralnervesystemet (CNS) er fremdeles en av de vanligste årsakene til både død og funksjonshemning, til tross for intens forskning på å oppnå nevrogenese og reparasjon av synapser for å gjenopprette synaptisk kobling av CNS nevroner. Ingen av dagens terapistrategier promoterer regenerasjon og gjenvekst av nevralt celler/aksoner. *In vivo* og *in vitro* studier har vist at CNS aksoner kan regenereres når de er lokalisert i et miljø som tillater det og det finnes områder i den voksne hjernen hvor nerveregenerering skjer, og et eksempel er luktelappen (olfactory bulb).

Olfactory ensheathing celler (OECs) finnes i luktelappen og de sekreterer nevrotrofiske stoffer, produserer nødvendige ECM molekyler og substrater for aksonforlengelse og myelinisering. Cellene aktiverer ikke inhibitoriske molekyler, eller hypertrofi i astrocytter og er derfor en lovende kandidat til cellemidert reparasjon av CNS.

Hovedmålene med dette prosjektet var å undersøke om innkapsling av OECs i forskjellige typer alginatmatriser ville øke cellenes viabilitet over tid og inducere morfologiendringer i cellene, siden et fremtidig mål er å transplanterer OECs inn i CNS. Levende OECs i 1.8% Ca^{2+} UP-LVG alginatkapsler i opp til 14 dager har blitt rapportert av Kristin Karstensen i hennes masterprosjekt (Karstensen, 2010), og lignende resultater ble oppnådd i et forsøk i dette prosjektet. Indikasjoner på cellekonsentrasjonsavhengig levedyktighet ble observert i dette forsøket, med høyere levedyktighet i kapsler med lav cellekonsentrasjon (1.5 millioner celler/mL alginat, 3.0 mill/mL og 5.0 mill/mL).

Det ble besluttet å gjennomføre innkapslinger av høy og lav OEC konsentrasjon (4.0 mill/mL og 1.0 mill/mL) i 1.0% UP-LVG $\text{Ca}^{2+}/\text{Ba}^{2+}$ alginat, for å undersøke om lavere alginatkonsentrasjon ville ha innvirkning på celleviabiliteten. Resultatene var lovende, med en prosentandel på 50% levende celler i prøven med lavest cellekonsentrasjon etter 51 dager. Den tilhørende prøven med høy cellekonsentrasjon ble forkastet etter 22 dager med anslagsvis 30% levende celler. Dette resultatet styrket hypotesen om at lavere cellekonsentrasjonen forbedret celleviabilitet, og bekreftet at lavere alginatkonsentrasjon forbedret celleviabilitet betydelig. Det andre forsøkets resultater støttet disse indikasjonene.

1.5 mill/mL og 5.0 mill/mL konsentrasjoner av OECs ble innkapslet i 1.0% epimerisert Ca^{2+} alginat med og uten 0.2% RGD peptid koblet på. Eksperimentet viste ingen effekt av RGD peptid, på verken celleviabilitet eller morfologi. Levedyktigheten til cellene ble utvidet med en uke og levende celler kunne observeres i 22 dager. I dette eksperimentet var effekten av lavere cellekonsentrasjon mindre uttalt, men indikerte ytterligere at en lavere alginatkonsentrasjon hadde en gunstig effekt på cellenes levedyktighet.

Stjerneformede kanaler ble observert i alle kapsler i dette eksperimentet, og en stor andel av døde celler var lokalisert inne i disse kanalene. Dette eksperimentet ble senere gjentatt med epimerisert alginat med $\approx 0.4\%$ RGD peptid koblet på fra en annen kilde, med sammenlignbare resultater med tanke på viabilitet og morfologi.

To innkapslinger med 1.5 mill/mL cellekonsentrasjon i 1.0% UP-LVG $\text{Ca}^{2+}/\text{Ba}^{2+}$ alginat blandet med tre ulike konsentrasjoner av gelatin (0.5%, 1.0% og 2.0%) ble gjennomført, med sikte på å observere kapselstabilitet og celleviabilitet. I det første eksperimentet syntes kapselstabiliteten å være omvendt proporsjonal med gelatin konsentrasjon. Dette ble ikke bekreftet da forsøket ble gjentatt, da prøven med 1.0% gelatinkonsentrasjonen ble oppfattet som mest stabil. Cellen levedyktighet var generelt høy for begge innkapslingene.

Til slutt ble fire prøver med 1.5 mil/mL OECs innkapslet i 0.9% UP-LVG $\text{Ca}^{2+}/\text{Ba}^{2+}$ alginat blandet med en type ECM molekyl, med konsentrasjon på 1.0 mg/mL. Sulfatert MG alginat ble blandet med 0.9% UP-LVG $\text{Ca}^{2+}/\text{Ba}^{2+}$ alginat med konsentrasjon på 1.0 mg sulfatert alginat per mL UP-LVG alginat, og inkludert i forsøket. Forsøket ble avsluttet på dag 28, med varierende celleviabilitet i de ulike prøvene. Felles for alle prøvene var en generell lavere celleviabilitet sammenlignet med levedyktigheten observert for celler med tilsvarende konsentrasjon innkapslet i ren 1.0% UP-LVG $\text{Ca}^{2+}/\text{Ba}^{2+}$ alginat, men kapslene viste seg å være relativt stabile gjennom hele forsøket.

Det ble funnet at å redusere alginatkonsentrasjon fra 1.8% til 1.0% hadde merkbar positiv effekt på cellelevedyktighet i kapslene. Høy cellekonsentrasjon i alginatkapsler viste seg å ha en negativ innvirkning på celleviabilitet, men denne effekten var mest tydelig i kapsler av UP-LVG alginatgel. Den negative effekten på celleviabilitet relatert til høy cellekonsentrasjon var ikke så tydelig i kapsler av

epimerisert Ca^{2+} alginat gel.

RGD-peptid koblet på alginat viste ingen entydig effekt på celleviabilitet og ingen effekt på cellemorfologi, uavhengig av 0.2% peptidkobling eller \approx . peptidkobling. Gelatin-1.0% UP-LVG alginatblandingene mislyktes også på å inducere morfologiendring i OECs. Heller ikke noen av ECM molekyl-1.0% UP-LVG alginatblandingene eller sulfatert alginat-1.0% UP-LVG alginatblanding påvirket morfologien til cellene. Cellene innkapslet i kapsler av gelatin-alginatblanding vises en generelt høy levedyktighet, mens cellene innkapslet i ECM molekyl-0.9% UP-LVG alginatblanding og sulfatert alginat-0.9% UP-LVG alginatblanding viste lavere levedyktighet enn celler innkapslet i ren UP-LVG alginat.

Alle kapselvarianter viste generelt god stabilitet i kulturen, med unntak av gelatin-alginat blandingkapsler som gradvis ble oppløst i kultur over tid.

List of abbreviations

Ba ²⁺	Barium ions
Ca ²⁺	Calcium ions
CLSM	Confocal Laser Scanning Microscope
CNS	Central nervous system
DMEM	Dulbecco's Modified Eagle Medium
ECM	Extracellular matrix
EDTA	Ethylendiaminetetraacetic acid
EthD-1	Ethidium homodimer-1
FBS	Fetal bovine serum
G-block	Blocks of alternating guluronic and mannuronic acids in an alginate chain
G	Guluronic acid residues
HEPES	4-(2-hydroxyethyl)-1-piperazineethanesulfonic acid
HSPGs	Heparan sulphate proteoglycans
M-block	Blocks of alternating guluronic and mannuronic acids in an alginate chain
M	Mannuronic acid residues
MG-block	Blocks of solely guluronic acid monomers in an alginate chain
MTT	3-(4,5-dimethylthiazol-2-yl)-2,5-diphenyl tetrazolium bromide
MW	Molecular weight
OECs	Olfactory ensheathing cells
PBS	Phosphate Buffered Saline
PBS	Phosphate Buffered Saline
RGD-peptide	Arginine-glycine-aspartic acid-peptide
SEM	Scanning Electron Microscope
UP-LVG	Ultra-Pure low viscosity guluronic acid sodium alginate

1. Theory

1.1. Alginate

Alginate was discovered by Stanford in 1881 (Draget, 2002) and is produced in marine brown algae (Phaeophyta) (Draget, 2005) and some bacteria, such as *Azotobacter vinelandii* (Gorin, 1966) and several *Pseudomonas* species (Painter T.J., 1983). In brown algae alginate accounts for 40% of the dry weight and its main purpose is to provide the seaweed with strength and flexibility. The composition and structure of alginate can vary, both in the same plant and between species. The supply of alginate is considered to be unlimited and about 30000 metric tons are produced from brown algae annually (Draget, 2002).

Alginate consists of two monomers, β -D-mannuronic (M) and its C5 epimer α -L-guluronic (G) acid bound by 1 \rightarrow 4 glycosidic linkages in randomly arranged linear structures of alternating MG blocks, homopolymeric M-blocks or G-blocks, all of varying length. The chemical structure of alginate and is shown in figure 1.1 together with block composition (Smidsrød, 1974).



Figure 1.1: Alginate chemical structure. (a) Illustration of the Haworth formulas of the two monomers. M = β -D-mannuronic acid and G = α -L-guluronic acid. (b) Block composition in alginates (excerpt directly reproduced from (Mørch, 2008)).

The sequential structure in alginate is determined by measurements of diads and triads frequencies. There are four diad frequencies; F_{GG} , F_{GM} , F_{MG} and F_{MM} and eight possible triad frequencies; F_{GGG} , F_{GGM} , F_{MGG} , F_{MGM} , F_{MMM} , F_{MMG} , F_{GMM} and F_{GMG} . These can be measured by NMR techniques. From these measurements the average consecutive length of both G ($F_{(G<1)} = F_G - F_{MGM} / F_{MGG}$) and M ($F_{(M<1)} = F_M - F_{GMG} / F_{MMG}$) blocks can be calculated (Smidsrød and Skjak-Braek, 1990).

The ring conformations of the different alginate chains are shown in figure 1.2.

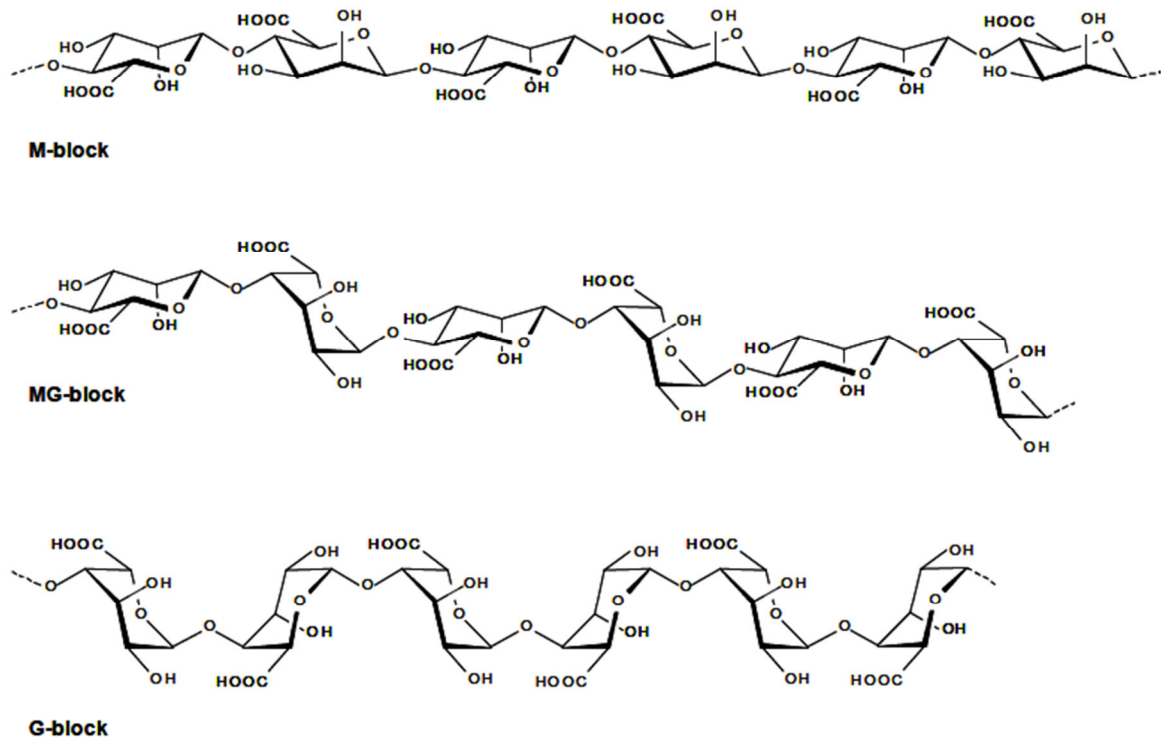


Figure 1.2: The ring conformation of the different alginate chains (Excerpt directly reproduced from (Mørch, 2008))

1.1.1. Alginate in solution

It has previously been thought that chain stiffness of alginate in solution has varied with block composition, but recent work has shown that chain stiffness is similar for G-blocks, M-blocks and MG-blocks (Vold et al., 2006).

The intrinsic viscosity of alginate depends on molecular weight, composition and sequence of M and G as well as the ionic strength of the solution (Draget et al., 2006). The viscosity of a solution of alginate will depend on the alginate concentration and its molecular weight. Alginate is a random coil molecule, and the viscosity of an alginate solution will therefore also depend on the ionic strength of the solution. A chain with fixed charges will expand in a solution with low ionic strength due to internal repulsion of charges within the molecule, and this will increase the viscosity. In a solution with high ionic strength the counter ions will shield the charges and cause the alginate molecule to contract, hence lowering the viscosity (Smidsrød O., 1995).

1.1.2. Mannuronan C-5 epimerases

Alginate from both algae and bacteria is initially synthesized as mannuronan with 100% M-residues. G-residues are introduced in a post-polymerization step by enzymes called C-5 epimerases that catalyse conversion of mannuronic acid residues into guluronic residues without breaking the glycosidic bond.

Seven different mannuronan C-5 epimerases from *Azotobacter vinelandii* have been sequenced, cloned and produced recombinantly in *Escherichia coli*. Some create G-

blocks (AlgE2, AlgE5 and AlgE6), while AlgE4 create MG-blocks (Campa et al., 2004) AlgE1 and AlgE3 are bifunctional epimerases and produce both G and MG-blocks (Steigedal et al., 2008) Lyase activity has been observed in AlgE7 (Svanem et al., 2001).

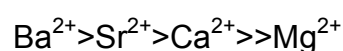
For AlgE4 from *A. vinelandii* the MG-blocks generated are on average 10 residues epimerized for each enzyme-substrate encounter and the enzyme has been shown to work progressively. The G-block forming enzymes create different patterns that vary in terms of both G-block length and relative amount of alternating structures (Campa et al., 2004). With knowledge of the sequences generated and the ability to recombinantly produce the enzymes, it is now possible to engineer alginate with desired and known structure (Morch et al., 2007, Morch et al., 2008) Bifunctional epimerases are also discovered and researchers have also constructed new epimerases from known parent enzymes by interchanging modules between different epimerases. This possibility enlarges the spectra of engineered alginate (Bjerkan et al., 2004).

1.1.3. Alginate gel

The ratio of G and M monomers together with their exact sequence affect the properties of alginate gel. When divalent ions such as Ca^{2+} , Sr^{2+} , and Ba^{2+} are added to a solution of alginate, a gel will be formed. It has been shown that alginate with large fractions of M and MG-blocks create soft and compact gels, while alginate containing a lot of G-blocks generates gels with an open and stiff network with higher porosity (Martinsen et al., 1989a, Draget, 2006a) It has also been shown that MG-blocks are participating in junction formation, forming MG-MG junctions and MG-GG junctions (Donati et al., 2005).

Calcium will bind to four G-monomers in a G-block forming a cavity in the chain, ideal for binding divalent ions. This binding causes two chains to bind to each other in an “eggbox” fashion, i.e. with the ion resembling an egg in a box as shown in figure 1.3. The ion will bind to four G residues, two in each chain as shown in figure 1.3. It follows that an abundant amount of G-blocks makes a stiffer and more stable gel as it enables more binding sites between the chains. It has also been suggested that the chains bind to each other laterally, further enhancing the stability of the gel (Stokke, 2000, Draget, 2006b) The “eggbox” model does only apply to Ca^{2+} ions, as Sr^{2+} and Ba^{2+} ions are larger and will bind to G-blocks in a different fashion (personal communication, Dr. Ing. Berit L. Strand, 10.04.2012).

The binding of ions to the G-blocks is highly selective and the order of affinity from highest to lowest is:



Barium has been shown to bind to both G and MG-blocks, while strontium only bind G-blocks (Morch et al., 2006) and barium is often added to gelling solution to stabilize gels because of its strong affinity with G-blocks. The gels tend to swell and dissolve

under physiological conditions when only calcium ions are used as a gelling ion. This is due to the networks sensitivity towards chelating agents such as lactate, citrate and phosphate and exchange of Ca^{2+} ions with non-gelling ions such as Na^+ and Mg^+ . Swelling leads to higher porosity and less elasticity due to fewer junctions (Flory, 1953). The use of barium should be limited, due to barium's potential cytotoxicity. A Ca^{2+} : Ba^{2+} relationship of 50:1 has been shown to stabilize gels sufficiently (Morch et al., 2006) (Morch et al., 2007). Another strategy to avoid swelling is to use alginate with a high G-block content, as it introduces more junctions (Martinsen et al., 1989a) (Thu et al., 1996).

The gel strength of alginate gels has been shown to be proportional with the square of alginate concentration (Strand et al., 2002a) and the gel stiffness has been shown to increase proportionally with increased alginate concentration (Kong et al., 2003).

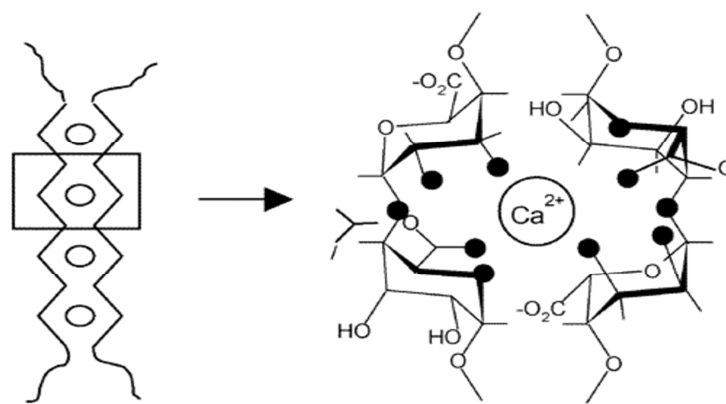


Figure 1.3: Schematic depiction of the interaction between calcium ions and the G-blocks of alginate. The divalent positive ion will be captured between two strands of G-blocks, and resembles an egg in an egg box (Braccini and Perez, 2001).

Gel formation is autocoperative. This is explained by the fact that the first binding of divalent ion to G-blocks is entropically unfavourable, while the subsequent bindings are not (zipper mechanism) (Moe, 1995). The minimum amount of G monomers adjacent to another required to form a gel is shown to vary between 8 and 20 residues, depending of the affinity for the ion (Kohn and Larsen, 1972, Stokke, 1993). Ions for which the G-blocks has high affinity, requires shorter G-block lengths (Stokke et al., 1993).

Syneresis is the phenomenon of gel shrinking , which causes release of water, hence the reduction of gel volume. It has been proposed that MG blocks are particularly involved in the syneresis mechanisms (Morch et al., 2008). This may be due to their ability to be compressed due to additional crosslinking with calcium in addition to the crosslinks formed by the G-blocks (Donati et al., 2005). Syneresis is mainly affected by the composition of alginate (Strand et al., 2003).

1.1.4. Alginate as a biomaterial

According to Lee and Mooney, a biomaterial is defined: “as a material intended to interface with biological systems to evaluate, treat, augment or replace any tissue,

organ or function of the body". The evolution of biomaterials has gone from wood, to ceramics and is now focused on nature-derived materials that are inherently biocompatible and in some cases able to interact with cells (Lee and Mooney, 2012).

Alginate hydrogel made from alginate and divalent ions is a natural biomaterial, which is biocompatible, has low toxicity, is relatively cheap and has mild gelation chemistry. It is a porous material with pores in the nanometer scale, which allows smaller molecules to diffuse through it. Alginate hydrogel is a polymeric network that contains 95-99% water and it does in many ways resemble the natural extracellular matrix that surrounds cells in the body (Partap et al., 2007). It is also hydrophilic, which reduces friction in body fluids and minimizes protein adsorption (de Vos et al., 2002) (Li, 1998) (Uludag et al., 2000) and is also easily stored and sterilized (Rowley et al., 1999).

These properties allow alginate to be used as a scaffold in tissue engineering where the aim is to replace lost or damaged tissue or organs with man-made tissue. Hydrogels such as alginate are able to deliver cells to a desired site and provide space, structure and control over engineered tissue (Lee and Mooney, 2012). Alginate can be utilized as an immobilizing matrix for cells, or as a scaffold for cells meant to migrate out of the matrix. In the latter case the gel has to be modified in order to obtain large enough pores for the cells to navigate through or be constructed to degrade *in vivo* (Augst et al., 2006). In the hydrogel, linear hydrophilic alginate chains crosslinked by divalent cations such as calcium or barium ions creates a scaffold that provides encapsulated cells or compounds with structural support and protects them from the surrounding environment (Freeman et al., 2008).

1.2. Alginate derivatives

Many alginate derivatives with biomedical applications have been constructed and different substituents have also been successfully attached to the monomers (Augst et al., 2006). These modifications allow control over solubility, pH sensitivity and affinity for specific proteins (Freeman et al., 2008) and interaction with cells. Examples of such substituents are the RGD peptide, YIGSR peptide (Augst et al., 2006) and sulphate groups (Freeman et al., 2008).

1.2.1

Covalently modified alginate

Alginate does not interact with mammalian cells and due to their hydrophilic nature they do not promote protein adsorption, therefore interaction cannot be mediated through serum proteins. Cellular anchorage is a prerequisite to survival for many cell types and cannot be met by pure alginate matrix. It is thus often necessary to culture aggregated cells to promote survival in pure alginate matrix. The interaction between cells and their environment is mediated through transmembrane receptors that binds adhesion ligands on the outside of the cell membrane and conveys signals to the

cell's interior. These are signals that govern migration, apoptosis, differentiation and proliferation.

It is possible to covalently modify alginates with cell specific adhesion molecules, most easily to the carboxylic group in the monomers (Rowley et al., 1999).

Alginate covalently linked to RGD peptide

The RGD peptide (arginine-glycine-aspartic acid) is commonly found in collagen and fibronectin in the extracellular matrix. It is the smallest sequence that integrin receptors can recognize and bind to. The modification is usually carried out by aqueous carbodiimide chemistry, where stable covalent amide bonds between the peptide and the alginate polymer are formed (Rowley et al., 1999). It is thought that a minimum concentration of RGD peptide is required to elicit cell adhesion and cell proliferation, and this minimum concentration is presumed to be cell specific (Augst et al., 2006).

Carbodiimides are compounds with the chemical formula 'RN=C=NR' and act as zero-length crosslinking agents that couples carboxyl groups to primary amines. The reaction forms an unstable amin-reactive o-acylisourea intermediate, which is stabilised by N-hydroxysulfosuccinimide sodium salt (s-NHS). The salt reacts with o-acylisourea and forms an amine- reactive ester that binds to peptide. RGD peptide has two carboxyl groups and one nucleophilic group and the presence of several functional groups increases the probability of side reactions. Some common by-products include N-acylourea and amides (Braccini and Perez, 2001). The RGD peptide is shown in figure 1.4.

It has been shown that mouse skeletal myoblasts adhere, proliferate and express a differentiated phenotype on RGD coupled alginate in 2D culture (Rowley et al., 1999). Recent work in our lab done by Kristin Karstensen (Karstensen, 2010) has demonstrated that OECs attach to RGD peptides and change morphology due to this attachment in 2D culture.

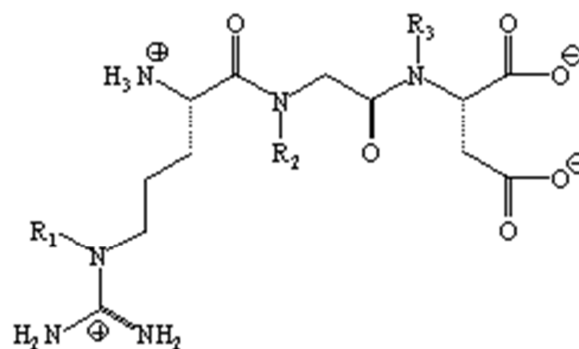


Figure 1.4: The RGD peptide (Hersel et al., 2003).

Sulfation of alginate

Sulphated polysaccharides can either be manufactured chemically or are found in

nature. The most commonly known sulphated polyaccaride is heparin, which prevents blood clotting and acts as an anticoagulant (Pawar and Edgar, 2012).

Heparin is also known to bind growth factors, such as fibroblast growth factor-1 (FGF-1), which is believed to modulate olfactory axon growth. This feature is also associated with the heparin-like molecule heparin sulphate proteoglycans (HSPGs), which are located on cell membranes and in the extracellular matrix. The HSPGs are known to activate FGF by presenting it to the high affinity signal transducer receptors on cell surfaces and it has been shown that FGF-1 is localised to sites of axonal growth and synaptic neuropil in the olfactory pathway. FGF-2 is believed to have a more global effect in both brain and spinal cord and is expressed in both glia and neurons (Key et al., 1996).

It is possible to synthesise sulphated alginate as reported by Yumin *et al* who used chlorosulfonic acid in formamide as shown in figure 1.5. The sulphate groups will bind to the OH groups on the uronic acids and it is believed that they will mainly bind to C2 and C3 in the mannuronic acid and guluronic acids, as these peaks will shift downwards during characterisation by ^{13}C NMR. This indicates that the sulphate groups are added to either one or both hydroxyl positions (Pawar and Edgar, 2012).

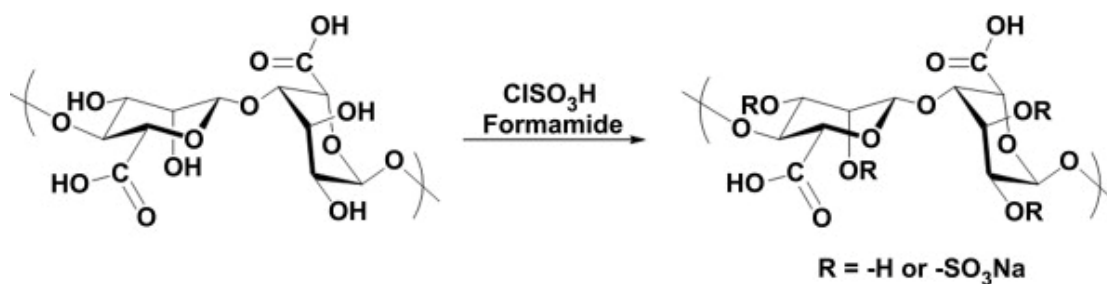


Figure 1.5: Sulfation of alginate by ClSO_3H in formamide (Pawar and Edgar, 2012).

In the study by Yumin et al it was also found that the sulphated alginate displayed anticoagulant activities comparable to heparin by the intrinsic coagulation pathway (Pawar and Edgar, 2012). Recently, sulphation of alginate has been carried out in our lab, showing that the mannuronic acid binds two sulphate groups and that the guluronic acid binds one, giving an average of 1.5 sulphate groups per monomer yielding a total sulphation of 150% per monomer (Personal communication from Øystein Arlov, 15.04.2012). It is known that heparin has >70% sulfation while heparin sulphate has <50% sulfation (Bruce Alberts, 2002), and compared to these values the sulphated alginate has a relatively high content of sulphate groups.

1.3. Encapsulation

When foreign cells are transplanted to an organism, the immune system will inevitably reject the implanted cells and try to destroy them in order to protect the organism. Immunosuppression has been one alternative to circumvent this obstacle, but it has many side effects such as increased cancer prevalence, frequent infections

and general toxicity. Other options are therefore highly requested. Immunoisolation obtained by encapsulation of cells in alginate microbeads (100-1000 μm in diameter) is one alternative. The alginate microbead forms a selective membrane around the implanted cells that allows small molecules such as nutrients, oxygen, electrolytes and biotherapeutic agents to pass through it, but shields the foreign cells from the immune system (Mørch et al., 2008). Alginate microcapsules have been shown to protect both allo-grafts and xeno-grafts against destruction in mice (Omer et al., 2005). Desired properties in alginate gels utilized in encapsulation are; high mechanical and chemical stability, controllable swelling properties, low content of toxic, pyrogenic and immunogenic contaminants, defined pore size and a narrow pore size distribution (Orive et al., 2004).

The encapsulation process is both simple and versatile as it is a one-step procedure that does not require extensive training in biopolymer chemistry. An aqueous solution of alginate is mixed with cells and dripped into a gelling bath containing divalent ions such as Ca^{2+} , Ba^{2+} or Sr^{2+} . The divalent ions will diffuse into the droplet and create hydrogel spheres where the cells are trapped inside a three-dimensional network of ionic cross-linked polymers. Beads with a diameter of $<200 \mu\text{m}$ can be manufactured with a bead generator as shown in figure 1.6, and a narrow size distribution is easily obtained.

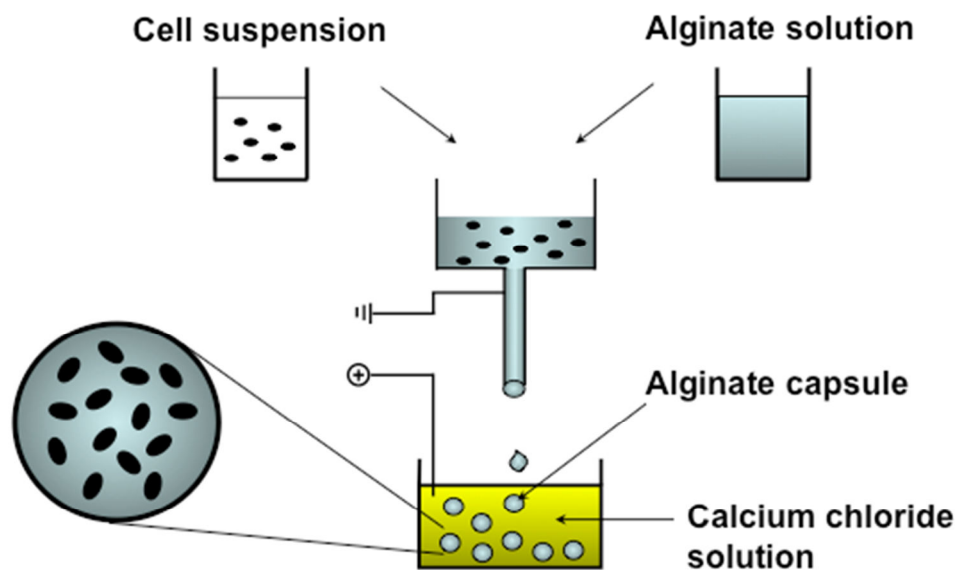


Figure 1.6: Encapsulation of cells using an electrostatic bead generator shown schematically (directly reproduced from (Mørch, 2008)).

The sizes of the beads depend on several factors, such as the viscosity of the alginate, needle size, flow rate and the voltage magnitude. The electrostatic bead generator creates an electrostatic potential between the tip of the needle and the gelling batch, usually between 1-20 kV. This potential causes the droplet to be pulled from the needle and into the batch, and allows control over the bead size by regulating the voltage (Strand et al., 2001).

The permeability of alginate capsules is determined by the gels porosity. Small molecules have been shown to diffuse almost unhindered through alginate, while glycol and ethanol exhibits a diffusion rate close to 90% of that in water (Tanaka et al., 1984) (Oyaas et al., 1995). Proteins up to $3,5 \cdot 10^5$ Da will diffuse through alginate gel with some difficulty, and even larger proteins will be able to escape the capsules with a rate depending on molecular weight, shape and pH in the solution (Tanaka et al., 1984) (Martinsen et al., 1989a). Gels with high G content will have large pores and an open and rigid network, due to the high number of junctions between the G-blocks, compared to gels with lesser G content (Morch et al., 2008).

The size of capsules is another parameter that affects cell survival and capsule properties. Smaller capsules have a larger surface to volume ratio that enhances exchange of nutrients, cell products/waste and oxygen (Morch et al., 2007). In capsules with a diameter 250 μ m of with islets of Langerhan's encapsulated, differences in oxygen tension throughout the capsule has been reported, as well as anoxia in the center of the capsule (Colton, 1995).

On the other hand, smaller capsules may provide less immunoisolation than larger capsules (Rokstad et al., 2001), and in addition they are more vulnerable to osmotic stress and swelling (Strand et al., 2002a).

1.4. Olfactory Ensheathing Cells and CNS repair

1.4.1. Damage in the Central nervous system (CNS)

CNS damage is still one of the major causes of both death and disability, despite intense research efforts to achieve neurogenesis and restore functional synaptic connection of CNS neurons. This process was believed to be impossible due to the non-permissive physical and chemical environment created after trauma in the CNS but this belief was disproved in the early 1980s, when researchers showed that axotomised CNS neurons regrew their axons in the presence of peripheral nerve grafts (David and Aguayo, 1985). Since then a tremendous effort has been put into creating a permissive environment and promote neuroregeneration in CNS, but the task has proven to be very difficult as the processes connected to both degeneration and regeneration of neurons are very complex (Sandvig, 2011).

1.4.2. Cell Transplant mediated repair

Current therapy after traumatic brain injury and spinal cord injury is limited to preventing inflammation, prevent secondary cell death and increase plasticity in spared circuits. None of these strategies promote regeneration or regrowth of neural cells/axons. *In vitro* and *in vivo* studies has shown that CNS axons can regenerate when located in a permissive environment (David and Aguayo, 1985) and it is known that on-going neurogenesis occurs in certain areas of the adult brain. Extensive research is performed with the aim to create such permissive environments at lesion sites, and many different strategies have been tested. The most promising techniques are transplantation of biomatrices and cell mediated transplant therapy

(McCreedy and Sakiyama-Elbert, 2012), where cells are implanted into CNS and deliver active molecules involved in repair of neurological damages (Li, 1998). Relevant cell types include embryonic stem cell (ESCs), neural stem/progenitor cells (NSPCs) and oligodendrocyte precursor cells (OPCs). Another promising candidate are olfactory ensheathing cells (OECs), which enwrap olfactory axons in the olfactory bulb, one of the areas in the brain where neurogenesis occurs throughout life (Barnett and Chang, 2004). Systemic delivery of therapeutic agents to the CNS is often hampered by the blood-brain barrier, and the cell candidates for cell-mediated transplant therapy are often short lived and labile. An alternative to systemic delivery is to encapsulate cells that produce therapeutic agents in alginate microcapsules and directly engraft the capsules into the brain or spinal cord, as the capsules provides the cells with a protective microenvironment (Li, 1998).

1.4.3. Olfactory ensheathing cells

Olfactory ensheathing cells (OECs) are found in the olfactory mucosa and olfactory bulb. They were first discovered by Golgi (1875) and Blanes (1889), and soon after proved to be a distinct glial cell type. OECs express GFAP and S100 β , a trait normally associated with astrocytes (Higginson and Barnett, 2011). OECs display a certain plasticity regarding to their phenotype and two main types are recognized, the astrocyte-like and the non-myelin forming Schwann-cell like morphology. The astrocyte-like form is distinguished by the fact that it has more cytoplasm around its nucleus, is flat and stellate-shaped and it can display a larger concentration of expressed filamentous GFAP (Higginson and Barnett, 2011).

The Schwann-like OECs expresses the p75^{NTR} receptor and is spindle-shaped. It is suggested that the two morphologies are associated with different cell migratory patterns and that OECs have the ability to spontaneously interchange between the two. It is also suggested that the Schwann-like cells are superior in supporting neurite outgrowth compared to the astrocyte-like OECs (Higginson and Barnett, 2011).

OECs enwraps developing and regenerating axons of olfactory receptor neurons (ORNs) from the olfactory mucosa through the cribriform plate, and into the olfactory bulb glomeruli, where ORNs synapse with second order neurons (Lindsay et al., 2010), as shown in figure 1.7. Before 1980 it was thought that neurogenesis ceased to happen in the CNS after development, but recent research proved that there are areas in the brain where neurogenesis happens (Lindsay et al., 2010). the primary olfactory system being one of them (Lindsay et al., 2010). It is suggested that this property is due to the fact that olfactory receptor neurons can frequently be exposed to damaging toxins and subsequently need to be replaced, as the olfactory bulb also is characterized by ORN regeneration (Lindsay et al., 2010).

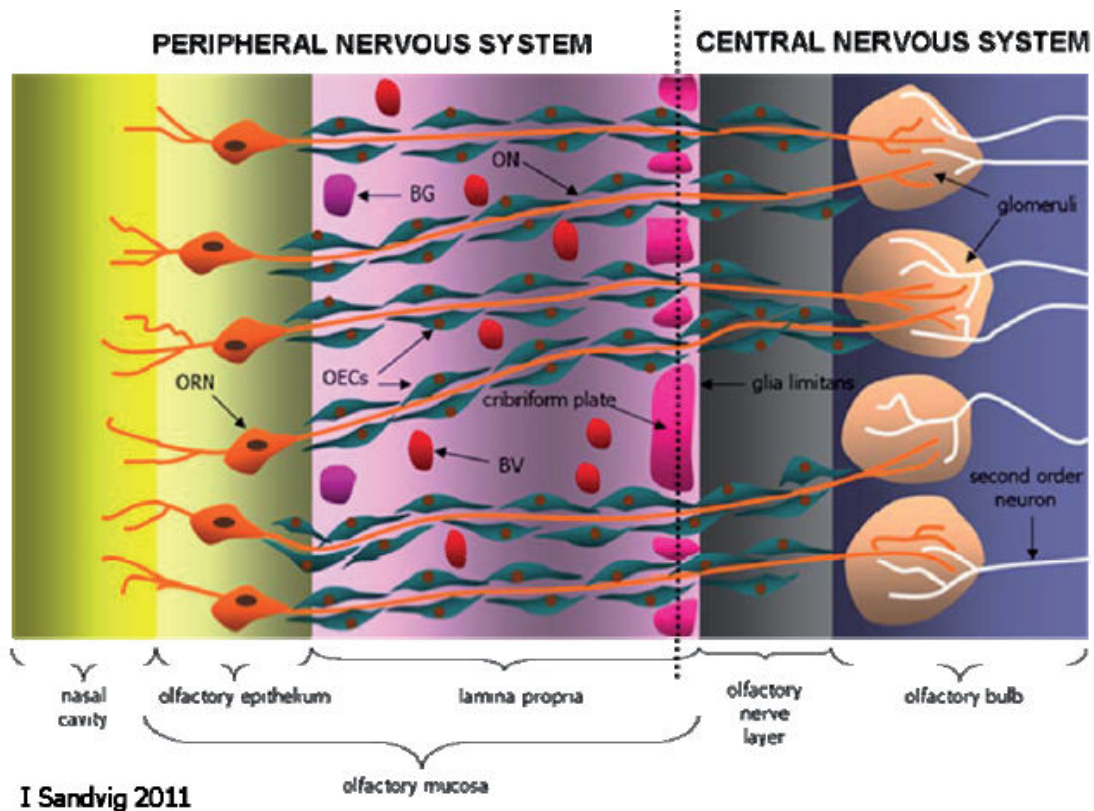


Figure 1.7: The ORNs trajectory from the olfactory bulb to the nasal cavity. OECs are wrapped around the ORNs and are shown as blue cells in this figure (directly reproduced from (Sandvig, 2011)).

OECs secrete neurotrophins, provide necessary ECM molecules and substrates for axon elongation and myelination. In contrast to Schwann cells they do not activate and induce inhibitory molecules, including chondroitin sulphate proteoglycans and hypertrophy in astrocytes, and are therefore believed to be a better candidate for cell-mediated repair of the CNS. Schwann cells have also been shown to promote axon regeneration, but unlike OECs they are not able to promote growth that goes beyond the local graft area and into CNS (Barnett and Chang, 2004).

As mentioned above there are different morphologies of OECs, and the relationship between the two principal morphologies (Schwann- and astrocyte-like) is not known. One hypothesis is that the astrocyte-like cell is an immature form of the Schwann-like cell, similar to real Schwann-cells that also have an immature and non-active flat stellar-shaped precursor. Another theory states that the two morphologies are mature forms of OECs with different tasks, and this theory is perhaps supported by the fact that the cells are found to have different antigenic profiles in the olfactory system based on their location, indicating that they perform different tasks. Both theories are depicted in figure 1.8 (Barnett and Chang, 2004).

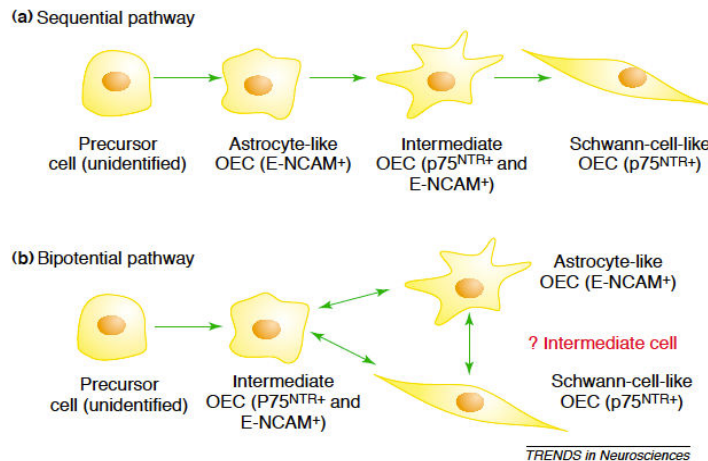


Figure 1.8: The two theories concerning OECs morphologies and origin as well as relationship to each other. The protein expression associated with the different morphologies is also mentioned in the figure (Directly reproduced from (Barnett and Chang, 2004)).

To obtain successful restitution of functional synapses and regrowth of neurons it is necessary for glia cells, neurons and ECM to communicate with each other. It is perhaps utopian to expect all this from a single cell type, and a realistic approach may include transplantation of several different cell types combined with suppression of inhibitory factors (Barnett and Chang, 2004).

1.5. 3D culture

Culturing cells in 3D cultures is thought to be more physiologically relevant than 2D cultures as most cells *in vivo* reside in 3D environments (Augst et al., 2006).

Mesenchymal stem cells encapsulated in RGD peptide grafted alginate have been shown to change differentiation pathway in response to the rigidity of three-dimensional microenvironments. Stiff gels (11-30 kPa) induced osteogenesis, and softer gels (2.5–5 kPa) induced an adipogenic lineage. In contrast to cells grown on 2D cultures of variable stiffness, no morphological change was observed in cells grown in 3D capsules with variable stiffness, as the cells appeared to be more or less spherical. Small protrusions were detected, but their numbers were not correlatable with the stiffness of the 3D matrix. The fate of the stem cell seemed to be related to the number of adherence bonds between the gel and cells, not the morphological changes. The cells were shown to alter the receptors used to adhere to RGD peptide in the 3D microenvironment compared to 2D culture (Huebsch et al., 2010).

In another experiment done by Fischbach *et al* carcinoma cells were encapsulated in alginate grafted with RGD peptide with a RGD density that correlated with the density found in tumors *in vivo*. In this study it was revealed that 3D microenvironmental cues affected cell signaling and tumor vascularization. 3D integrin engagement was shown to be critical regulators of IL-8 secretion in carcinoma cells. This is knowledge that can be utilized in cancer research (Huebsch et al., 2010).

1.6. Molecules in the extracellular matrix (ECM)

The composition of the ECM can vary and enables an enormous diversity in the tailoring of biomaterials, from calcified structures in bone to the transparent structure of the cornea. Despite these differences, the molecular classes that are the components of ECM are for the most part the same and they differ only in their organization and relative amounts (Bruce Alberts, 2002).

The ECM in the brain has several important tasks such as providing structural support, regulate synaptic functions and neuronal plasticity. Both neuronal and glial cells produce its constituents and the main components are hyaluronic acid, proteoglycans, lectican-link proteins and phosphacan. The most prominent feature of the brain ECM is the perineural nets that are assembled around cell bodies and axons during the postnatal maturation of ECM (Zimmermann and Dours-Zimmermann, 2008). These loose flexible nets consist of hyaluronic acid polymer that protrudes from the cells and binds to the end of a lectican proteoglycan. This binding is stabilised by link proteins collectively called hyaluronic acid and proteoglycan binding link proteins (HAPLs). The other end of lectican is bound to an arm of a tenascin oligomere that can bind three or six lecticans (dependent of the type of tenascin) and thus creates bridges between different lectican-link protein-hyaluronic acid complexes. Tenascins are large multimeric glycoproteins that bind to many constituents in the ECM, among them lecticans, integrins, cell surface HSPGs and cell adhesion immunoglobulines. It has been observed that the migration of neurons into the outer layers of the olfactory bulb in adult knockout mice deficient of tenascin R (Tn-R) is impaired, thus, it has been hypothesized that Tn-R has a role as a positive cue for neuronal migration (Zimmermann and Dours-Zimmermann, 2008).

1.6.1. Integrins

Integrins are some of the most widely studied members of cell receptors, and are found in all nucleated cells of multicellular organisms. They are essential for cell-cell interaction and cell-matrix adhesion, and contribute to development, homeostasis and immune responses. Integrins do also play a part in autoimmune diseases and cancer. These proteins are both mechanic links as well as being involved with bidirectional signalling over the cell membrane (Lowell and Mayadas, 2012).

Integrins are $\alpha\beta$ heterodimeric transmembrane proteins. The α subunit has four subclasses in mammals, while the β unit has three subunits with two represented in vertebrates. The combination of different α and β subunits determines the function of the integrin. Group 1 of α subunits ($\alpha3$, $\alpha6$ and $\alpha7$) combined with B1 subunits will act as laminin receptors, while group 2 α subunits ($\alpha1b$, αv , $\alpha5$ and $\alpha8$) combined with B1 or B3 will form receptors for the RGD peptide (Arg-Gly-Asp motif), as an example. The β subunits in vertebrates are organized in two groups; A ($\beta1$, $\beta2$ and $\beta7$) and B ($\beta3$, $\beta4$ and $\beta5$), with $\beta1$ subunit most widely expressed throughout the body (Lowell and Mayadas, 2012). The β subunit is rich in Cys residues, which enables many intrachain disulphide bonds. The α unit contains many binding sites for Ca^{2+} ions, which has to be bound for the integrin to become activated. As can be seen in figure

1.9 the integrin has a short cytoplasmic extension with one transmembrane helix and a large ECM domain with ligand binding site. The most prominent ligands include the RGD motif in collagen, laminin and heparan sulphate proteoglycans (HSPGs) (Albert L. Lehninger, 2008).

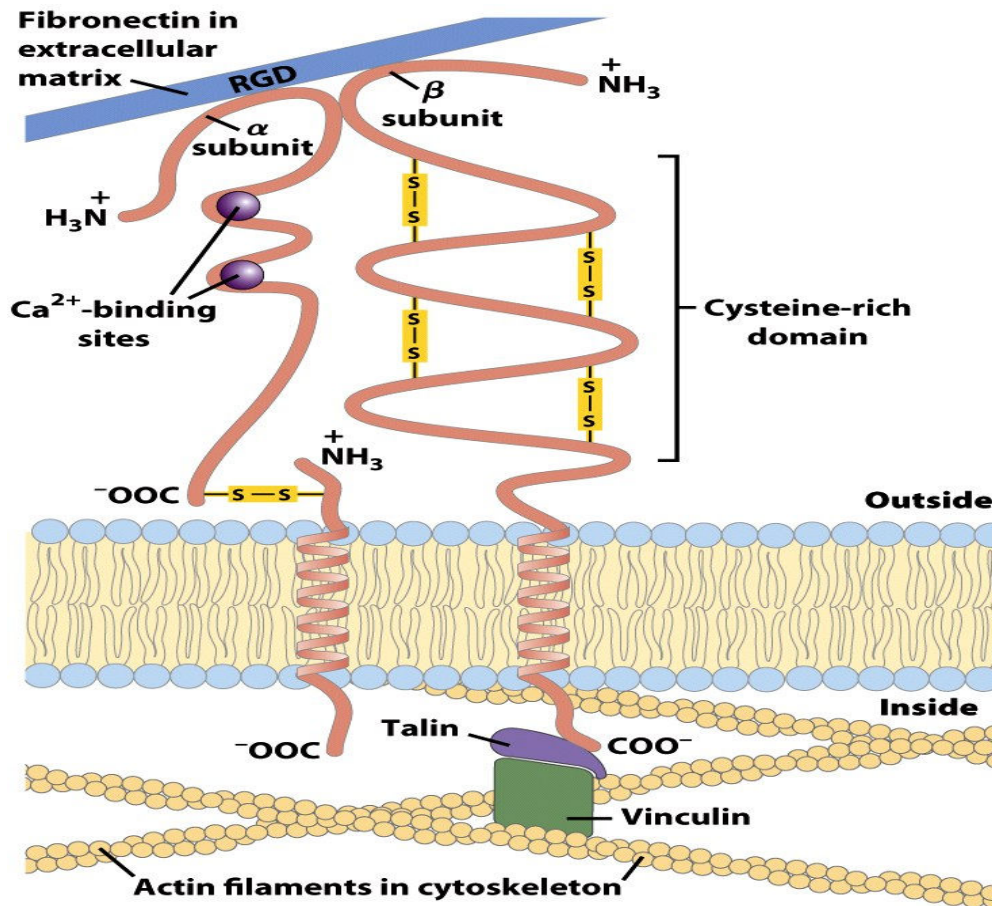


Figure 1.9: Overview of the organization of the transmembrane integrin dimer (Directly reproduced from(Albert L. Lehninger, 2008)).

The expression of integrins on the cell membrane are controlled by gene transcription which in turn can be regulated by signals relayed by the integrins themselves and the process is known as “inside-out” signalling. The regulation is dynamic, which allow the cell to control their adherence to other cells as well as ECM and this is especially important during migration. It can activate the integrins by making them change their conformation from closed to open, as well as order accumulation of integrins at specific locations in the cell membrane. When an integrin is activated by a ligand situated in ECM it leads to an assembly of many cytoplasmic proteins and this links the integrin to actin filament and microtubule cytoskeletal network. The activated integrin can reorganize the cytoskeleton and modulate ECM, as well as transmitting intracellular signals, which is known as “outside-in” signaling (Lowell and Mayadas, 2012)

Integrins play an important part in the central nerve system (CNS). It is known to guide migration of nerve precursor cells and stabilize neural synapses. Knockout

mice deficient of β 1 integrins will for display relatively normal neural migration, but have a completely disorganized cortex, due to lack of contact between cortex structures and the meningeal basement membrane. This deficit will also affect the peripheral nervous system (PNS), and leads to severe perturbations of the system caused by defective migration through the embryonic ECM (Lowell and Mayadas, 2012).

1.6.2. Hyaluronic acid

Hyaluronic acid is produced by the enzyme hyaluronic acid synthase (HAS) located on the inner cell membrane of astrocytes (foundation, 1989) and the linear polymer protrudes out from the cell and into ECM. It consists of repetitive disaccharides; glucuronic acid and N-acetylglucosamide. Three different isotopes of the HAS enzyme are found in mammals and in the brain HAS2 and HAS3 predominates. Hyaluronic acid binds proteoglycans of the lectican family and is the main constituent of the ECM in the brain (Zimmermann and Dours-Zimmermann, 2008).

1.6.3. Proteoglycans

Proteoglycans are variable N- and O- linked oligosaccharides that contain at least one long glucosaminoglycan polysaccharide (GAG) covalently bound to a core protein. The main proteoglycans found in the brain are of either lectican or hyalectican family, which both bind to hyaluronic acid, tenascin and link proteins (HAPLs). The GAG sequence in the proteoglycan determines the class and the different classes in the brain are heparan/heparin-, dermatan- or chondroitin-sulphate proteoglycan (Zimmermann and Dours-Zimmermann, 2008).

1.6.4. Collagen

Collagen is the most abundant protein in ECM and is known to interact with cells via several receptors, such as glycoproteins, heparan sulphate proteoglycans and most prominently, integrins, as well as discoidin domain receptors in the tyrosine kinase family. It is known to be involved with cell adhesion and migration, differentiation and wound healing, aside from being the main contributor to biomechanical properties of tissue (Leitinger and Hohenester, 2007).

Collagen consists of three different polypeptide α -chains, intertwined in a triple helix conformation. Each of the α -chains comprises about 1000 different amino acids and the triple helix is 300 nm long and has a diameter of 1,4 nm. Collagen is made intracellularly and starts out as pro-collagen with additional non-helical residues located at the terminal ends. These residues are primarily involved with transport and aggregation and are cleaved off when the triple helix is finished, with the exception of 9-26 amino acids called telopeptides. Collagen contains large amounts of two unusual amino acids; 4-hydroxyproline and ϵ -hydroxylysine, both manufactured by post-translational modifications done by special enzyme systems. The ϵ -hydroxylysine can also be glycosylated by other enzyme systems and the degree of glycosylation varies between the different types of collagen. 33% is glycine, 22% is proline and hydroxyproline and the remaining 45% is some 17 different amino acids

with a relatively high share of basic and acidic amino acids. Some observations indicate that the carbohydrates participate in intra- and inter-molecular covalent crosslinking, but their exact function is still not known. Both hydroxylation and glycosylation are restricted to growing chains, and the helix stability is dependent on the content of hydroxyproline content.

Up until now 19 different types of collagen has been discovered. Type I is mainly found in bone and skin, and is used to produce gelatin industrially. Type II is primarily found in cartilage and type III is also found in skin (the ratio decreases with age) (Babel, 1996). All of these three collagens are water-soluble until they are crosslinked and turned first into microfibrils of 2-8 collagen molecules and these are further turned into fibrils by enzyme-catalysed steps outside the cell membrane. The structure of collagen I is shown in figure 1.10, with proline in the X-position and hydroxyproline in the Y-position (Friess, 1998).

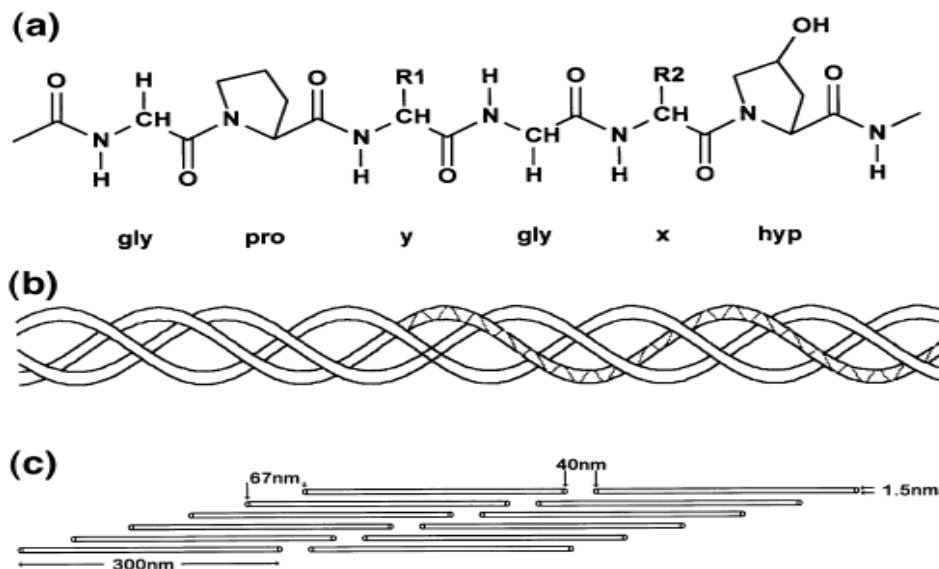


Figure 1.10: Overview of the collagen structures where (a) is the chemical structure of collagen I, (b) shows the primary amino acid sequence and (c) is a schematic presentation of the quaternary staggered sequence (Friess, 1998).

Gelatin

Gelatin is formed from collagen by gentle conversion of highly cross-linked and water-insoluble raw material into water-soluble gelatin. The collagen is obtained from by-products from slaughtered calves, cattle and pigs. The skin from animals is often treated with acids, and bone is treated with alkaline suspensions. The main goal of these procedures is to hydrolyze residual fat and crosslinks, and extract non-collagenous proteins, nucleic acids and carbohydrates. After such treatment, the raw materials are washed to remove excess acid/base and the gelatin is extracted. Historically, the same result was obtained with boiling of raw materials, and this way of converting collagen to gelatin is experienced by all of us when cooking meat to

make it tenderer. The partial thermal hydrolysis is schematically shown in figure 1.11.(Babel, 1996).

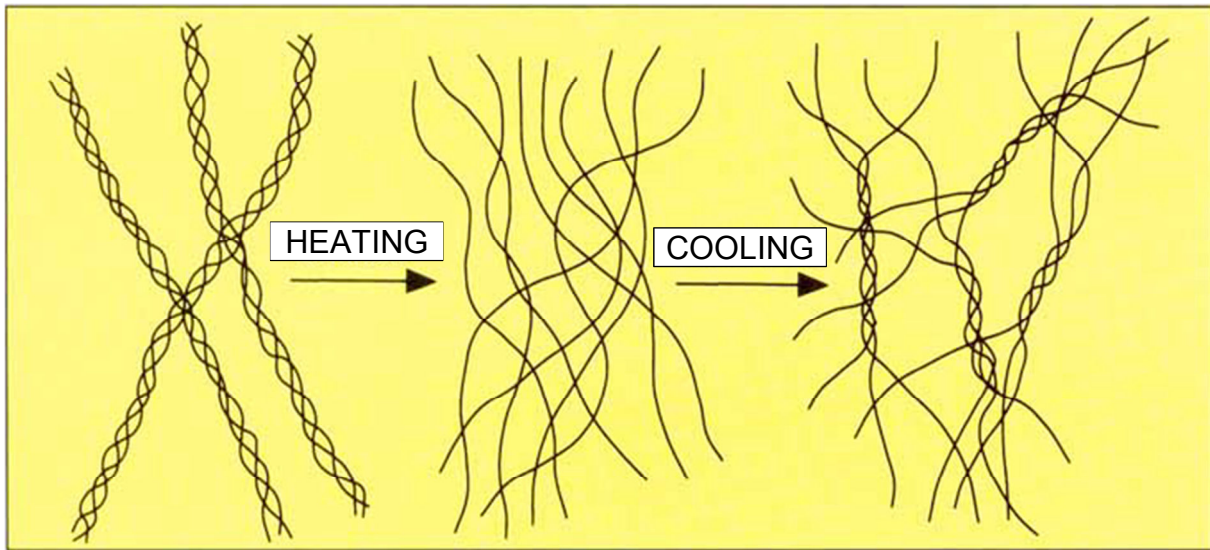


Figure 1.11: Partial thermal hydrolysis of collagen into gelatin (directly reproduced from (Babel, 1996)).

Gelatin has a molecular weight ranging from 10000 to several million daltons and contains amino acids that possess side chains with amino-carboxyl and hydroxyl groups. These groups allow altering of chemical and physical properties of the gelatin. Gelatin is able to interconvert between sol and gel thermo-reversibly. If an aqueous solution with higher gelatin concentration than 0.5% is allowed to cool below 35-40°C it will form a gel. This process is reversible by heating the solution again. It is thought that the gelling occurs due to association of dissolved α -chains via hydrophobic structural elements that form ordered helical structures. Further on, crystal formation of two or three such helical structures occurs. The structure is stabilized by hydrogen bonds within and between the helices, as well as the addition of water molecules that form hydrogen bonds with the hydrophilic OH-groups of the corresponding amino acids. The viscosity of the gel is dependent of concentration of gelatin in the solution as well as pH, temperature and additives present. The viscosity increases with higher gelatin concentration and decreases with increasing temperatures (Babel, 1996).

1.6.5. Fibronectin

Fibronectin is associated with cell migration and organization of ECM. It is a non-collagen glycoprotein with many domains that binds both other matrix molecules and cell receptors. It consists of two large subunits that form a dimer, joined by two disulphide bindings near the C-termini. Each subunit is folded into series of functional domains with flexible polypeptide regions separating them. Fibronectin can be solubilized in body fluid as single chains, but can also be assembled into insoluble fibrils. The fibrils are only formed when the fibronectin is anchored to a structure in ECM and attached to an appropriate cell receptor, causing the protein to stretch and

thereby reveal binding sites where other fibronectin molecules can cross-link with additional disulphide bonds. This feature ensures that fibrils are only formed at appropriate locations in the organism as shown in figure 1.12 (Bruce Alberts, 2002).

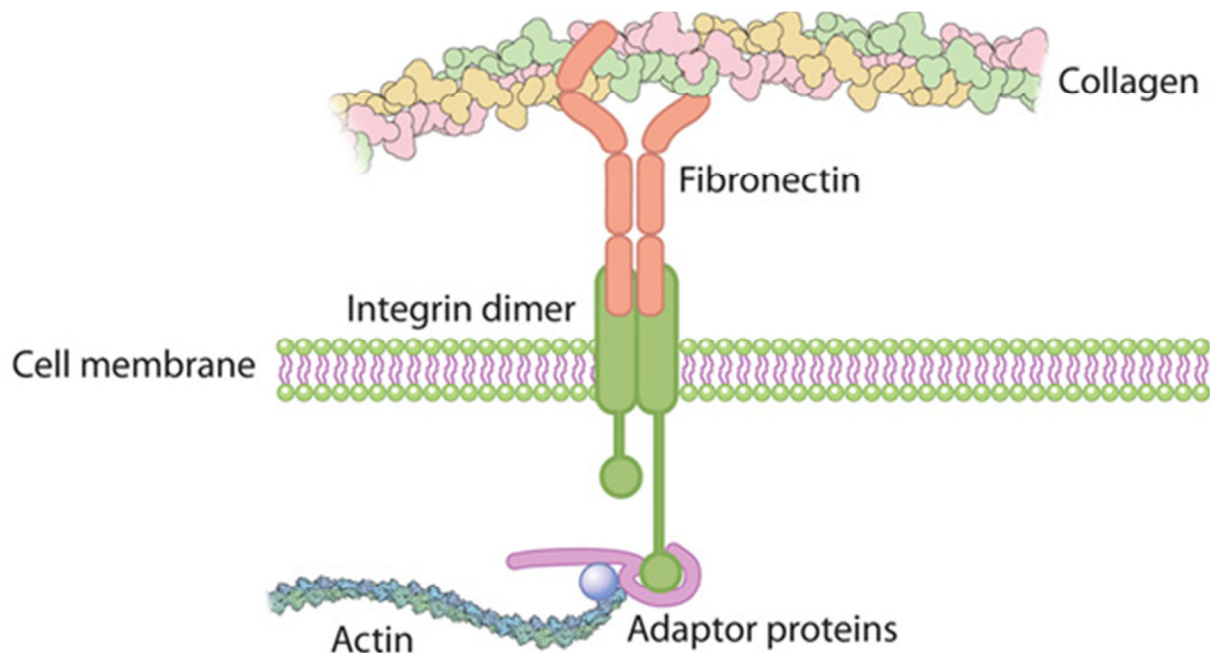


Figure 1.12: Fibronectin anchored to collagen in the ECM and an integrin receptor in the cell membrane (Education, 2011).

The different domains in fibronectin bind to heparin, collagen and cell receptors. The type III fibronectin domain contains the RGD peptide (Arg-Gly-Asp) that bind to integrins, and occurs 15 times in each subunit allowing fibronectin to bind cells strongly (Bruce Alberts, 2002).

Fibronectin is found in the embryonal nervous system and is expressed in a specific spatial and temporal manner important for both neuronal migration and outgrowth during development. It is also associated with remodelling of injured brain tissue where it promotes nerve generation and activates astrocytes (A. Alovskaya, 2007).

1.6.6. Laminin

Laminin is a large heteromeric glycoprotein consisting of three polypeptide chains; α , β , and γ and is shaped like a cross. To date there are found five α -chains, four β -chains and three γ -chains and when these are combined they make up 16 different types of laminins in mammals. Laminins are the main constituents of the basal membrane, also known as the basal lamina, and their main task is to anchor the cells to the membrane. Its receptors include eight different integrins, dystroglycan and other non-integrin molecules. The integrin receptors bind to specific sequences of the α -chain. The structure of laminin is shown in figure 1.13 (Shay et al., 2008).

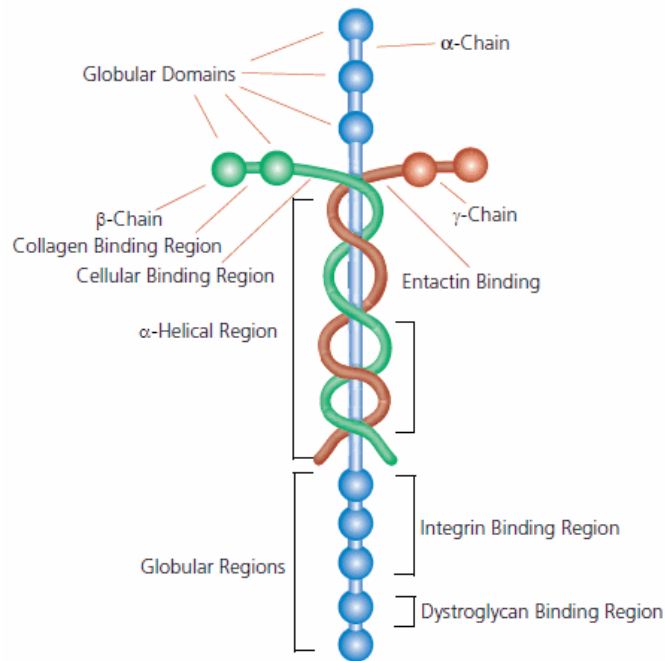


Figure 1.13: A schematic overview of the protein laminin (Sitterley, 2008).

Laminin-1 has been observed to play a role in olfactory development in earlier studies and is expressed *in vivo* by OECs. *In vitro* it stimulates ORN migration and promotes axon extension. During glomerular development in mice the OECs express laminin-1 in all regions of the olfactory pathway. It has also been observed that laminin-1 is expressed before HSPGs and Tenascin-R during development (Shay et al., 2008).

Several domains and peptide sequences in the laminin protein are shown to promote axon growth *in vitro*. Some examples are P1543 peptide, YIGSR peptide, IKVAV peptide and p20 peptide. When NB2a neuroblastoma cells from mouse were cultured on discs with three different concentrations of YIGSR peptide conjugated onto alginate, it was shown that the adhesion of cells did not follow the increase of YIGSR concentration proportionally. Comparing to the control of native alginate, an increase of peptide concentration from 0.5 mg/g alginate to 1 mg/g alginate prompted an increase of cell adhesion from 9,5% to 44%. When comparing 1mg/g peptide concentration to 2mg/g peptide concentration, the cell adhesion percentage only increases from 44% to 63%. It was deduced that the minimum critical ligand density was represented somewhere between the two lowest concentrations. A disc coated with regular laminin produced a cell adhesion percentage of 63%, comparable to the disc with the highest YIGSR concentration (Dhoot et al., 2004).

When laminin was coated onto the alginate dish it displayed much lower ability to promote axonal growth, compared to when coated onto a tissue culture dish and treated with differentiation media. This suggests that the active sites that promotes axonal growth is either masked by alginate or that the alginate poses steric hindrance to axonal growth. The peptide density also seemed to have an impact on the length

of the axons, as the highest concentrations displayed the longest axons (Dhoot et al., 2004).

Laminin has a great affinity for Ca^{2+} ions, which may cause the gel to dissolve over time. It is also a large protein that may occlude diffusion of substances out of alginate microbeads (Dhoot et al., 2004).

It has been shown that extracellular matrix, via the $\beta 1$ integrin component of laminin receptors, is important in myelination (Barnett and Chang, 2004).

2. Materials and methods

2.1. Alginate characteristics

The characteristics of the different alginate types that were used in this project are listed in table 2.1 and the alginates are more closely described below.

Ultra Pure Low Viscosity Guluronic acid (UP-LVG) sodium alginate

UP-LVG alginates are ultra purified and contains at least 60% G monomers. It can be modified in several ways, and is approved for use in pharmaceutical, biomedical, biotechnology and tissue engineering applications. The term ultra pure implies that the endotoxin levels in the alginate are <100EU/g (Systems, 2012). The UP-LVG alginate used in this project originated from batch FP 603-04 and was purchased from NovaMatrix.

Peptide grafted alginate I

Mannuronan (batch 512-215-01 TP) was isolated from an epimerase negative mutant of *Pseudomonas fluorescens* and modified by coupling GRGDSP peptide (RGD peptide) onto the C5 carboxylic group on mannuronic acid monomers using carbodiimide chemistry, yielding 0.2% grafted RGD peptide.

The grafted alginate was epimerized by the mannuronan from C-5 epimerases AlgE4 and AlgE6 from *Azotobacter vinelandii* produced in *Hansenulia polymorpha* and *Escherichia coli*, respectively. AlgE4 created MG-blocks and AlgE6 created G-blocks. A similar mannuronan without peptide was also modified with these epimerases and used as a non-peptide coupled reference. The composition of both alginates can be found in table 2.1. The alginates were dissolved in 0,3 M mannitol and stored in a refrigerator, and sterile filtered before utilized in this project. Kristin Karstensen made this alginate during her master thesis (Karstensen, 2010).

Alginate mixed with gelatin

Alginate was mixed with gelatin in three concentrations (0.5%, 1.0% and 2.0%) to establish whether gelatin could resemble the extracellular matrix (ECM) molecule collagen in capsules, and determine if it induced any changes in cell morphology and/or viability.

Freeze dried UP-LVG alginate (batch FP 603-04) was dissolved in sterile water to 1.0% concentration by stirring with a magnet. Gelatin (Gelatin type A, Gelita®, Pigskin gelatin, 260 Bloom, 628305, provided by Ingvild Haug) was also dissolved in sterile water heated to approx. 40°C and stirred by a magnet until it dissolved. The gelatin was kept at 40°C to avoid gelation until mixed with alginate.

Both dissolved gelatin and dissolved alginate was mixed with stock solution containing 200 mM NaCl and 0,6 M mannitol, before the gelatin and alginate were

mixed together to yield three different concentrations of gelatin in three batches; 0.5% gelatin, 1.0% gelatin and 2.0% gelatin. All three batches had a final concentration of 1.0% UP-LVG alginate, 60 mM NaCl and 0,18 M mannitol, and pH was adjusted to 7,2-7,4 before sterile filtering and storage in sterile test tubes.

Alginate mixed with ECM molecules

Alginate was mixed with four different ECM molecules; collagen, hyaluronic acid, fibronectin and laminin. Olfactory ensheathing cells (OECs) were encapsulated in these mixtures with the goal of observing any morphological changes and/or viability changes, as well as to monitor the capsules' shape and stability throughout the experiment.

2 mg collagen (powdered collagen from rat tail, purchased from SigmaAldrich, product no: C7661) was solved in 0.5 mL 0,01M HCl and stirred by magnet until the collagen had dissolved (approx. 2 hours). The solution was sterile filtered and stored in a sterile tube in a refrigerator until mixed with alginate.

2 mg hyaluronic acid (lyophilized hyaluronic acid sodium salt from bovine vitreous humor, purchased from SigmaAldrich, product no: 53728 FLUKA) was dissolved in 0.5 mL sterile water by magnet stirring. The solution was sterile filtered and stored in a sterile tube in a refrigerator until mixed with alginate.

1 mg fibronectin (lyophilized bovine plasma fibronectin, purchased from Invitrogen, cat.no: 33010.018) was solved in 0.25 mL sterile water by magnet stirring. The solution was sterile filtered and stored in a sterile tube in a refrigerator until mixed with alginate.

0,024 g HEPES (hydroxyethyl piperazineethanesulfonic acid) buffer was added to 4 mL 1,2% UP-LVG alginate solution to a concentration of 25 mM HEPES and 1,2% alginate. The pH was adjusted to pH: 7,2-7,4 with 1 M NaOH.

0.25 mL of each protein solution described above was mixed with 0,75 mL alginate solution, yielding three different batches of 1 mL ECM molecule-alginate mix.

1 mg laminin (natural mouse laminin, purchased from Invitrogen, cat.no: 23017-15) in 1 mL 50mM Tris-HCl buffer (pH: 7,4) with 0,15 M NaCl were stored in a sterile test tube until mixed with UP-LVG alginate to yield 0.9% concentration of alginate and 1mg/mL laminin. The laminin-alginate mix was sterile filtered before use.

All ECM-molecule-alginate mixes had a final ECM-molecule concentration of 1mg protein per mL 0,9% alginate.

Sulphated alginate

Sulphated alginate produced by Øystein Arlov was included in this experiment because it was hypothesized that the sulphated alginate would resemble the sulphated ECM protein heparin, and to a lesser degree HSPGs. The alginate had an

estimated sulphation percentage of 1-2,5% per monomer and consisted of MG-blocks. 4 mg of the freeze-dried alginate was dissolved in 0.25 mL sterile water and sterile filtered before it was stored in a sterile test tube until mixed with 1,2% alginate.

0.25 mL of sulphated alginate was mixed with 0,75 mL UP-LVG alginate buffered with 25mM HEPES and pH adjusted to pH: 7,2-7,4 with 1M NaOH. The final concentration of sulphated alginate was 1 mg per mL 0.9% UP-LVG alginate.

Peptide grafted alginate II

Ultrapure polymannuronan from NovaMatrix (Ref. H3:512-216-01TP, $F_M = 1$) was coupled with GRGDYP-peptide by carbodiimide chemistry, yielding approximately 0.1-0.4% grafted RGD peptide. The RGD peptide graft percentage is probably nearer 0.4%, as measured by ^1H NMR spectroscopy (personal communication, Birgitte McDonagh, 10.05.12)

High molecular mass mannuronan from epimerase-negative mutant of *P. fluorescens* was produced by SINTEF (batch: 206-011-01-TP, $F_M = 1$).

Polymannuronan from this latter source was used as a non-peptide coupled reference.

The epimerase AlgE4 from *H. polymorpha* was used to introduce alternating MG-blocks to while the epimerase AlgE6 from *E. coli* was used to insert G-blocks in both alginates described above. The samples were filtrated by active coal and dialysis was performed in sterile water until the conductivity was below 2micropμ Siemens. The pH was adjusted to 7.0 and the samples were freeze-dried. This work was performed by Birgitte McDonagh.

Table 2.1: The characteristics of the different alginate types that were used in this project.

Composition Alginate									
	F_G	F_M	F_{GG}	$F_{MG/GM}$	F_{MM}	$F_{GG/MMGG}$	F_{MGM}	F_{GGG}	$N_{G<1}$
UP-LVG*	0,670	0,330	0,550	0,120	0,21	0,050	0,090	0,500	12,0
Alg Epi RGD I**	0,550	0,450	0,200	0,350	0,10	0,400	0,340	0,160	5,0
Alg Epi I **	0,520	0,480	0,160	0,360	0,13	0,040	0,340	0,120	4,0
Alg Epi RGD II***	0,340	0,660	0,059	0,280	0,39	0,023	0,280	0,032	3,0
Alg Epi II***	0,500	0,500	0,110	0,390	0,11	0,038	0,500	0,079	4,0
Sulphated alginate****	0,47	0,530	-	1,000	-	-	1,000	-	1,0

* Given by Wenche Strand

** Given by Kristin Karstensen

*** Given by Birgitte McDonagh

**** Given by Øystein Arlov

2.2. Cell purification and culture

Experimental: OECs were purified from the olfactory bulb of neonatal rats (n=5-6) at P7 or P8 by enzymatic digestion in L-15 (Leibovitz) medium (Sigma), incubation in

O4 (IgM at 1:4) and anti-galactocerebroside (IgG3 at 1:2) primary antibodies followed by goat anti-mouse IgM phycoerythrin and goat anti-mouse IgG3 fluorescein secondary antibodies (1:100, Southern Biotech, Cambridge, UK) and FACS (Becton Dickinson, Oxfordshire, UK) sorting, selecting for O4-positive and galactocerebroside-negative cells. The above work was performed by Ioanna Sandvig, PhD, Department of Circulation and Medical Imaging, NTNU.

Primary cells were plated on PLL-coated cell culture flasks (BD Biosciences) and fed with OEC media made with DMEM-Glutamax (GIBCO) supplemented with 250 $\mu\text{L}/\text{mL}$ gentamicin (GIBCO), 41.6% SATO media, 5.5% FBS (Autogen Bioclear), 2.7% FGF (Peprotech), 0.27% Heregulin (Fischer Scientific), and 0.05% Forskolin (Sigma). The cells were maintained at 37°C with 7% CO₂ and passaged at confluence.

Cells were harvested by trypsinisation, placed in cryotubes at approx. 1.5-1.8 million cells/mL of freezing media (made with 5 mL FBS, 4 mL DMEM and 1 mL DMSO (Fischer Chemicals)) and stored at 80°C for a couple of days, before being transferred into a liquid nitrogen freezer. Frozen cells were rapidly thawed in a water bath at 37°C, suspended in 4 mL FBS 10% (made with 22.5 mL DMEM, 2.5 mL FBS and 125 μL L-glutamine (Gibco)), and centrifuged at 310 G. After centrifugation, the supernatant was removed and the cells resuspended in OEC media before encapsulation or culture.

The above work was performed in collaboration with Ioanna Sandvig, PhD, Department of Circulation and Medical Imaging, NTNU.

2.3. Gelling solution

Experimental: Two gelling solutions were utilized during this project, with and without barium ions. The gelling solution containing Ba²⁺ ions produce more stable gels as the high G alginate has stronger affinity to Ba²⁺ ions than calcium ions (Smidsrod and Skjak-Braek, 1990). On the downside, Ba²⁺ ions are cytotoxic and it is not preferable if the capsules are to be transplanted *in vivo* (Morch et al., 2006). The capsules made with gelling solution containing Ba²⁺ also proved difficult to dissolve with citrate with the aim of performing RNA extraction from the cells trapped inside the capsules. Also, the epimerized alginate utilized in this project is engineered to be gelled with only Ca²⁺ as gelling ion.

It was therefore decided to make capsules with gelling solution with only calcium ions, to avoid toxicity and enable the capsules to be dissolved by citrate.

Gelling solution with barium ions

CaCl₂ (50 mM), BaCl₂ (1 M), HEPES buffer (10mM) and mannitol (0,15 M) were dissolved in 2000 mL sterile water by stirring with a magnet. The pH was adjusted to 7,2-7,4 with 10M/5M NaOH in sterile water. The solution was filter sterilized by vacuum filter into a sterile plastic bottle and kept in RT until used.

Gelling solution without barium ions

CaCl₂ (50 mM), HEPES buffer (10mM) and mannitol (0,15M) were dissolved in 2000 mL sterile water by stirring with a magnet. The pH was adjusted to 7,2-7,4 with 10M/5M NaOH in sterile water. The solution was filter sterilized by vacuum filter into a sterile plastic bottle, and kept in RT until used.

2.4. Encapsulation of OECs

Experimental: Twelve encapsulations of OECs in different types of alginates were performed during the project, and they are summarized in table 2.2 below. The basic protocol for encapsulation is described in the following paragraph, with deviations from protocol stated beneath.

Table 2.2: Overview of the different alginates and cell concentrations used in the project. Deviations from protocol are indicated with x in the last column, and are described below.

Experiment	Type of alginate	Cell concentration	Deviations from main protocol
A	A1: 1.8% UP-LVG	A1a: 1.5 mil/mL A1b: 3.0 mil/mL A1c: 5.0 mil/mL	
B	B1: 1.0% Alg LG Epi RGD I B2: 1.0 % Alg LG Epi I	B1a: 1.5 mil/mL B1b: 5.0 mil/mL B2a: 1.5 mil/mL B2b: 5.0 mil/mL	X
C	C1: 1.0 % UP-LVG	C1a: 1.0 mil/mL C1b: 4.0 mil/mL	
D	D1: 1.0 % UP-LVG	D1a: 1.5 mil/mL D1b: 5.0 mil/mL	
E	E1: 1.0 % UP-LVG with 0.5% gelatin E2: 1.0 % UP-LVG with 1.0% gelatin E3: 1.0% UP-LVG with 2.0% gelatin	E1: 1.5 mil/mL E2: 1.5 mil/mL E3: 1.5 mil/mL	} X
F	F1: 1.0 % UP-LVG with 0.5% gelatin F2: 1.0 % UP-LVG with 1.0% gelatin F3: 1.0 % UP-LVG with 2.0% gelatin	F1: 1.5 mil/mL F2: 1.5 mil/mL F3: 1.5 mil/mL	} X
G	G1: 0.9 % UP-LVG with laminin (1mg/mL) G2: 0.9 % UP-LVG with fibronectin (1mg/mL) G3: 0.9 % UP-LVG with hyaluronic acid (1mg/mL) G4: 0.9 % UP-LVG with collagen (1mg/mL) G5: 0.9 % UP-LVG with sulphated alginate (1mg/mL)	G1: 1.5 mil/mL G2: 1.5 mil/mL G3: 1.5 mil/mL G4: 1.5 mil/mL G5: 1.5 mil/mL	} x
H	H1: 1.0 % Alg LG Epi RGD II H2: 1.0 % Alg LG Epi II H3: 1.0 % UP-LVG	H1: 1.5 mil/mL H2: 1.5 mil/mL H3: 1.5 mil/mL	X X X

Cryotubes containing 1.5 million olfactory ensheathing cells purified from neonatal rat olfactory bulbs in 1 mL freezing media, were taken out of -80°C liquid nitrogen freezer and melted in a water bath of 37°C. Each cryotube content was transferred to 4 mL 10% FBS and centrifuged down at 310 G. The supernatant was removed and the cells were resuspended in 4 mL OEC-media before counted using Countess automated cell counter (Invitrogen).

After another centrifugation with the same settings the cells were resuspended with 0,1 mL OEC growth media.

0,1 mL cell suspension and 0,9 mL alginate were mixed in a 3 mL syringe and attached to an infusion pump. The syringe was connected to a needle through a plastic tube and the cell-alginate mix was dripped into a-gelling bath by an electrostatic bead generator.

The electrostatic bead generator was adjusted to the following settings:

Voltage: 7.0 kV

Distance between needle and gelling bath: 2.5 cm

Flow: 8 mL/hour

Needle size: 0.35 mm (one needle)

Each batch of capsules was allowed to gel in the gelling bath for approximately 7 minutes. Gelling solutions with Ba^{2+} was used in almost all experiments, exceptions are mentioned below. The capsules were filtered out of the gelling bath and washed three times with 10 mL Hanks Buffered Salt Solution (HBSS). The capsules were suspended in approximately 1 mL of HBSS and 9 mL of OEC growth media was added, giving a total volume of 10 mL of capsule suspension. The capsule suspension were transferred to 75 cm² culture flasks and cultured in 37°C with 7 % CO₂. The media was changed every other week or more often, and media was withdrawn for use in assays such as alamarBlue®, Live/dead, protein gel electrophoresis and actin/nucleus staining were replaced immediately with fresh media.

Deviations from encapsulation protocol

B: Gelling solution with only Ca^{2+} was used to gel the capsules, as the capsules are made with alginate especially designed with many of MG and G blocks to form a stable gel without Ba^{2+} ions present in the gelling solution (Morch et al., 2007).

E: The gelatin/alginate-mixes were kept in an incubator with 37°C for approximately 1 hour prior to encapsulation to prevent the gelatin to gel.

F: The gelatin/alginate mixes and gelling solution were kept in heated water (approx. 40°C) to prevent the gelatin to gel. The plastic tube was isolated with cotton and aluminium foil with the aim of preserving the elevated temperature for as long as possible.

G: 0.9% alginate concentration.

H (all): Gelling solution with only Ca^{2+} was used to gel the capsules.

H1: The capsules became very small and had to be centrifuged for 2 minutes at 800 RPM before washing, instead of filtered.

H2: As batch H1 consisted of very small capsules and the alginate used in H2 were the same as the alginate used in H1, but without RGD peptide, it was attempted to avoid such small capsules in batch H2. This was partially avoided by reducing flow time to 7,0 mL/hour and voltage to 5,8 kV.

2.5. alamarBlue®

Principle: alamarBlue® (produced by Invitrogen) is an assay for quantitative measurement of cell proliferation, viability and/or cytotoxicity. It is an oxidation-reduction sensitive dye, which fluoresces and changes colour in response to growth and inhibition of growth. The active ingredient of alamarBlue® is resazurin, a non-toxic, non-fluorescent and cell permeable compound. Live cells have a natural reductive power that converts resazurin into a fluorescent molecule called resorufin. Viable cells continue to do so over time, which enables a quantitative measurement of viability and cytotoxicity. The amount of fluorescence produced is thus proportional to the number of living cells (Page et al., 1993).

Both fluorescence and absorbance measurement instrumentation can be used to collect data, however, fluorescence is considered to be the more sensitive. Absorbance is measured at 570 and 600 nm (Page et al., 1993).

Experimental: Different protocols of alamarBlue® assay were tested during this study, as method 1 (described below) did not work adequately for all experiments. The different methods are described below.

2.5.1. Method 1- OECs encapsulated in 1.8% UP-LVG alginate

Five parallel samples of capsules and media estimated equal to 5000 cells were taken from each culture flask, and transferred to a clear-bottomed 96 well plate. Media from the corresponding culture flask were added up to a volume of 180µL in each well.

Five parallels of 180µL media controls from each culture flask were transferred to the well plate. As a final control, five parallels of new unused OEC culture media were added to the well plate. 18µL of alamarBlue® reagent was added to each well and the plate was incubated in room temperature for four hours.

The fluorescence intensity was measured by a multilabel microplate reader (Victor Wallac, Perkin Elmer) at 535/590 nm.

2.5.2. Method 2 - OECs encapsulated in 1.0% Alg Epi RGD I

Certain difficulties were experienced when applying method 1 to the cells encapsulated in 1.0% alginate gel. The fluorescence values turned out negative when subtracting the blank control sample values from the sample value. It was thus decided to increase the incubation time from 4 to 6 hours and check whether a prolonged incubation time would enable the cells to reduce the reagent sufficiently. After six hours of incubation the fluorescence values were negative for the lower cell concentrations (1.5 mil/mL).

2.5.3. Test round - OECs encapsulated in 1.0% UP-LVG alginate.

The negative results obtained from the alamarBlue® assay using Method 2 spurred a test round where three different protocols were tried and their results compared. All three methods were performed on two concentrations of OECs encapsulated in 1.0% UP-LVG alginate; 1.0 mill/mL and 4.0 mil/mL.

Method 3 – test round

The third method was basically the same as method 2, except that the samples were incubated in 37°C and 7% CO₂ for four and six hours. The fluorescence values were measured after four and six hours by a multilabel microplate reader (Victor Wallac, Perkin Elmer) at 535/590 nm.

Method 4 – test round

A volume of media and capsules corresponding to 50 000 cells were taken out from each culture flask and placed in transparent 6-well plate. Media from the corresponding culture flask was added to a total volume of 5,1 mL in each well. 0.51 mL of alamarBlue® reagent were added to each well in the 6-well plate.

Five parallels of control samples with a volume of 180 µl were withdrawn from each culture flask and placed in a 96 well plate. The control samples were each added 18 µl alamarBlue® reagent.

Both the 6-well plate containing capsules and media and the 96-well plate containing controls were incubated in 37°C and 7% CO₂.

Five samples of 180 µl from each batch in the 6-well plate were withdrawn and placed in a 96-well plate at three time points; 2, 4 and 6 hours after incubation. The fluorescence values of both samples and controls were measured by a multilabel microplate reader (Victor Wallac, Perkin Elmer) at 535/590 nm.

Method 5 – test round

Five parallels of 180 µl control samples were withdrawn from the media supernatant in each culture flask and placed in a 96-well plate. 18µl alamarBlue® reagent was added to each well sample.

After withdrawal of control samples, 1 mL of alamarBlue® reagent were added directly to the culture flasks (total volume in flask: 10 mL). The control samples and the culture flasks were incubated in 37°C and 7% CO₂.

Five parallels of 180 µl were withdrawn from the flasks at three time points; 2, 4 and 6 hours. The samples were placed in a 96-well plate and the fluorescence intensity was measured by a multilabel microplate reader (Victor Wallac, Perkin Elmer) at 535/590 nm. The control samples were measured at the same time points.

2.6. MTT assay

Principle: The MTT assay was developed by Tim Mossman in 1983 and is a versatile and quantitative method for measuring live cells quantitatively in homogenous cell cultures. The light yellow tetrazolium salt MTT (3-(4,5-dimethylthiazol-2-yl) 2,5-diphenyl tetrazoliumbromide) contains a tetrazodim ring that is cleaved by various dehydrogenases in active mitochondrias, giving the insoluble dark blue crystal formazan. Adding DMSO will dissolve the formazan crystals and an absorbance measure device can measure the resulting colored solution. As activated cells produce more formazan than dormant cells, the assay can be used to distinguish between active and dormant cells as well as live and dead cells (Mosmann, 1983).

Experimental: In this project the MTT assay was performed to see if the results corresponded with the results obtained by the alamarBlue assay. Both assays were performed on OECs encapsulated in 1.0% UP-LVG with a concentration of 1.5 mil cells/mL alginate, on day 8, day 13 and day 21.

Part I: Three parallels of 33 μ L capsules suspended in media were placed in three wells in a 24 well plate (PerkinElmer), EACH containing 40 capsules on average. 1 mL media from the related culture flasks and 100 μ L of MTT solution (5 mg MTT/mL PBS, Invitrogen and Gibco®, respectively) was added to each well and the plate was incubated at 37°C and 7% CO₂ for four hours. After incubation the capsules were washed three times with 1 mL 0.9% NaCl and sealed with tape and stored in 1 mL 0.9% NaCl in a refrigerator.

Part II: The liquid was pipetted off, and the number of remaining capsules were counted. 400 μ L of DMSO (Fischer Chemicals) were added to the wells before incubation in RT for 1 hour. After incubation 50 μ L of Sorensen's solution (0,1 M glycine and 0,1 M NaCl adjusted to pH 10.5 by 1 M NaOH) was added to each well. Two parallels of 200 μ L from each well were transferred from the 24-well plate onto a 96 well plate before measuring the absorbance at 570nm by an iMark Microplate Absorbance Reader (BioRad).

2.7. Live/Dead

Principle: The LIVE/DEAD Viability/Cytotoxicity Assay Kit (Molecular Probe) is an assay that simultaneously shows live and dead cells, utilizing two fluorescent probes. The polyanionic non-fluorescent dye calcein AM is enzymatically converted to the intensely fluorescent calcein in live cells due to their intracellular esterase activity. This enzyme is not active in dead cells. Calcein is well retained in live cells and fluoresces in an intense green color (ex/em 495nm/515nm). Ethidium homodimer-1 (EthD-1) enters cells with damaged cell membranes and binds to the nucleic acids. This binding causes a 40-fold enhancement of bright red fluorescence (ex/em 495/635). EthD-1 is excluded by the intact plasma membrane of live cells. There is virtually no background fluorescence because the dyes are not fluorescent before interacting with cells. Thus, both live and dead cells are dyed simultaneously and the

analysis is performed using a confocal microscope as shown in figure 2.1 (Invitrogen, 2005).

Experimental: A Live/Dead Viability Kit was purchased from Invitrogen. A working solution of 3 mL PBS (Gibco®), 0,8µL calcein AM and 1,3µL ethidium bromide was made and vortexed to ensure proper mixing. The work solution was stored in the refrigerator for no more than a week. 200 µL of pure PBS were added to capsules (≈ 0.5 mL) in a cryotube (Nunc cryotubes™) followed by 200µL work solution.

A volume of 200µL from each batch was transferred to a glass bottom microwell dish (MaTek Corporation) and examined with laser scanning confocal microscope (LSM 510 by Carl Zeiss). Calcein was excited with an argon laser at 488 nm and EthD-1 was excited with a helium-neon laser at 543 nm. A 10x water immersion objective was used during analysis.

The same Live/Dead protocol was followed in all experiments, and the Live/Dead ratios were qualitatively estimated from the pictures taken with CLSM.

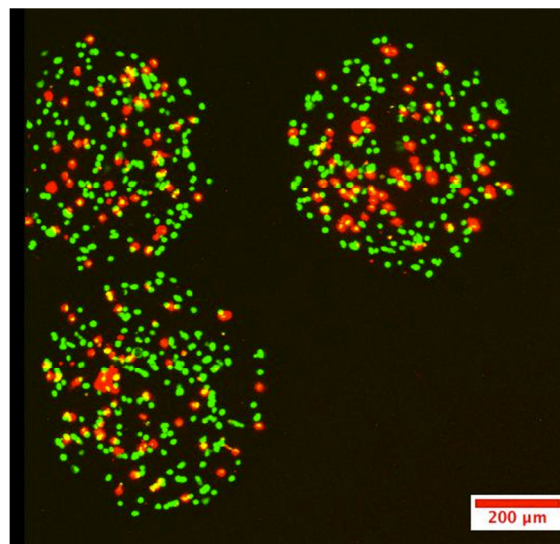


Figure 2.1: The green cells are live cells, while the red cells are dead cells.

Settings for the CLSM:

Scan Mode; Plane, original data, multi track, 8 bit

Objective; C-Apochromat 10x/0.45W

Beamsplitters; MBS-1: HTF UV/488/543/633

DBS1-1: Mirror

DBS1-2: Mirror

NDD MBS1-1: None

MBS-2: HTF UV/488/543/633

DBS1-2: Mirror

DBS2-2: NFT 545

NDD MBS1-2: None

MBS-3: HTF UV/488/543/633

NDD MBS: None
Lasers; Argon (488nm)
HeNe (543nm)
Filters; BP 505-530, LP 650
Pinholes; 199 μ m

2.8. Actin filament and nucleus staining using Phalloidin and DRAQ5

Principle: Phalloidin is a probe that binds specifically to filamentous actin. It is isolated from the deadly *Amanita phalloides* mushroom and it is a bicyclic peptide. Phalloidin has virtually equal binding properties with F-actin from different species, both plants and animals with high selectivity and low non-specific binding. Invitrogen has conjugated the peptide to a photostable green fluorescent dye, Alexa Fluor 488® that enables both visualization and quantification of actin. Before staining, cells have to be both fixated and permeabilized. Alexa Fluor 488® is excitable at 495 nm and has emission at 518 nm (Wulf et al., 1979).

Deep red fluorescent bisalkylaminoanthraquinone (DRAQ5) has a high affinity for DNA and is capable of entering both live and dead cells. The fluorescent dye is 100% synthetic and derived from intercalating cytostatika. It is excitable at 646nm and emissions at 681nm. Coloring of DNA takes place in a matter of seconds, and is enhanced by incubation at 37°C. DRAQ5 is classified as cytotoxic, and not suitable for experiments where long term cell viability is a prerequisite Figure 2.2 depicts an example of an OEC that has been encapsulated in UP-LVG alginate and stained with phalloidin (green) and DRAG5 (red) (Smith et al., 2004).

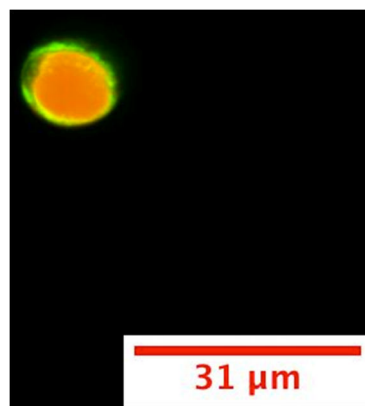


Figure 2.2: An olfactory ensheathing cell stained with phalloidin (green) and DRAQ5 (red). The green color represents F-actin, while red stains DNA. (Figure taken from this project).

Experimental: Alexa Fluor 488® phalloidin was purchased from Invitrogen. DRAQ5™ was purchased from Biostatus Limited.

50 μ L of capsules in media suspension were pipetted into an Eppendorff tube and the capsules were allowed to sediment before the media was pipetted off. The capsules were washed with 100 μ L of 0.9% NaCl solution with 2 mM CaCl₂, before

100 μ L of 0.9% NaCl solution with 2 mM CaCl₂ with 3,7% FAH were added as fixation media. The Eppendorff tubes were incubated in 37°C with 7% CO₂ for 15 minutes.

Excess fixation media was removed by washing 3 times with 100 μ L 0.9% NaCl solution with 2 mM CaCl₂, before 50 μ L 0,05% Saponin in 0.9% NaCl solution with 2 mM CaCl₂ was added. The samples were then incubated in RT for 10 minutes.

The two dyes were added, Phalloidin (25 μ L) and DRAQ5 (1 μ L) and thoroughly mixed before the tubes were incubated for about 10 minutes in 37°C with 7% CO₂.

The capsules were washed with 100 μ L 9% NaCl solution with 2 mM CaCl₂ before imaging by a confocal microscope (LSM 510 by Carl Zeiss). The following settings were applied:

Scan Mode: Plane, original data, multi track, 8 bit

Objective: C-Apochromat 10x/0.45W, C-Apochromat 40x/1.2W, C-Apochromat 63x/1.2 W

Beamsplitters: MBS-1: HTF UV/488/543/633 DBS1-1: Mirror DBS1-2: NFT 610 NDD MBS1-1: None MBS-2: HTF UV/488/543/633 DBS1-2: Mirror DBS2-2: NFT 610 NDD MBS1-2: None MBS-3: HTF UV/488/543/633 NDD MBS: None

Lasers: Argon (488nm) HeNe (633nm)

Filters: BP 505-530 LP 650

Pinholes: 166 μ m, 212 μ m

Some changes were applied to the original protocol, which states that 0,1.0% BSA in PBS should be used as washing solution and in the fixation media. This solution proved to dissolve the capsuled before imaging and it was therefore decided to replace it with 0.9% NaCl solution with 2 mM CaCl₂, which worked satisfactorily.

The amount of DRAQ5 was reduced from 1 μ l to 0.5 μ l in the last assay (Day 20 on batch H), as it was found to have much larger intensity than Alexa Fluor 488® phalloidin.

2.9. Capsule stability

The capsule stability was tested with different solutions with the aim of assessing the gel stability and to establish which method to use if it became necessary to extract cells from the capsules, that is, how to dissolve the alginate effectively without damaging the cells.

Experimental: The capsule stability was tested with sterile water, 0.9% NaCl, MG lyase (Sigma-Aldrich®), 50 mM citrate (KeboLab AB) solved in sterile water, and 50mM ethylenediaminetetraacetic acid (EDTA, Sigma) in 10mM HEPES (Sigma) buffer solved in PBS (Gibco®).

20 μ L of capsules (batch B1a, B1b, B2a and B2b, made with gelling solution containing only Ca²⁺ ions) suspended in OEC media were placed in 300 μ L sterile

water in a 96 well plate in RT. The capsules were monitored with a light microscope at 10x magnification every 10 minutes for 30 minutes.

20 μL of capsules (batch B1a, B1b, B2a and B2b, made with gelling solution containing only Ca^{2+} ions) suspended in OEC media were placed in 300 μL sterile 0.9% NaCl in a 96 well plate in RT. The capsule stability was checked every 10 minutes with a light microscope at 10x magnification.

MG lyase enzyme (8 units/mL) solved in 1 mL PBS was added to 0.5 mL capsules (batch C1a) suspended in 4 mL OEC growth media, and incubated in 37°C and 7% CO_2 for three days.

Citrate and EDTA solutions were sterile filtrated and pH adjusted to pH: 7,2-7,4 before use.

1 mL of citrate solution (50mM in 100 mL sterile water) was added to 100 μL suspension of capsules (batch C1a) in OEC media placed in a transparent 24 well plate. The capsules were monitored in a light microscope at 10x magnification every 5 minutes for 25 minutes. For every 5 minutes without any dissolving capsules, another 1 mL of citrate solution was added to the capsules. When the volume became larger than the well could contain, the capsules were transferred to a 25 mL test tube. The capsules were checked again after 1.5 hours.

600 μL EDTA solution (50 mM in 100 mL PBS with 10 mM HEPES) was added to 100 μL capsules (batch C1a) suspended in OEC growth media placed in a 24 well plate. The capsules were monitored in a light microscope at 10x magnification after one minute.

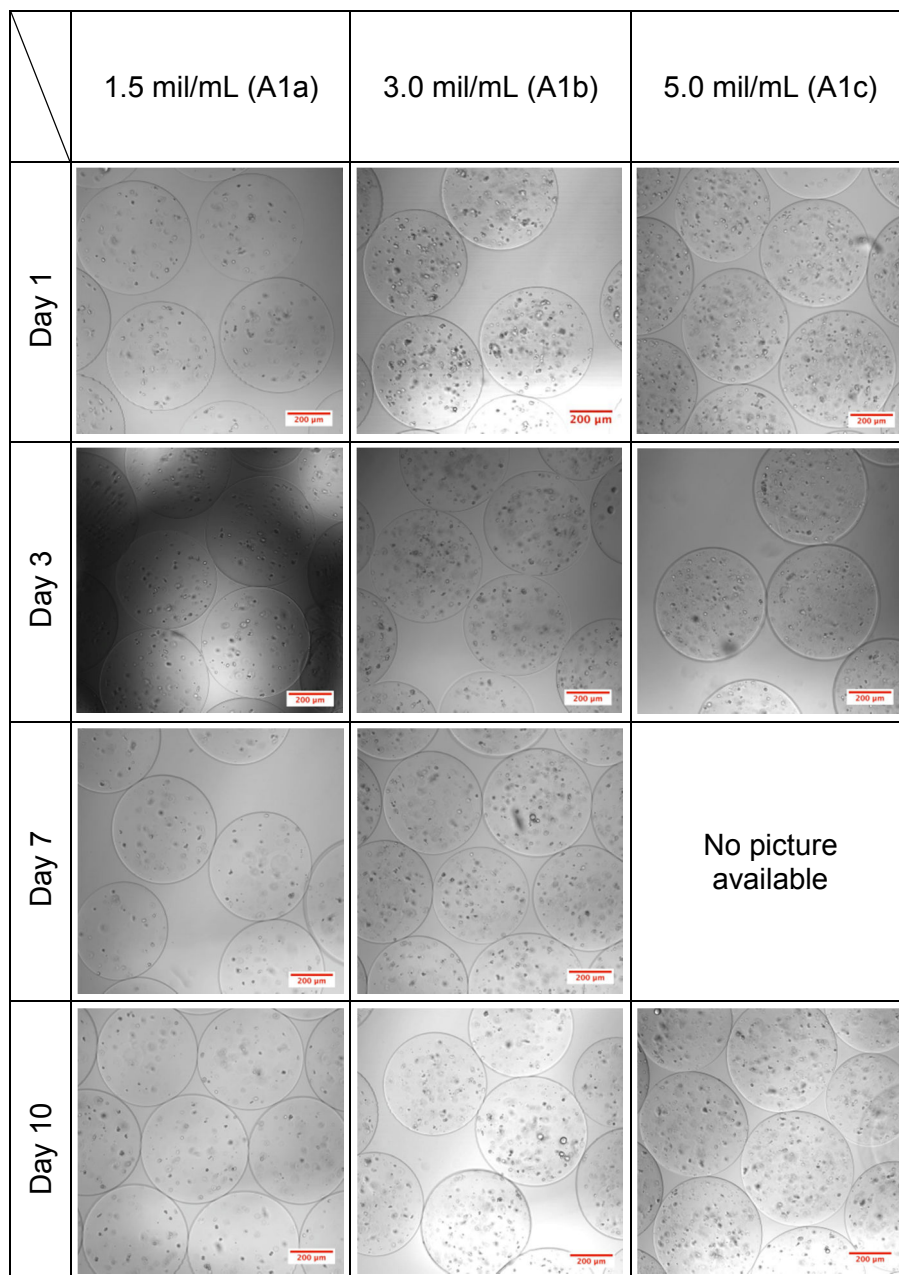
3. Results

3.1. Different concentrations of OECs encapsulated in 1.8% UP-LVG alginate

Three different concentrations of OECs were encapsulated in 1.8% UP-LVG $\text{Ca}^{2+}/\text{Ba}^{2+}$ alginate; 1.5 mil/mL, 3.0 mil/mL and 5.0 mil/mL with the aim of observing differences in cell viability related to cell concentration in the capsules. They will be denoted A1a, A1b and A1c, respectively, in accordance with table 2.2 in section 2.1.

The cells viability was measured by Live/Dead assay over a period of 14 days.

The distribution of live and dead cells was visualized by 3D Z stack projections by CLSM. Figure 3.1 displays cross sections through the equator of capsules overlaid with transmitted light.



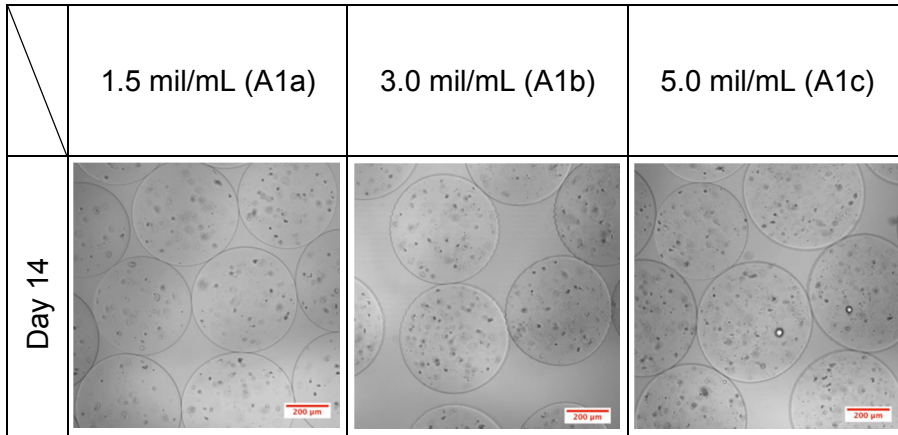
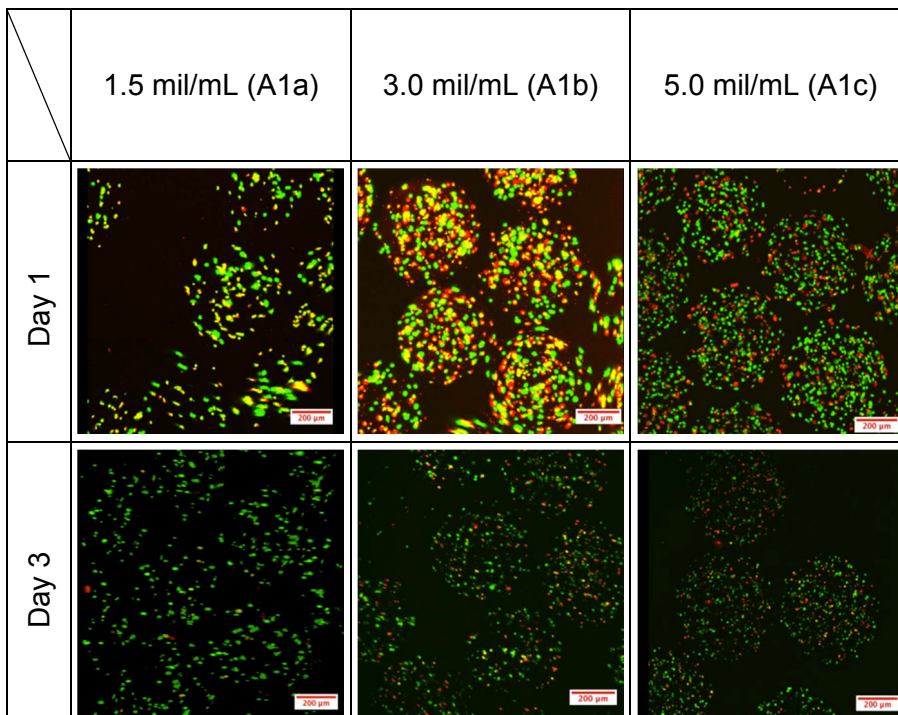


Figure 3.1: CLSM cross-sections through the equator of capsules made of 1.8% UP-LVG alginate gelled with gelling solution containing Ca^{2+} and Ba^{2+} ions, containing OECs overlaid with transmitted light. Green fluorescence indicates live cells and red fluorescence indicate dead cells. A 10x objective was used for image acquisition. The size bar is 200µm.

The capsules displayed a narrow size distribution with an approximate average diameter of 500µm. The structural integrity of the capsules remained intact throughout the experiment, with a few exceptions. These broken capsules were randomly distributed among the three different cell concentrations. The capsules retained their initial size throughout the experiment and showed no sign of swelling. The difference in cell concentration between the three batches can be clearly observed.

CLSM Z stacks 3D projections from the Live/Dead assay can be observed in figure 3.2.



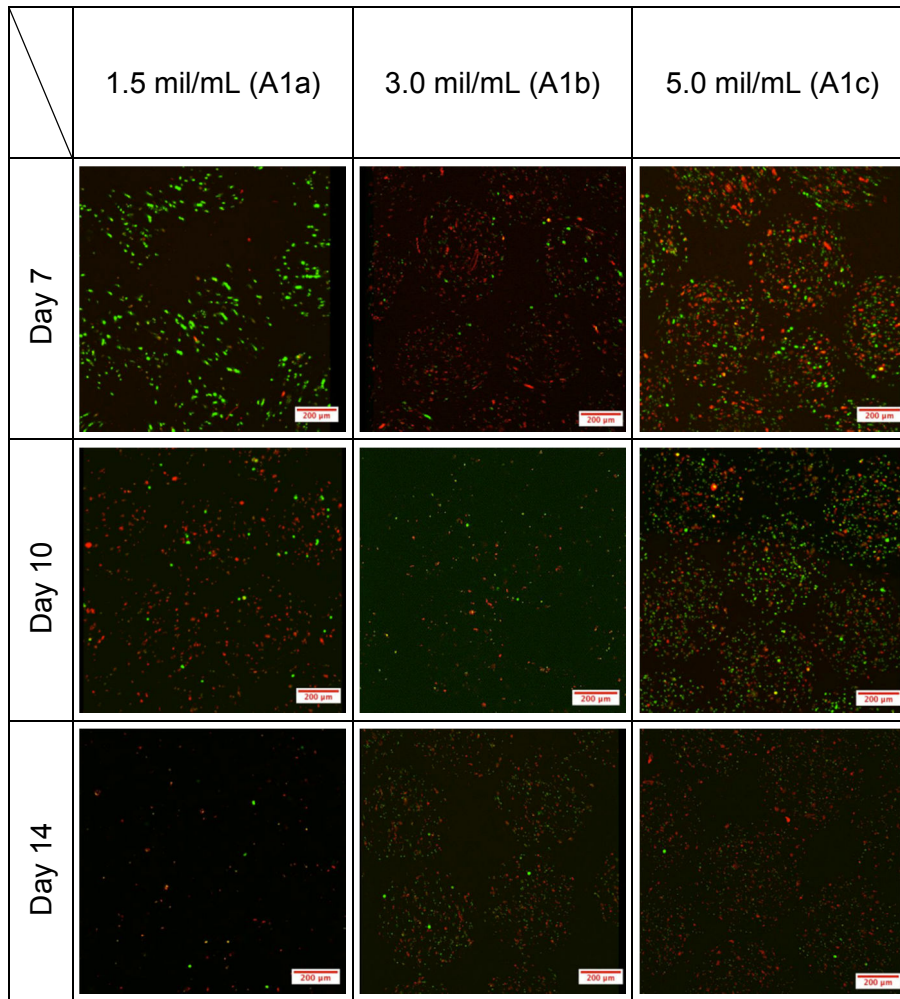


Figure 3.2: Live/dead assay. CLSM Z stacks 3D projections of OECs encapsulated in 1.8% UP-LVG alginate gelled with gelling solution containing Ca^{2+} and Ba^{2+} ions. Green fluorescence indicates live cells as opposed to red fluorescence, which indicates dead cells. Several capsules are shown in each picture. A 10x objective was used for image acquisition and the size bar is 200 μm .

At day 1 the cells in batch A1a displayed good viability with approximately 90% live cells. The A1b batch displayed lowest viability the day after encapsulation with 70% live cells, but the picture is overexposed, making the estimate inaccurate. Batch A1c had a viability of 80% at day 1.

The picture of the 3.0 mil/mL capsules at day 1 introduces an artefact, as the capsules were moving during image acquisition. The picture is also somewhat overexposed. This causes the colonies to appear more numerous and more intensely coloured than they really were.

It can be observed from figure 3.2 that the viability of the cells is declining rapidly for all cell concentrations over a period of 14 days. The estimated percentage of live cells is plotted in figure 3.3.

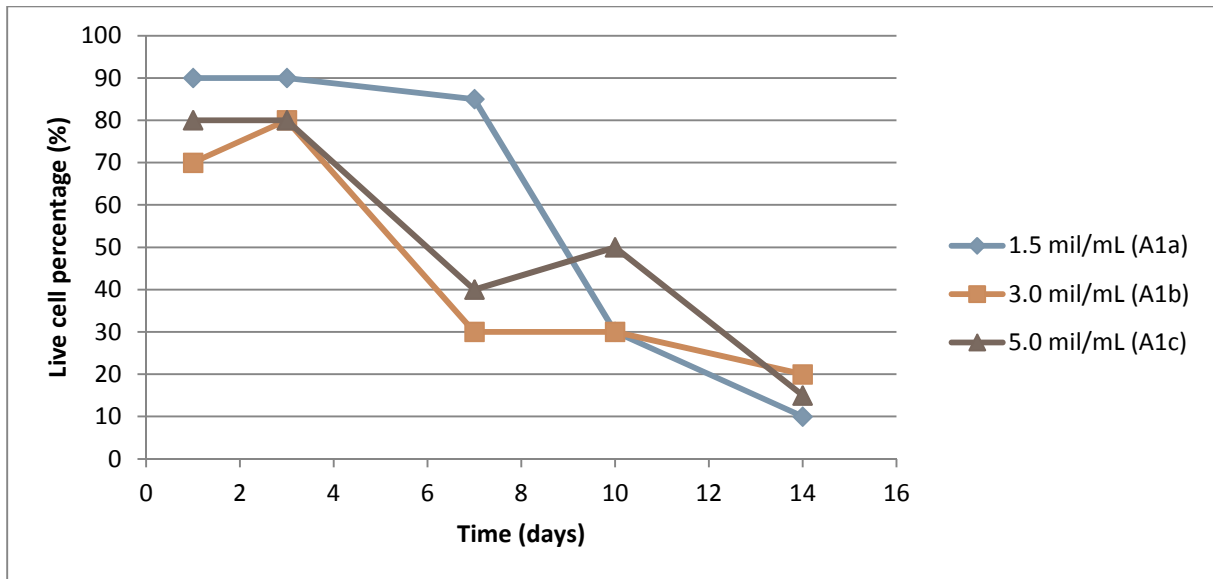


Figure 3.3: The estimated percentage of live cells in 1.8% UP-LVG capsules with different cell concentration, based on figure 3.2.

The A1a batch display a higher viability than A1b and A1c up until day 10 where it declines from an estimated percentage of 85% live cells at day 7 to 30% live cells at day 10 (fig. 3.2 and 3.3). The A1b and A1c batches seemed to decline in viability earlier than A1a, at day 7 where A1b plunged from 80% live cells to 30% live cells at day 7 and A1c went from 80% live cells to 40% live cells.

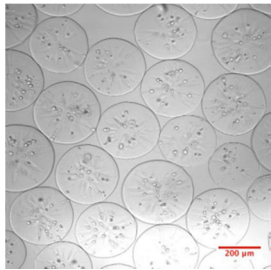
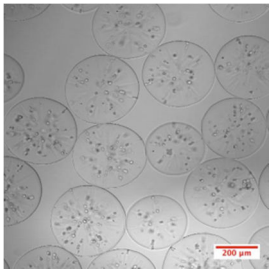
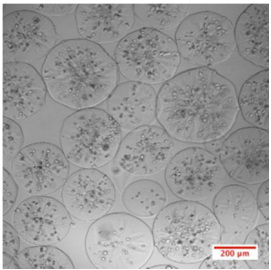
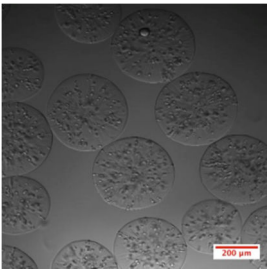
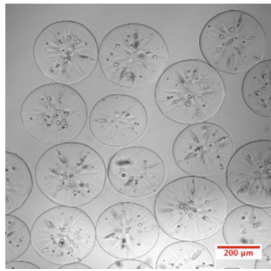
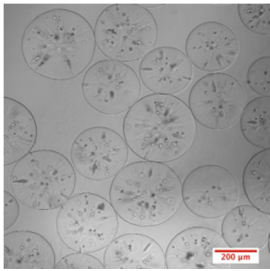
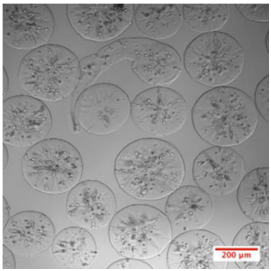
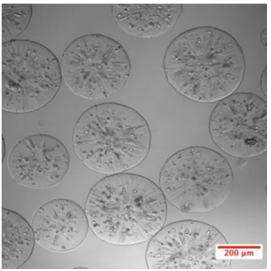
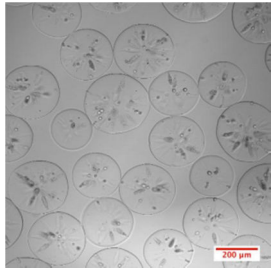
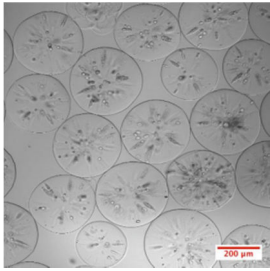
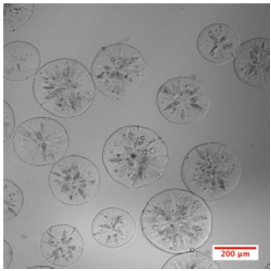
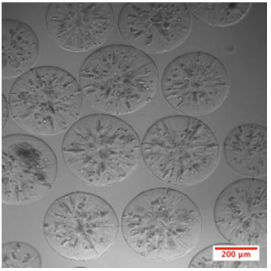
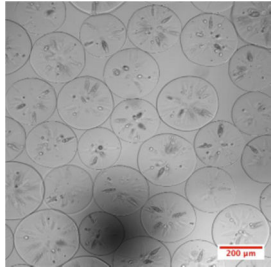
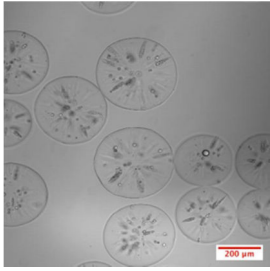
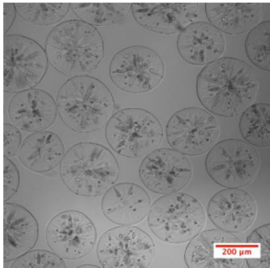
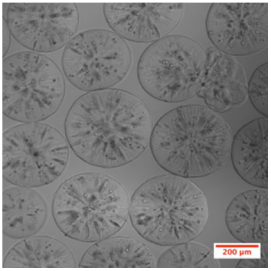
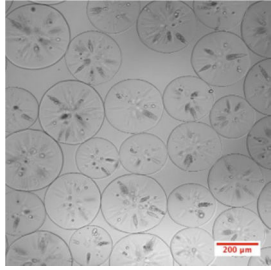
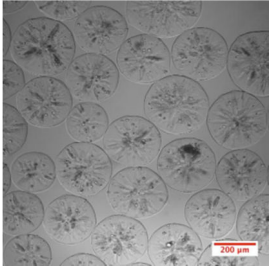
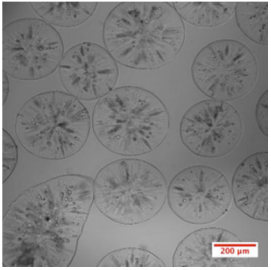
From day 7 to day 10 there was a slight increase from 40% to 50% in living cells in batch A1c, while batch A1b kept a constant percentage of 30% live cells. From day 10 to 14 all batches displayed a declined in viability and the experiment was terminated.

3.2. Encapsulation of OECs in 1.0% LG alginate grafted with 0.2% RGD peptide

1.5 mil/mL and 5.0 mil/mL OECs were encapsulated in 1.0% LG Ca²⁺ alginate epimerised with mannuronan C5 epimerases AlgE4 and AlgE6 and grafted with 0.2% RGD peptide. As a control, both concentrations of OECs were encapsulated in non-peptide grafted similar alginate. The purpose of this encapsulation was to see if the cells viability was affected by the RGD peptide grafted to alginate. Kristin Karstensen (Karstensen, 2010) observed attachment of OECs to RGD peptide in 0.2% RGD peptide grafted alginate gel 2D culture in her master project. However, no effect was observed of the RGD peptide upon OEC culture in 3D gels. She also observed a similar drop in viability upon 3D culture in 1.8% alginate concentration in these capsules. It was of great interest to see whether interaction would occur in a 3D environment in this experiment.

The cells viability was measured by Live/Dead assay over a period of 22 days, at day 1,3,7,10,14 and 22. The distribution of live and dead cells was visualized by 3D Z

stack projections by CLSM. Figure 3.4 displays cross sections through the equator of capsules overlaid with transmitted light.

	1.5 mil/mL Alg (B1a)	1.5 mil/mL Alg RGD (B2a)	5.0 mil/mL Alg (B1b)	5.0 mil/mL Alg RGD (B2b)
Day 1				
Day 3				
Day 7				
Day 10				
Day 14		No picture available		

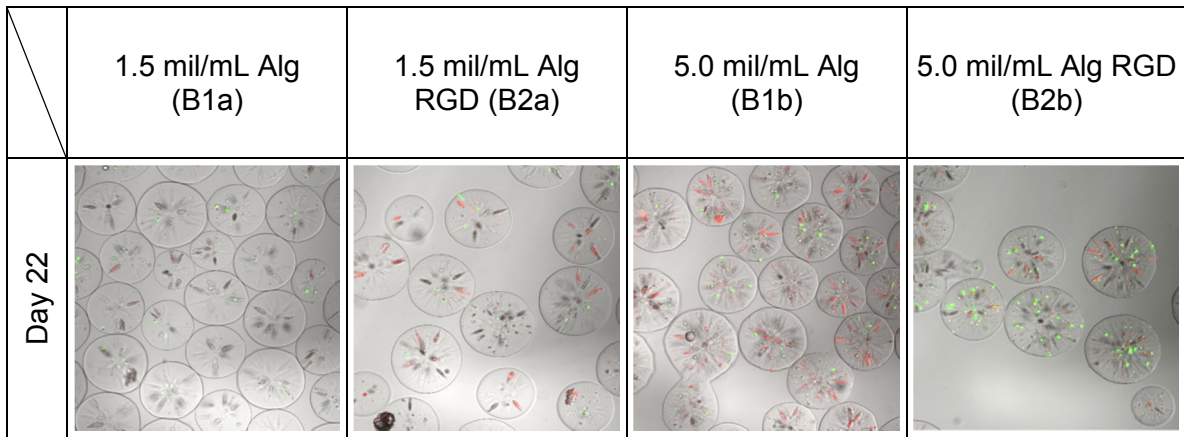
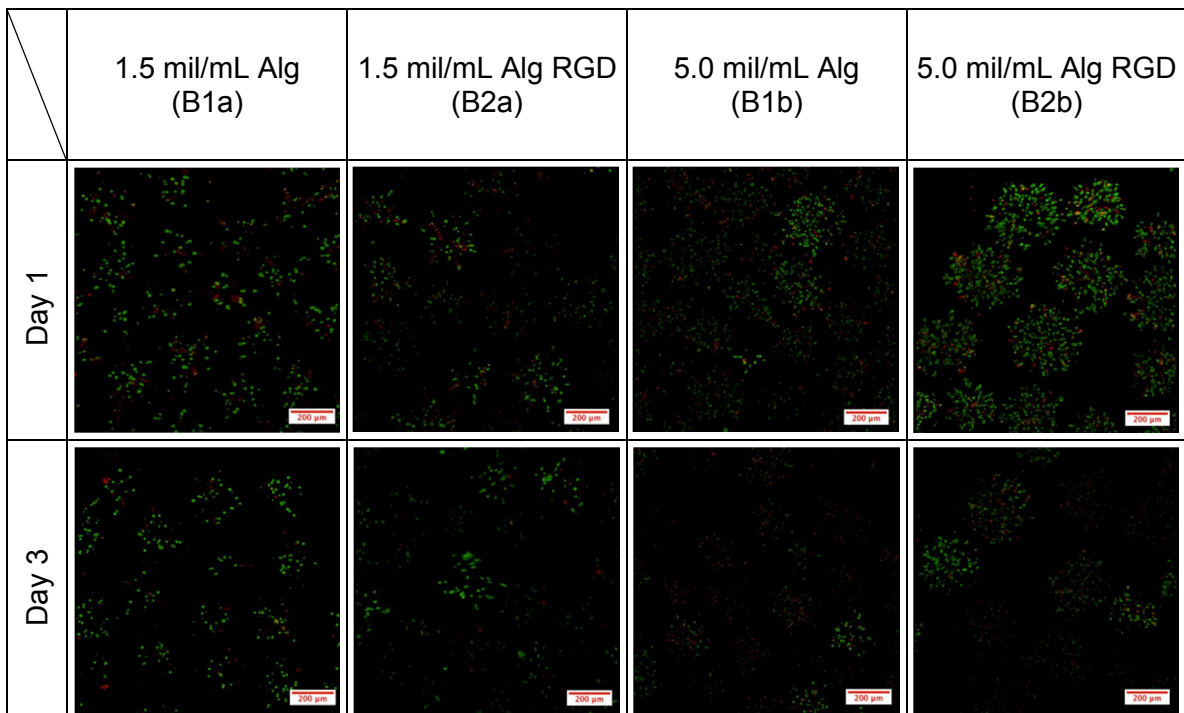


Figure 3.4: CLSM cross-sections through the equator of 1.0% epimerised Ca^{2+} alginate capsules containing OECs overlaid with transmitted light. A 10x objective was used for image acquisition. The size bar is 200 μm . Due to technical problems the pictures from day 22 lack a size bar.

The capsules displayed a larger variation in size than capsules made with 1.8% UP-LVG alginate, and capsules with a tail were observed. The capsules in this experiment were generally smaller than the capsules observed in experiment 3.1, with a diameter of approximately 350 μm on average. The capsules with 5.0 mil/mL cell concentration were perceived as larger than capsules with 1.5 mil/mL cell concentration on several occasions.

All capsules appeared stable over 22 days in culture with no observed swelling.

CLSM Z stack 3D projections are depicted in Figure 3.5.



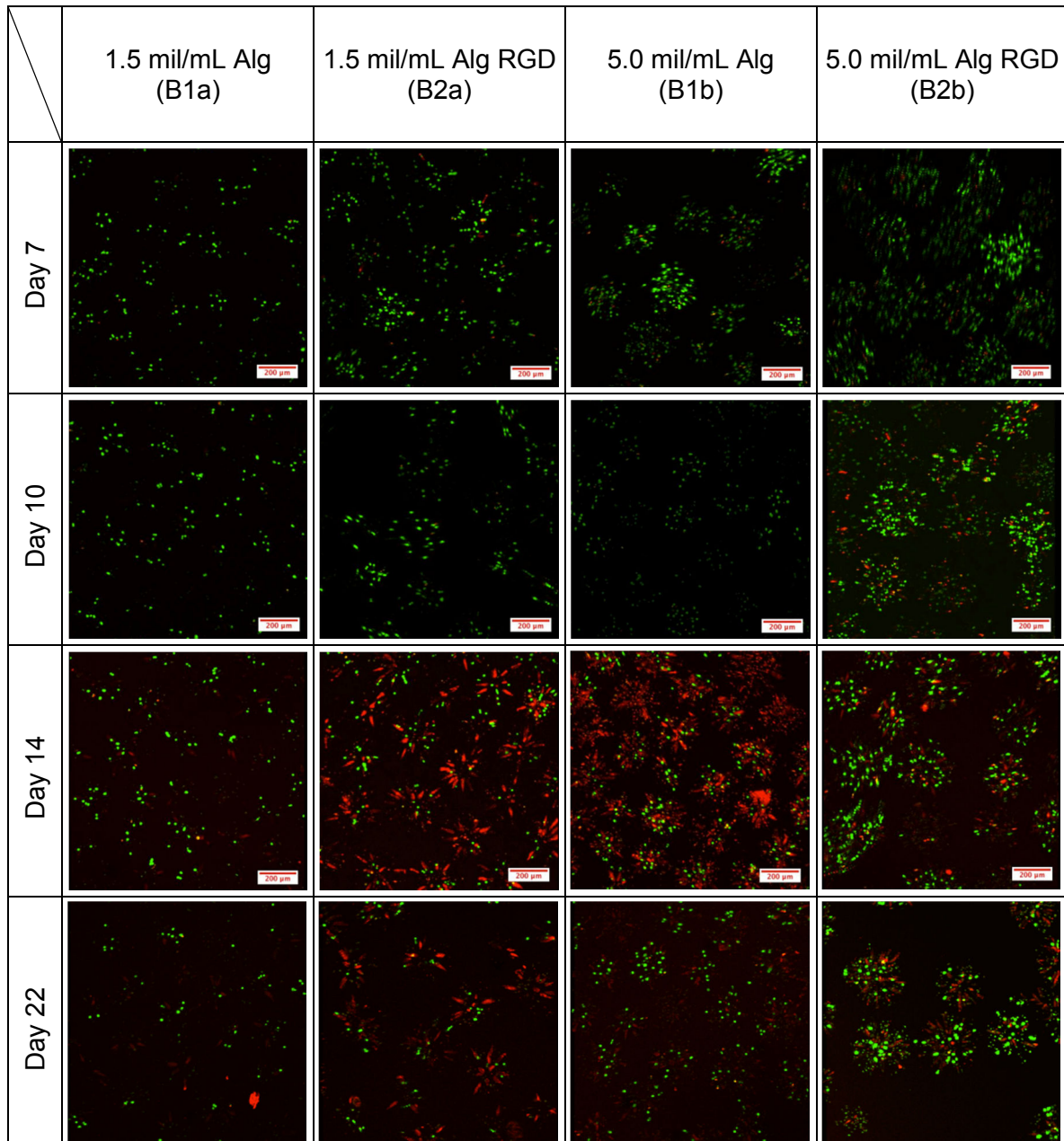


Figure 3.5: Live/dead assay. CLSM Z stacks 3D projections of OECs encapsulated in 1.0% epimerised Ca^{2+} alginate with and without RGD peptide graft. The pictures were taken at day 1, 3, 7, 10, 14 and 22 after encapsulation. Green fluorescence indicates live cells as opposed to red fluorescence, which indicates dead cells. Several capsules are shown in each picture. A 10x objective was used for image acquisition and the size bar is 200 μm .

The cells of all batches displayed very good viability at day 1 with live cell percentage > 90%. This indicated that the cells tolerated the encapsulation well. The pictures from day 1 and 2 for the B2a and B1b have low intensity, making the estimations insecure.

The viability of the cells in all batches was high (>85%) up until day 10. From day 10 to 14 many dead cells were observed in batch B2a and B1b. The dead cells were predominantly located inside the channel formations. A smaller fraction of dead cells

were observed at day 22, than day 14, especially in batch B2a and B2b. The live cells clusters seemed relatively constant in both batches in this time period. B1a displayed relatively high viability throughout the experiment, with an estimated decrease in live cell percentage from 95% to 70% after 22 days in culture as can be observed in figure 3.6. The cells in batch B2b displayed an estimated viability percentage of 50% when the project was terminated but in contrast to batch B2a and B1b the viability seemed to decline gradually, without any sudden drops.

The estimated live cell percentage is presented in Figure 3.6.

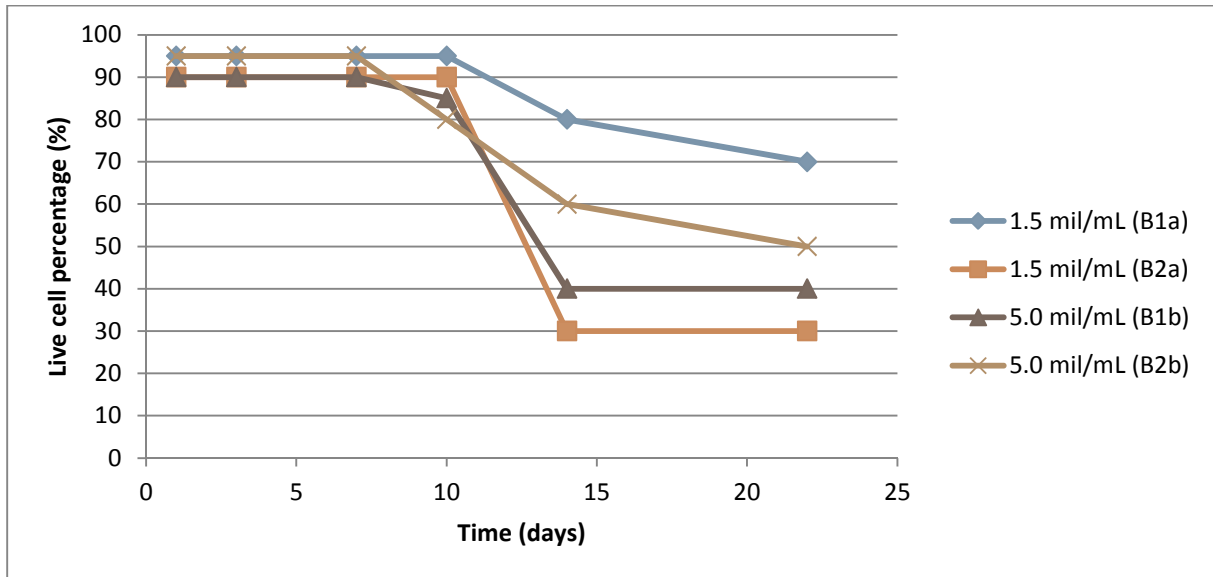


Figure 3.6: The estimated percentage of live cells in 1.0% epimerised Ca^{2+} alginate with and without RGD peptide graft capsules with different cell concentration, based on Figure 3.5.

No difference in viability between grafted (B2b and B2a) and non-grafted alginate (B1a and B1b) could be observed in this experiment. The two batches with relatively high viability were grafted and non-grafted, and consequently the two batches with low viability were also grafted and non-grafted alginate capsules. The lowest cell concentration (1.5 mil/mL) was represented on both ends of the viability scale, while the capsules with high cell concentration (5.0 mil/mL) both displayed low viability (<40%) after 22 days.

No interaction of cells with RGD peptide could be observed as changes in morphology in this experiment.

Figure 3.7 A clearly shows that most dead cells are located inside the channels, while live cells are situated in round, regular clusters. Figure 3.7 B and C may suggest that the round live clusters also are located inside channels.

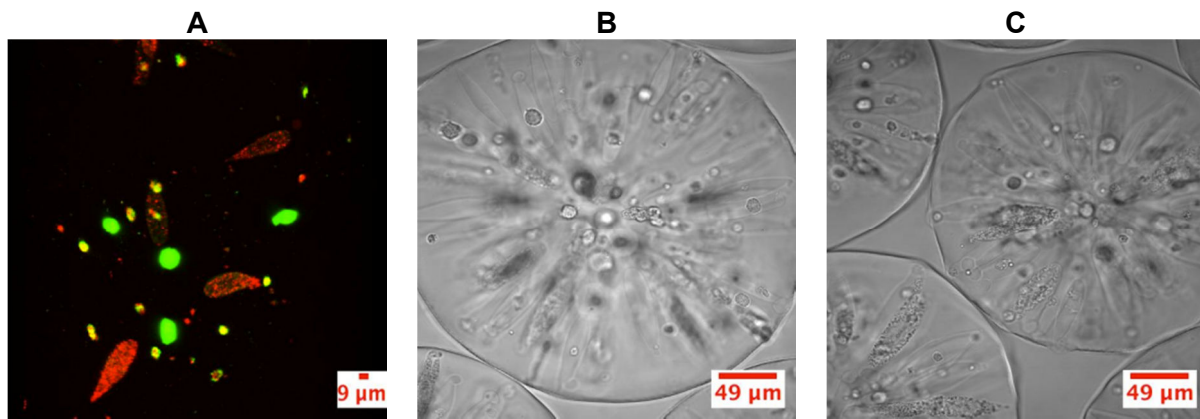


Figure 3.7: A: CLSM Z stack 3D projection of a capsule from the B1a batch. The picture was obtained at day 14. A 40x objective was used for image acquisition and the size bar is 9µm. B: CLSM cross-section through the equator of a capsule from the B2a batch overlaid with transmitted light. A 40x objective was used for image acquisition. The size bar is 49µm and the picture was obtained at day 14. C: CLSM cross-section through the equator of capsules from the B1b batch overlaid with transmitted light. A 40x objective was used for image acquisition. The size bar is 49µm and the picture was obtained at day 22.

Star shaped channels were observed in all of the capsules regardless of RGD-graft or not. In the capsules with high cell concentration (B1b and B2b) these channels seemed to push the surface of the capsules outwards, causing the capsules to appear angular shaped. An example of such a capsule is depicted in figure 3.7 C.

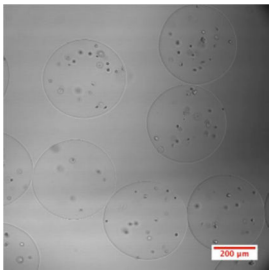
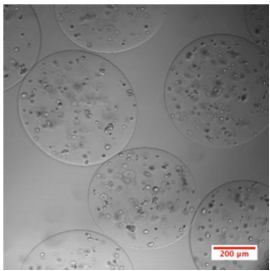
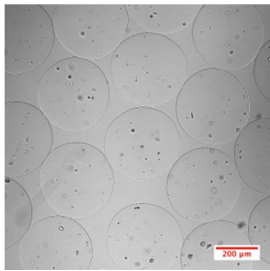
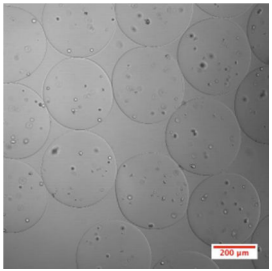
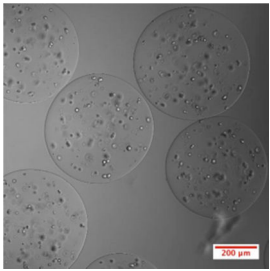
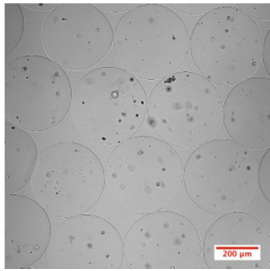
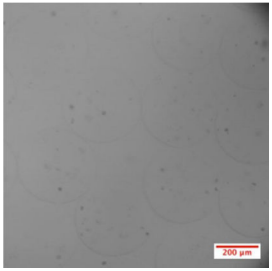
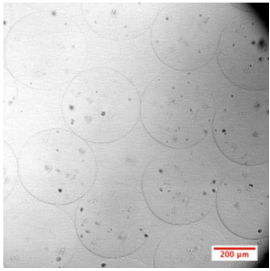
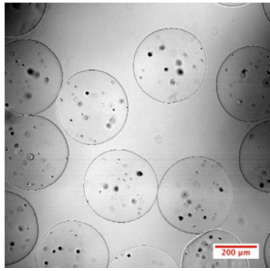
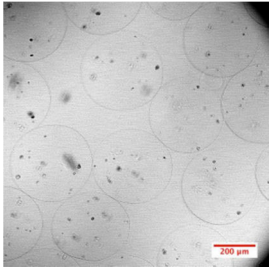
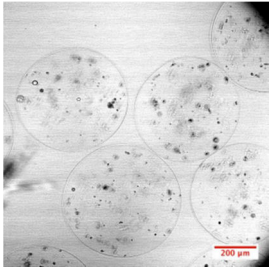
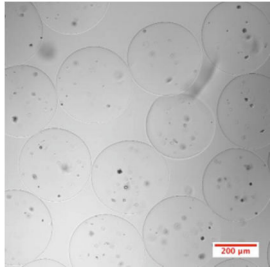
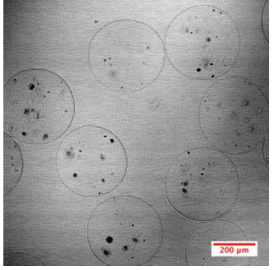
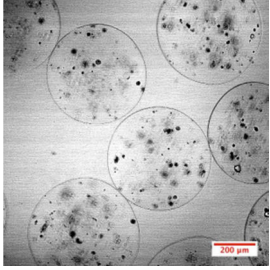
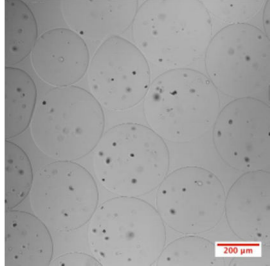
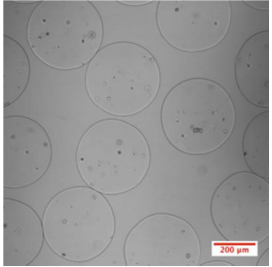
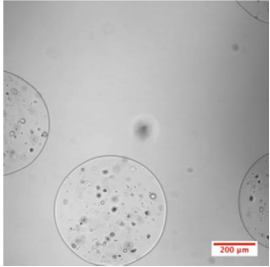
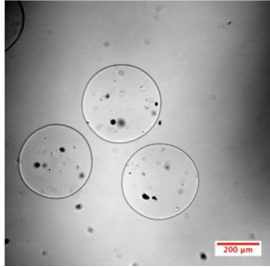
3.3. Encapsulation of OECs in 1.0% UP-LVG alginate I

Two different concentrations of OECs were encapsulated in 1.0% UP-LVG $\text{Ca}^{2+}/\text{Ba}^{2+}$ alginate; 1.0 mil/mL and 4 mil/mL, denoted C1a and C1b. The purpose of this encapsulation was to check if the increased viability observed in experiment 3.2 was due to softer gel caused by lower alginate concentration (1.8% alginate versus 1.0% alginate) or due to differences in the alginate properties (UP-LVG alginate *versus* 0.2% RGD peptide grafted alginate epimerized with mannuronan C-5 epimerases AlgE4 an AlgE6).

The cell viability was measured by Live/Dead assay. Because of lower cell concentration than expected (1.0 mil/mL and 4 mil/mL versus 1.5 mil/mL and 5.0 mil/mL), these batches were used to test different alamarBlue® protocols as described in the Materials and Methods section 2.5. It was decided not to use the alamarBlue® assay on these batches after the test round, as a new encapsulation (experiment 3.4) with cell concentration corresponding to the other experiments in this project.

Batch C1a was kept in culture for 51 days while batch C1b was discarded after 22 days, due to low cell viability.

The distribution of live and dead cells was visualized by 3D Z stack projections by CLSM. Figure 3.8 displays cross sections through the equator of capsules overlaid with transmitted light.

	1.0 mil/mL (C1a)	4 mil/mL (C1b)		1.0 mil/mL (C1a)
Day 1			Day 24	
Day 3			Day 29	
Day 9			Day 32	
Day 10			Day 36	
Day 14			Day 44	
Day 17			Day 51	

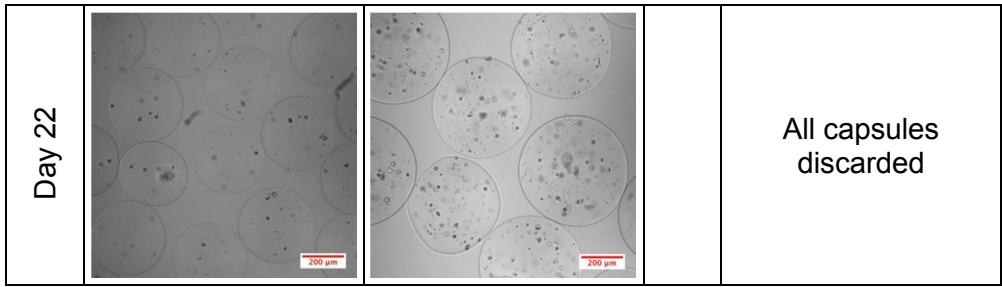
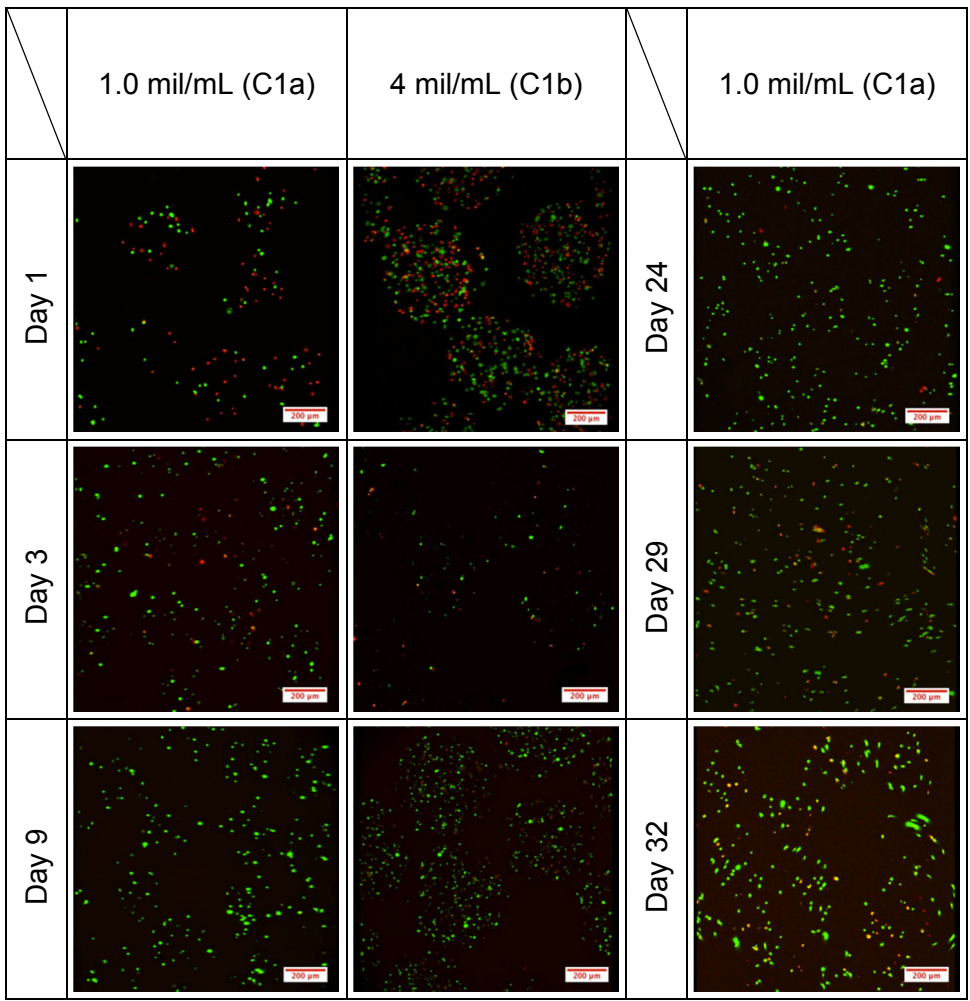


Figure 3.8: CLSM cross-sections through the equator of 1.0% UP-LVG $\text{Ca}^{2+}/\text{Ba}^{2+}$ -alginate capsules containing OECs overlaid with transmitted light. A 10x objective was used for image acquisition and the size bar is 200 μm . The 4 mil/mL cell concentration batch (C1b) was discarded at day 22 due to low cell viability.

The capsules exhibited a narrow size distribution with circular capsules and a few broken capsules distributed randomly between the batches. Batch C1b displayed a larger capsule diameter than batch C1a. On average the diameter of C1a was approximately 350 μm , while batch C1b displayed an approximate average diameter of 500 μm . The capsules retained their initial size during the experiment.

CLSM Z stack 3D projections are depicted in Figure 3.9.



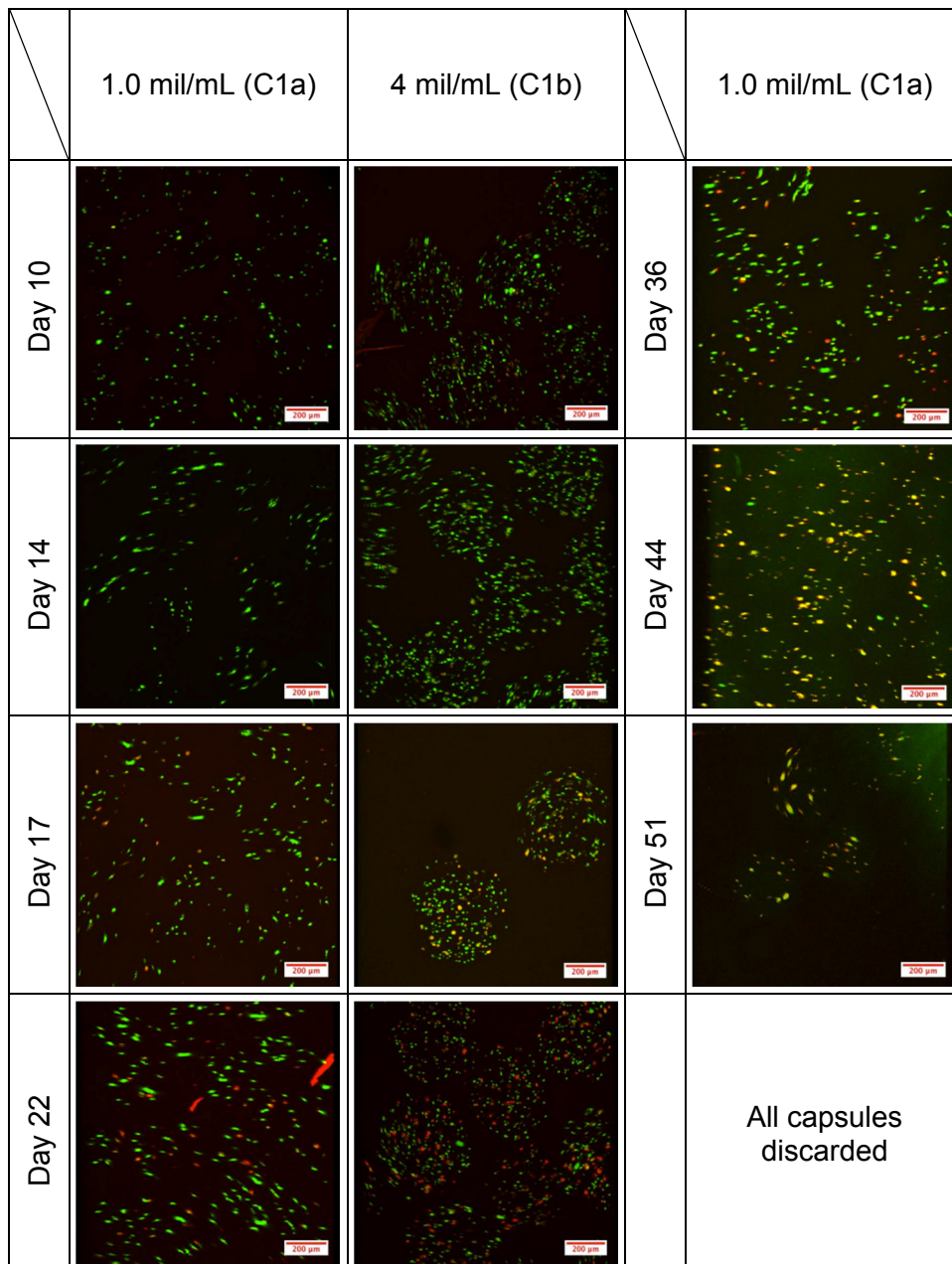


Figure 3.9: Live/dead assay. CLSM Z stacks 3D projections of OECs encapsulated in 1.0% UP-LVG $\text{Ca}^{2+}/\text{Ba}^{2+}$ alginate. Batch C1b was discarded at day 22 due to low cell viability. Green fluorescence indicates live cells as opposed to red fluorescence, which indicates dead cells. Several capsules are shown in each picture. A 10x objective was used for image acquisition and the size bar is 200 μm .

Both batches displayed high cell viability (estimated >75% live cells) up to day 17, with an exception of day 1 and 3 where the cell viability in both batches was roughly estimated to 50%. The dead cells are presumed to be washed out of the capsule, increasing the Live/Dead ratio in favour of live cells (figure 3.10). This may indicate that the cells in both batches did not tolerate the encapsulation process well. The viability of the cells in the C1b batch declined from day 17 to 22 from >75% live cells to approximately 50% live cells. These capsules were discarded at day 22.

Batch C1a displayed stable viability with an estimated live cell percentage over 75% up until day 36. From day 36 to 51 a slow decrease in viability was observed until the experiment was terminated at approximately 50% live cells in batch C1a.

The estimated live cell percentage for both batches are presented in Figure 3.10.

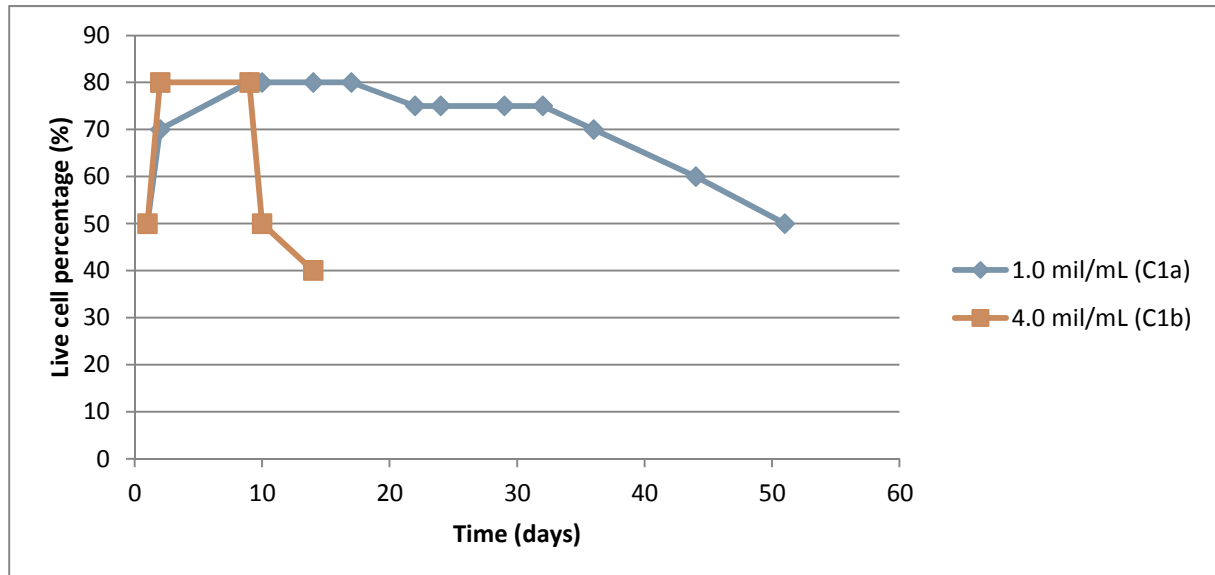


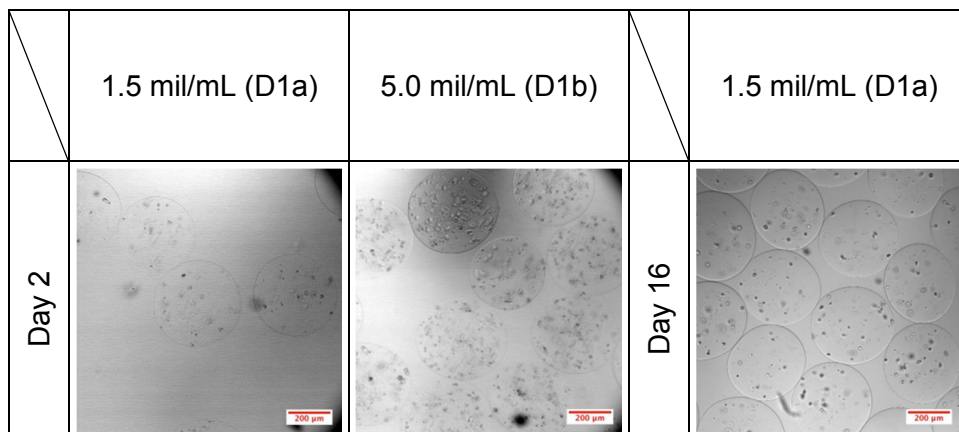
Figure 3.10: An estimate of live cell percentage of OECs encapsulated in 1.0% UP-LVG $\text{Ca}^{2+}/\text{Ba}^{2+}$ alginate, based on Figure 3.9.

3.4. Encapsulation of OECs in 1.0% UP-LVG alginate II

It was decided to repeat the encapsulation of two concentrations in 1.0% UP-LVG $\text{Ca}^{2+}/\text{Ba}^{2+}$ alginate because the cell concentrations became lower than expected in experiment 3.3. The two new batches denoted D1a and D1b obtained desired cell concentration 1.5 mil/mL and 5.0 mil/mL, respectively.

The cell viability was measured with Live/Dead assay and alamarBlue® assay, and batch D1a was kept in culture for 36 days, while batch D1b was discarded after day 14 due to low viability.

Figure 3.11 displays cross sections through the equator of capsules overlaid with transmitted light obtained by CLSM.



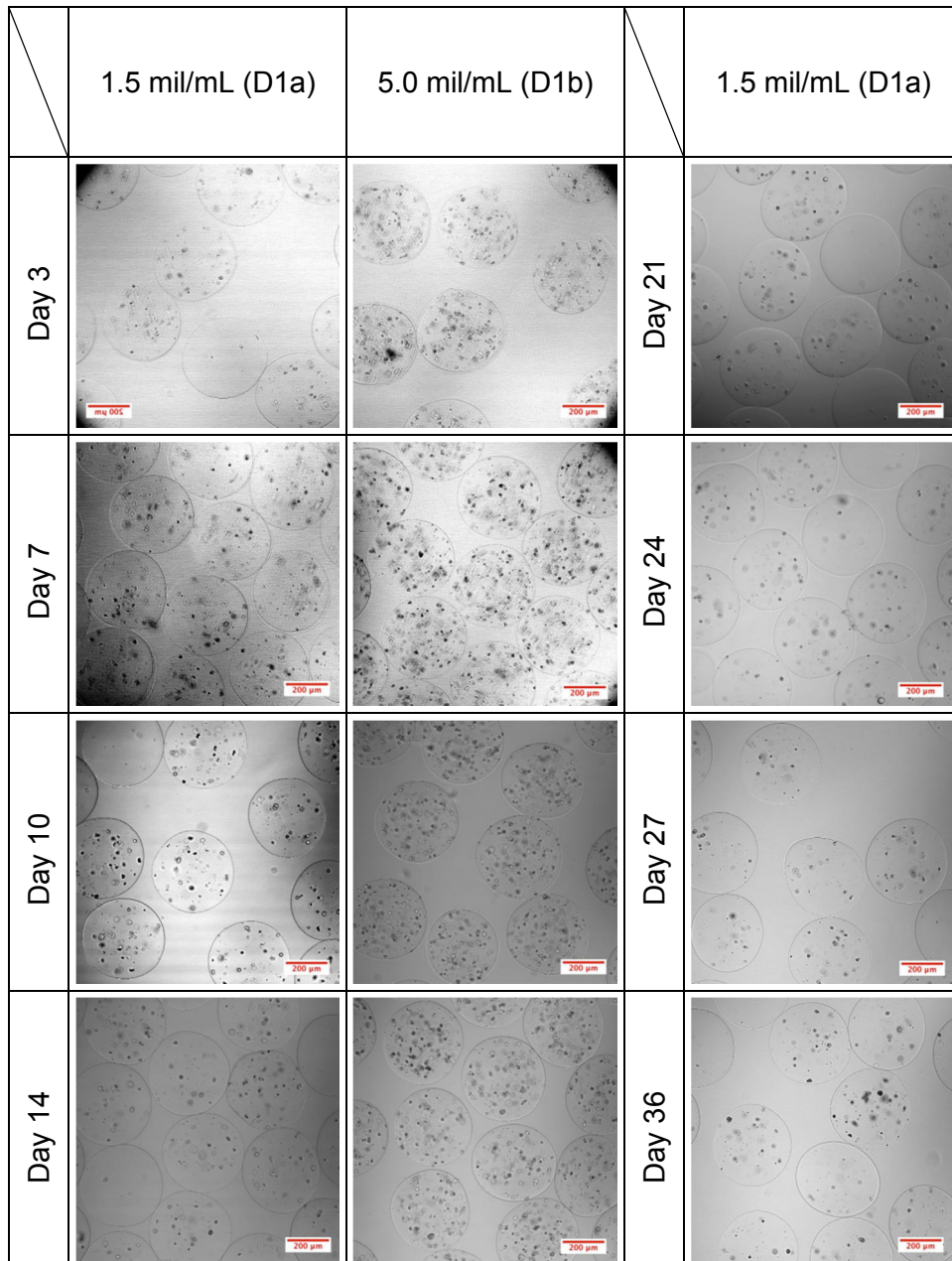


Figure 3.11: CLSM cross-sections through the equator of 1.0% UP-LVG $\text{Ca}^{2+}/\text{Ba}^{2+}$ capsules containing OECs overlaid with transmitted light. A 10x objective was used for image acquisition and the size bar is 200µm. The 5.0 mil/mL cell concentration batch (D1b) was discarded at day 14 due to low cell viability.

Both batches displayed an average diameter of approximately 400µm, with no notable difference in capsule size between the two cell concentrations. The capsules retained their initial size throughout the experiment and only few broken capsules were observed.

The distribution of live and dead cells was visualized by 3D Z stack projections by CLSM and is shown in figure 3.12.

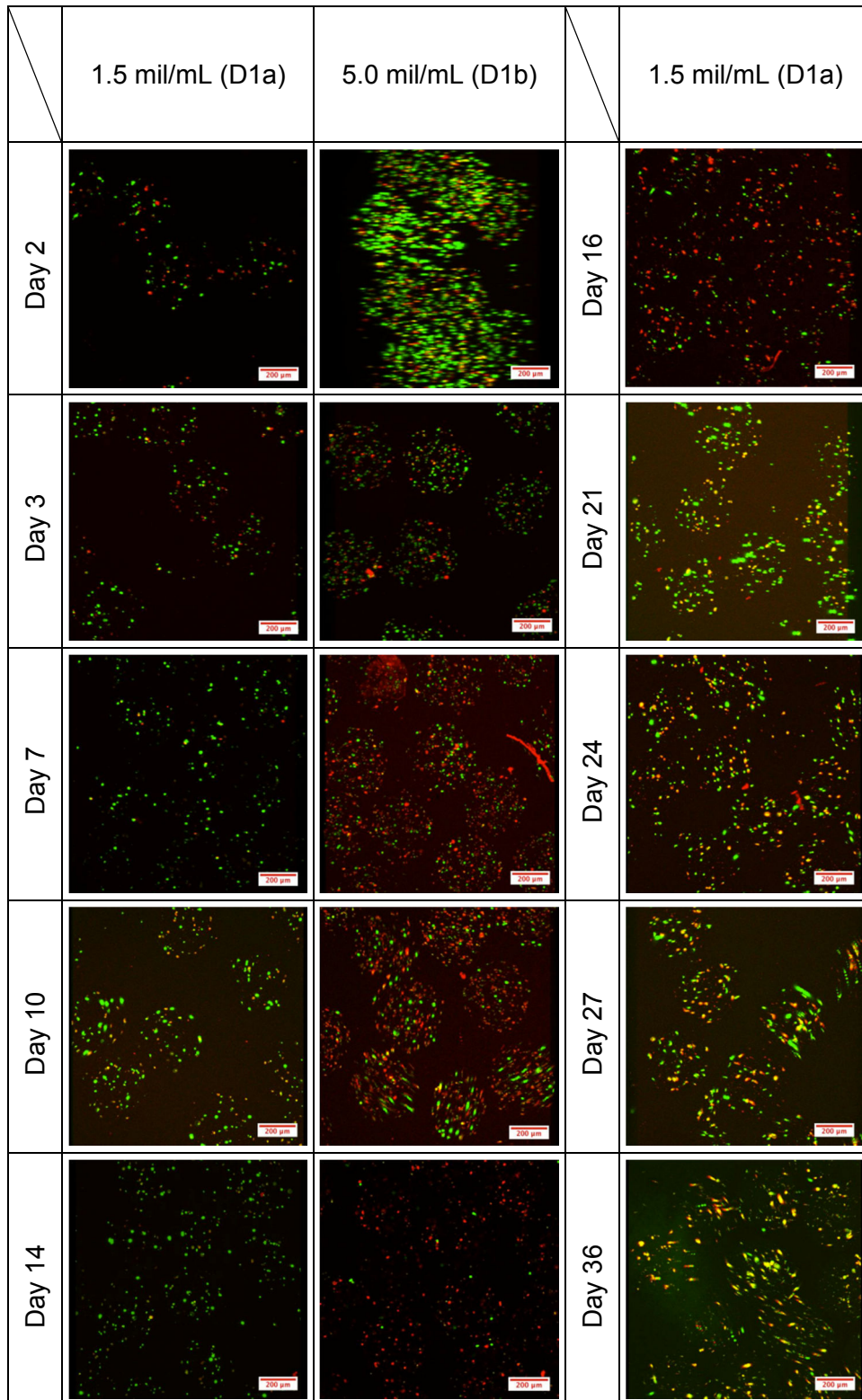


Figure 3.12: Live/dead assay. CLSM Z stacks 3D projections of OECs encapsulated in 1.0% UP-LVG Ca²⁺/Ba²⁺ alginate. Green fluorescence indicates live cells as opposed to red fluorescence, which indicates dead cells. Several capsules are shown in each picture. A 10x objective was used for image acquisition and the size bar is 200μm.

Both batches displayed an estimated viability of 60% at day 2, but the picture for the D1b batch is overexposed, rendering the estimate for this batch uncertain.

The picture of the 5.0 mil/mL capsules at day 2 introduces an artefact, as the capsules were moving during image acquisition. This causes the cell clusters to appear larger and more intensely green coloured than they really were. The pictures of day 24, 27 and 36 (batch D1a) are somewhat overexposed, which made it difficult to assess Live/Dead ratio. This introduces uncertainties in the qualitative analysis, which must be taken into account when interpreting figure 3.13.

As in experiment 3.3 the cells viability in batch D1a seems to increase from approximately 60% live cells to ca. 75% live cells after day 3 in the capsules. This does not apply for the cells in batch D1b, where the viability decreases rapidly from day 3 until termination of the batch due to low viability at day 14. It is probable that the cells that died during encapsulation in batch D1a were washed out of the capsules, and increased the Live/Dead ratio in favour of live cells.

Batch D1a displayed high viability (>75% live cells) up until day 21, where the viability decreased gradually to an estimated value of 50% at day 36 when the experiment was terminated. An exception is day 16, where the viability was estimated to 40% live cells.

The estimated live cell percentage for both batches are shown in figure 3.13.

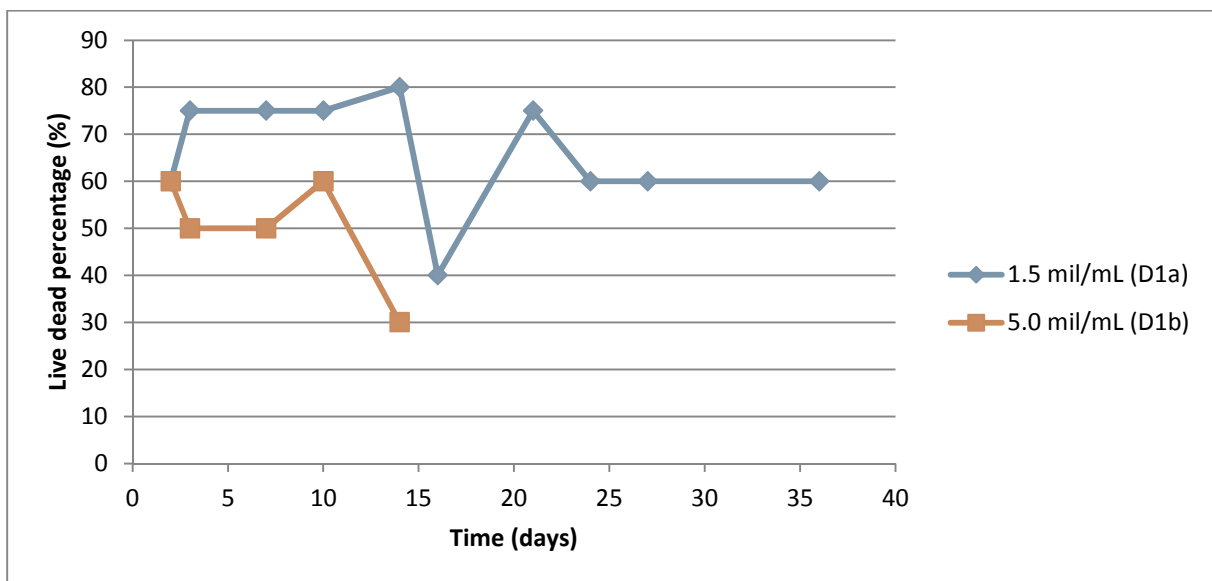


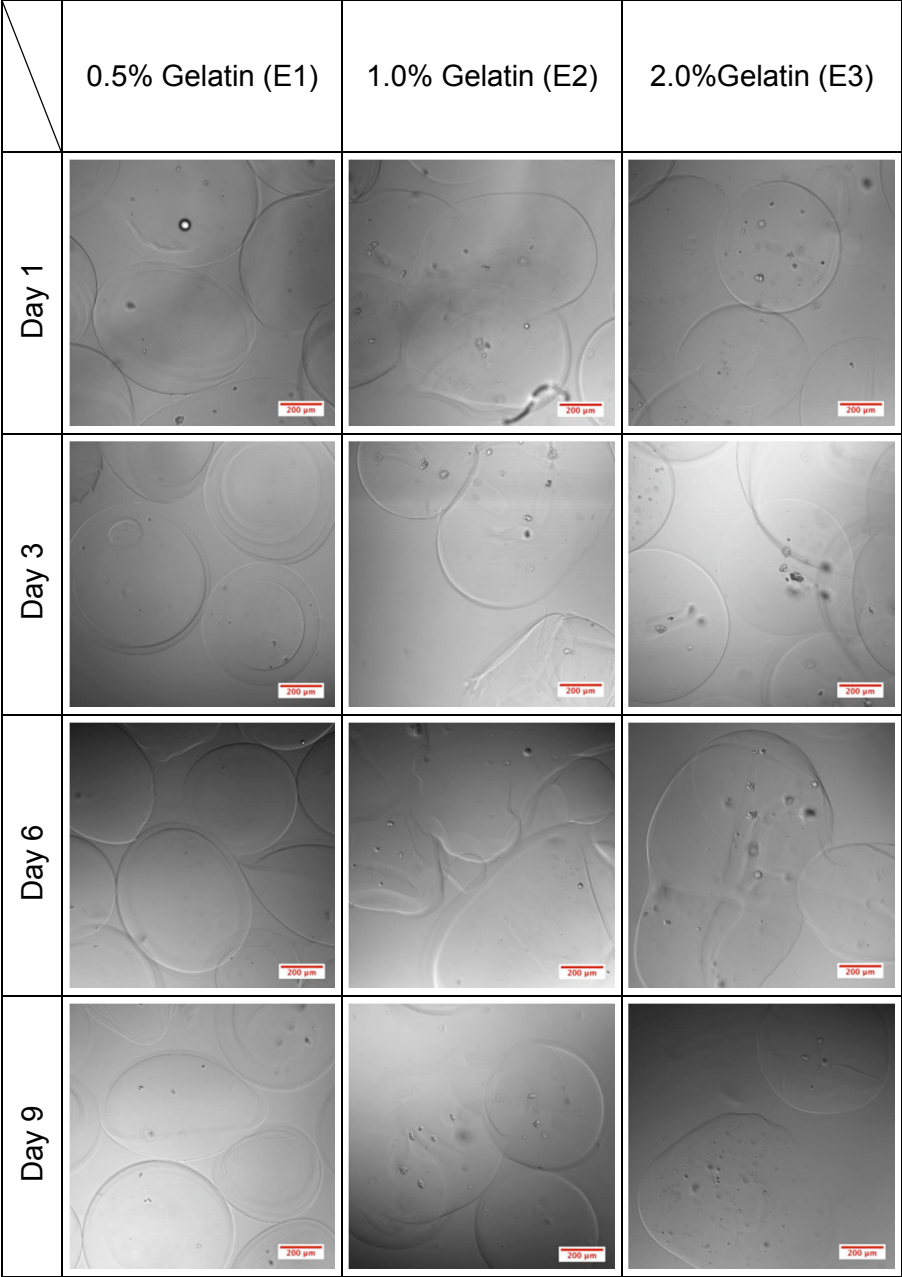
Figure 3.13: An estimated percentage of live cells encapsulated in 1.0% UP-LVG $\text{Ca}^{2+}/\text{Ba}^{2+}$ alginate , based on figure 3.12.

3.5. OECs encapsulated in 1.0% UP-LVG alginate mixed with different concentrations of gelatin I

OECs were encapsulated in 1.0% UP-LVG alginate mixed with gelatin to yield three different gelatin concentrations; 0.5 %, 1.0% and 2%, denoted E1, E2 and E3, respectively. All three batches had a cell concentration of 1.5 mil/mL and were gelled in gelling solution containing $\text{Ca}^{2+}/\text{Ba}^{2+}$ ions.

The purpose of this encapsulation was to make the alginate more similar to the ECM by mixing alginate with gelatin, and examine whether the gelatin influenced the cells, both in terms of viability and morphology. Gelatin may resemble collagen and collagen is the most abundant protein in the ECM. It was also of interest to monitor the capsule quality as well as the encapsulation process.

Figure 3.14 displays cross sections through the equator of capsules overlaid with transmitted light obtained by CLSM.



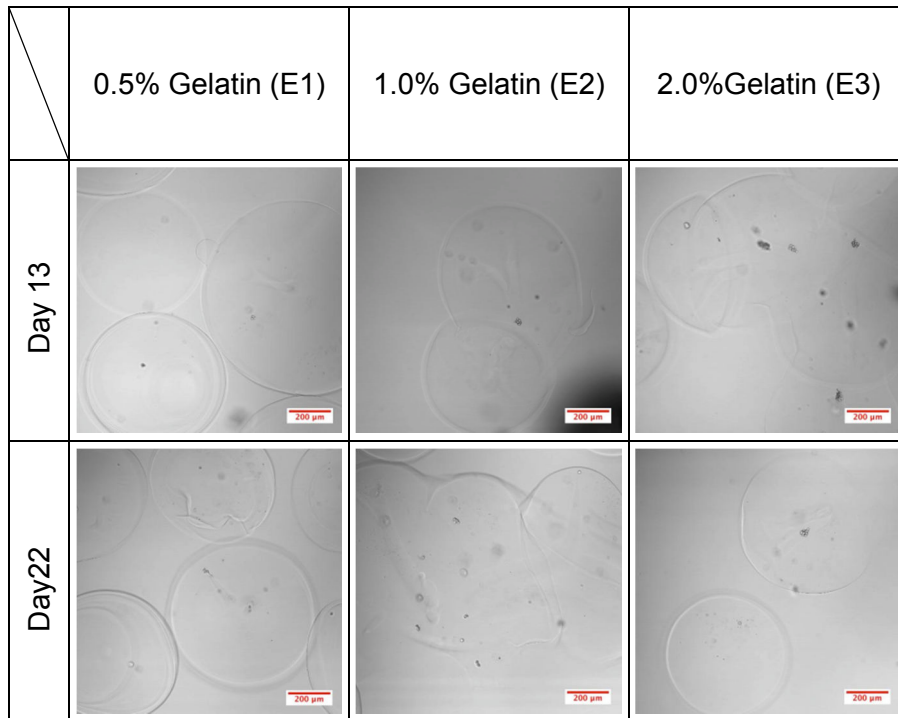


Figure 3.14: CLSM cross-sections through the equator of capsules made of 1.0% UP-LVG $\text{Ca}^{2+}/\text{Ba}^{2+}$ alginate mixed with gelatin containing 1.5 mil/mL OECs overlaid with transmitted light. A 10x objective was used for image acquisition and the size bar is 200µm.

As can be observed in Figure 3.14, the irregular shape of the capsules increased proportionally with increasing gelatin concentration. The average capsule diameter was approximately 500µm, but it was sometimes difficult to assess due to the capsules irregular shape. The stability of the capsules was also affected by increasing gelatin concentration, with more broken capsules and escaped cells attached to the culture flask bottom in the E3 batch, less in the E2 batch and the stability of the E1 batch was comparable with the experience with 1.0% UP-LVG capsule stability.

The cell colonies tended to be less dispersed and rather large compared to earlier experiments during this project. An example of two cell clusters can be observed in figure 3.15. The amount of cells in the capsules did also look smaller than in previous experiments.

Some difficulties were experienced during encapsulation, as gelatin gels below $\approx 35^\circ\text{C}$. It was a challenge to keep the temperature of the alginate-gelatin mix over this threshold before the ionic gelation with alginate took place and lack of experience and a proper protocol may have influenced the capsule result. It was decided to try another encapsulation with the same settings to improve the encapsulation process (described in section 3.6.), to see if the results obtained in this experience were reproducible.



Figure 3.15: Two cell clusters situated in a 1.0% UP-LVG alginate mixed with 1.0% gelatin capsule (E2). The picture was obtained by CLSM cross-sections through the equator of capsules overlaid with transmitted light. A 40x objective was used for image acquisition and the size bar is 49μm.

The distribution of live and dead cells was visualized by 3D Z stack projections by CLSM and is shown in figure 3.16. The alamarBlue® assay was also performed on these cells and the fluorescence values and calculations can be observed in appendix A9, while the graph is shown in appendix A10.

	0.5% gelatin (E1)	1.0% gelatin (E2)	2% gelatin (E3)
Day 1			
Day 3	Due to technical difficulties, no picture was available at day 3		

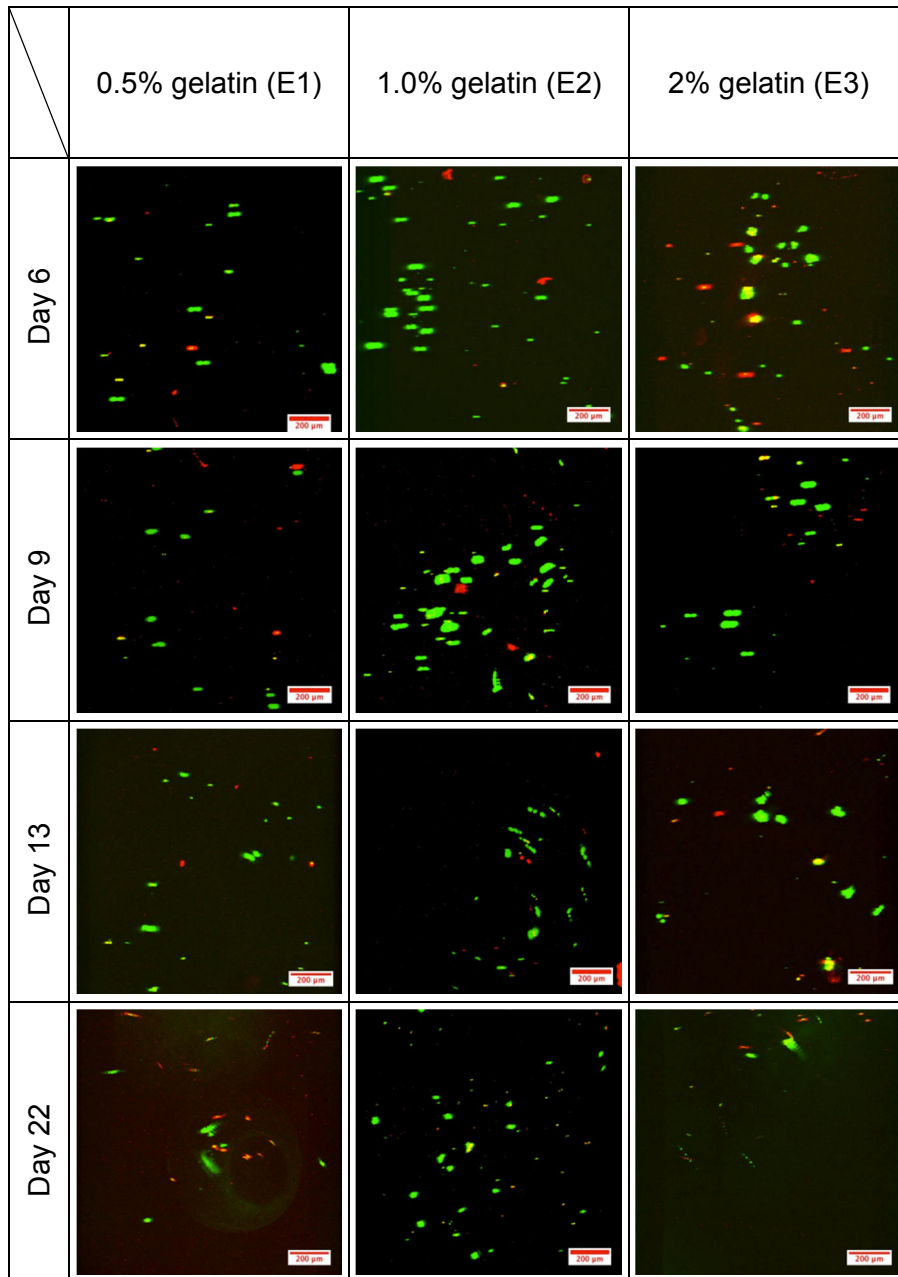


Figure 3.16: Live/dead assay. CLSM Z stacks 3D projections of OECs encapsulated in 1.0% UP-LVG $\text{Ca}^{2+}/\text{Ba}^{2+}$ alginate mixed with gelatin. Green fluorescence indicates live cells as opposed to red fluorescence, which indicates dead cells. Several capsules are shown in each picture. A 10x objective was used for image acquisition and the size bar is 200 μm .

At day 1 the viable cell percentage was estimated to 60% for all three batches and it increased for all batches until day 3. It is probable that the cells that did not tolerate the encapsulation well and died as a result of it, were washed out of the capsule.

The cells displayed overall high viability regardless of gelatin concentration, and it seemed like the viability of cells depended more on loss of capsules due to instability than on the material itself. As mentioned above, the cell clusters seem to be larger than experienced before, but the cell number appears lower than in the previous

experiments. Some background green fluorescence from the gel was experienced, which may have influenced image quality.

The estimated live cell percentage for both batches are shown in figure 3.17.

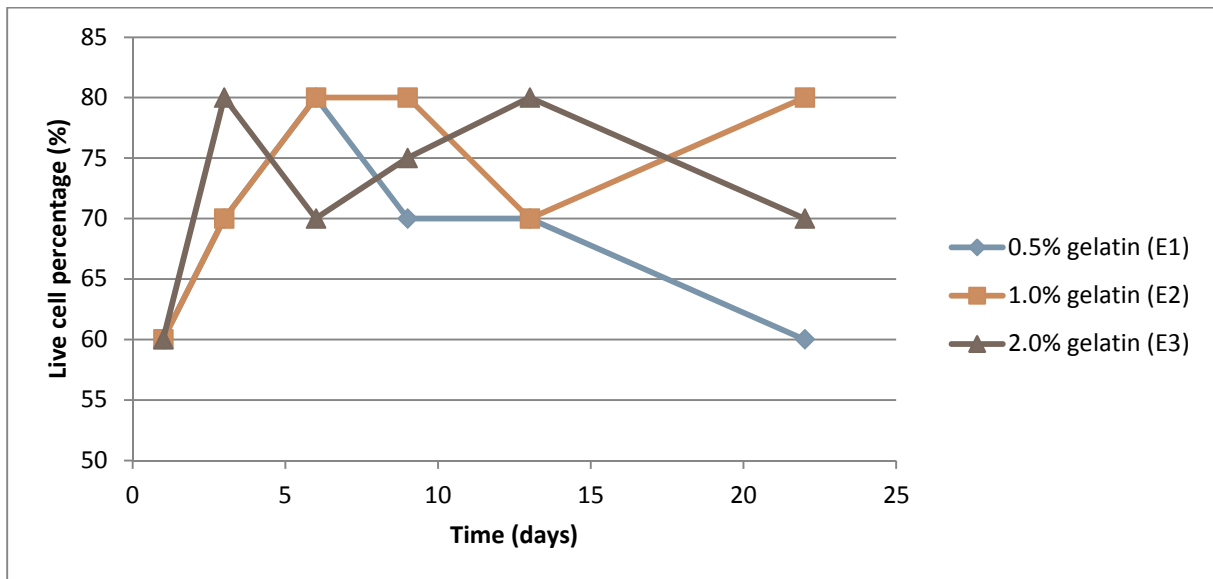


Figure 3.17: An estimated percentage of live cells encapsulated in 1.0% UP-LVG $\text{Ca}^{2+}/\text{Ba}^{2+}$ alginate mixed with gelatin, based on figure 3.15.

3.6. OECs encapsulated in 1.0% UP-LVG alginate mixed with different concentrations of gelatin II

The experiment described in section 3.5 above was repeated with the same settings, with the aim of improving the encapsulation process and gain a narrower size distribution and more circular capsules.

To improve the encapsulation it was decided to preheat both the gelling solution and alginate-gelatin mix to $\approx 40^\circ\text{C}$ in a water bath before encapsulation, as well as insulating the plastic tube from the syringe to the needle to avoid gelling of the gelatin.

Figure 3.18 displays cross sections through the equator of capsules overlaid with transmitted light obtained by CLSM.

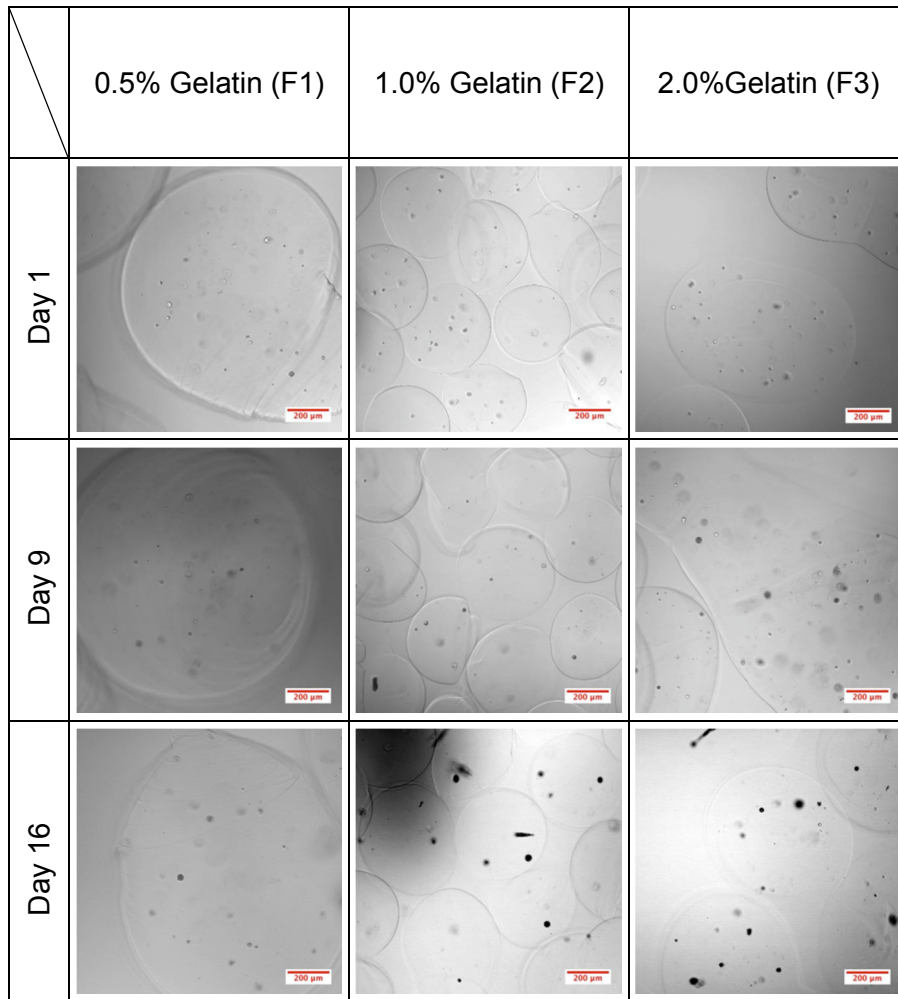


Figure 3.18: CLSM cross-sections through the equator of capsules made of 1.0% UP-LVG $\text{Ca}^{2+}/\text{Ba}^{2+}$ alginate mixed with gelatin containing 1.5 mil/mL cells overlaid with transmitted light. A 10x objective was used for image acquisition and the size bar is 200 μm .

The capsule quality did improve, perhaps with most impact on the F2 batch. For both batch F2 and F3 the edges of the capsules became more defined compared to the capsules obtained in experiment 3.5. The shape of the capsules did also improve for batch F2 capsules, and F3 capsules, albeit to a lesser degree for the latter in terms of circular shape of the capsules. At day 14 of the experiment there were few F2 and F3 capsules left in the culture flask, suggesting that they had dissolved at this stage.

The diameter of the capsules varied between 350-600 μm in order F1>F3>>F2.

The distribution of live and dead cells was visualized by 3D Z stack projections by CLSM and is shown in figure 3.19.

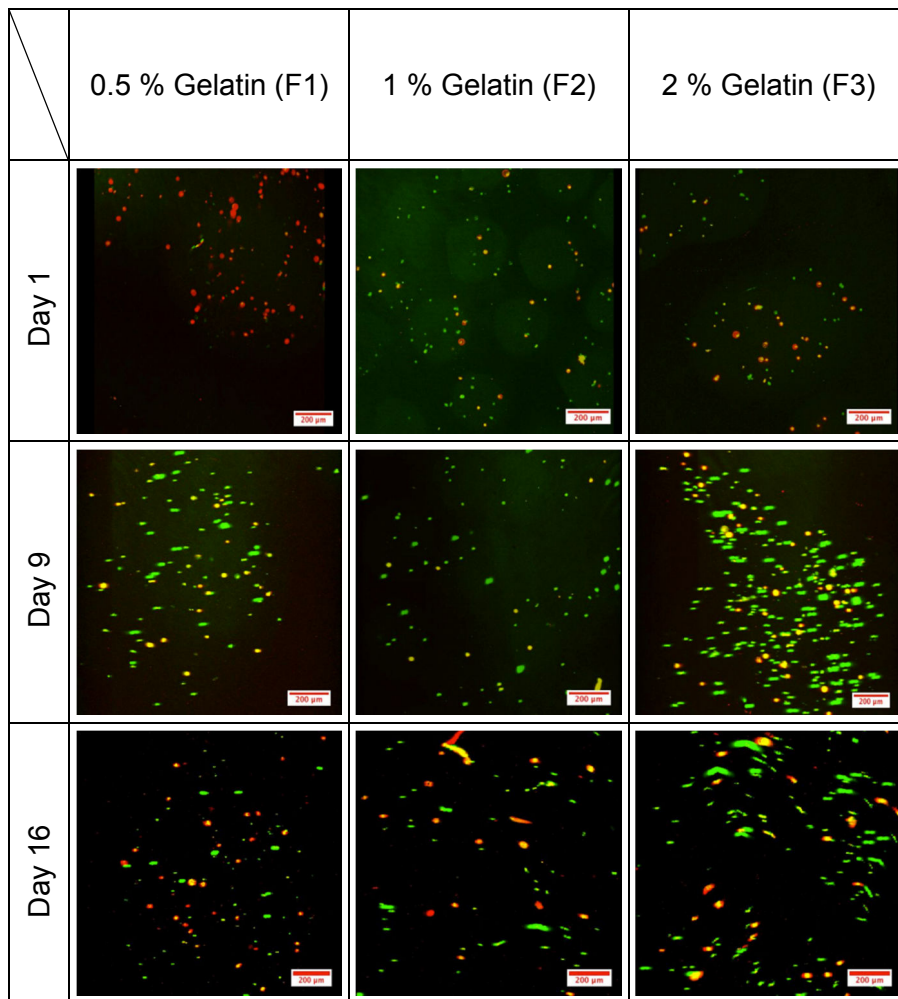


Figure 3.19: Live/dead assay. CLSM Z stacks 3D projections of 1.5 mil/mL OECs encapsulated in 1.0% UP-LVG Ca²⁺/Ba² alginate mixed with gelatin. Green fluorescence indicates live cells as opposed to red fluorescence, which indicates dead cells. Several capsules are shown in each picture. A 10x objective was used for image acquisition and the size bar is 200µm.

On day 1 batch E2 displayed a live cell percentage 60%, while E3 had 70% live cell percentage. As in the previous experiment (section 3.5) the cell viability was overall high throughout the experiment with no notable differences between the batches, with an exception of day 1 for batch F1. This picture was treated as an outlier and may be caused by unfortunate selection of capsules and was therefore excluded from figure 3.20. The capsules were only kept in culture for 16 days, because their main purpose was to improve the encapsulation process, and as can be observed in figure 3.20 the live cell percentage was > 70% when the experiment was terminated. The cell clusters may have been smaller and more dispersed than in the previous experiment (section 3.5). In the picture of F2 from day 1 green background fluorescence from the alginate-gelatin is clearly visible.

An estimate of live cell percentage in all batches is presented in figure 3.20.

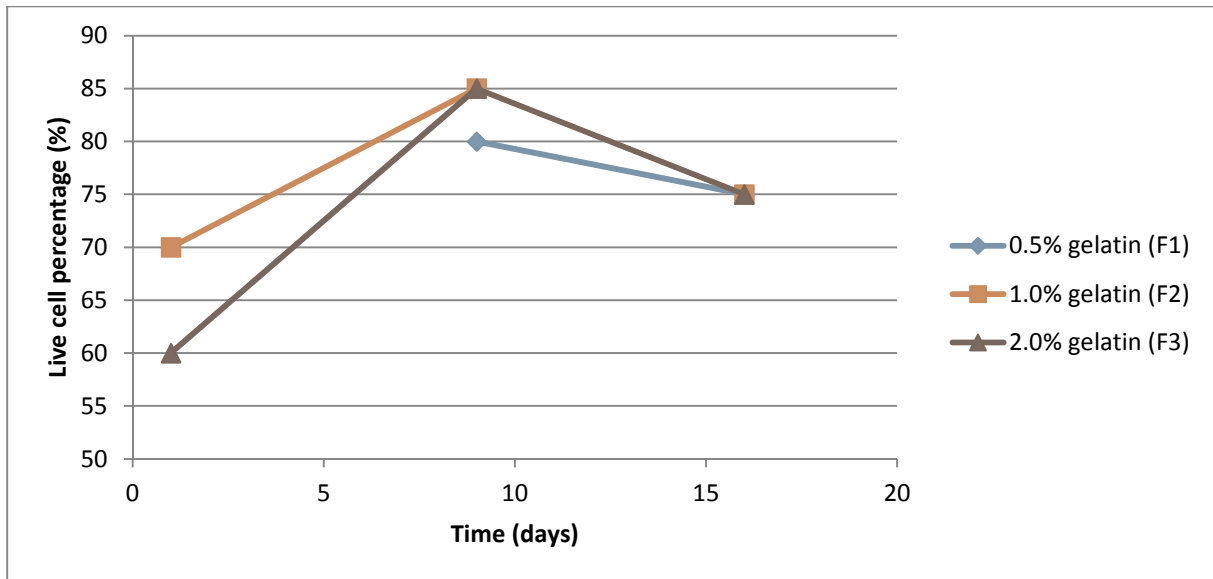


Figure 3.20: An estimated percentage of live cells encapsulated in 1.0% UP-LVG $\text{Ca}^{2+}/\text{Ba}^{2+}$ alginate mixed with gelatin, based on figure 3.19.

3.7. OECs encapsulated in 0.9% UP-LVG mixed with different ECM molecules and sulphated alginate

0.9% UP-LVG $\text{Ca}^{2+}/\text{Ba}^{2+}$ alginate was mixed with laminin, collagen, fibronectin and hyaluronic acid, creating four different batches with an ECM molecule concentration of 1.0 mg/mL. Sulphated MG-block alginate was mixed with 0.9% UP-LVG alginate to a concentration of 1.0 mg/mL. The purpose of the ECM molecule-alginate mixes were to mimic the environment in ECM, where all of these molecules may be present, and see if they affected the OECs in terms of viability or morphology. The sulphated alginate was included because of its likeness with the sulphated ECM molecule heparin and the same purpose in relation to OECs applied.

Figure 3.21 displays cross sections through the equator of capsules overlaid with transmitted light obtained by CLSM.

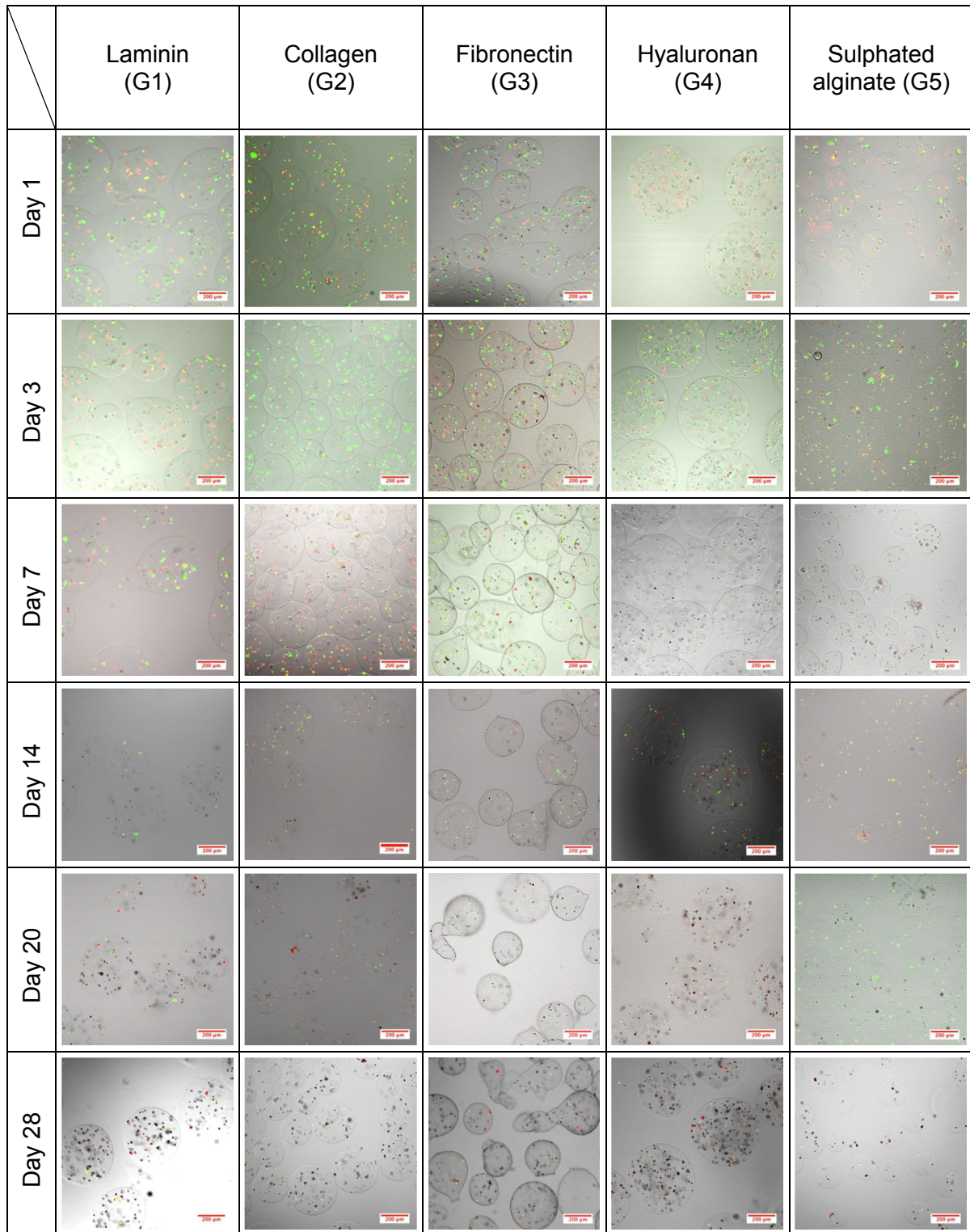


Figure 3.21: CLSM cross-sections through the equator of capsules made of 1.0% UP-LVG $\text{Ca}^{2+}/\text{Ba}^{2+}$ alginate mixed with 1.0 mg/mL different ECM molecules, and 1.0 mg/mL sulphated alginate containing 1.5 mil/mL OECs overlaid with transmitted light. A 10x objective was used for image acquisition and the size bar is 200 μm .

At day 1 the capsule diameter varied between the different samples. Capsules containing laminin and hyaluronic acid displayed the largest relative diameter, capsules containing fibronectin and collagen were middle sized and sulphated alginate capsules were by far the smallest. The size distribution did also vary for all

batches of capsules. Capsules containing fibronectin were the only batch with relatively large fraction of tail formation. All capsules were stable and few broken capsules were observed during the experiment.

The distribution of live and dead cells was visualized by 3D Z stack projections by CLSM and is shown in figure 3.22.

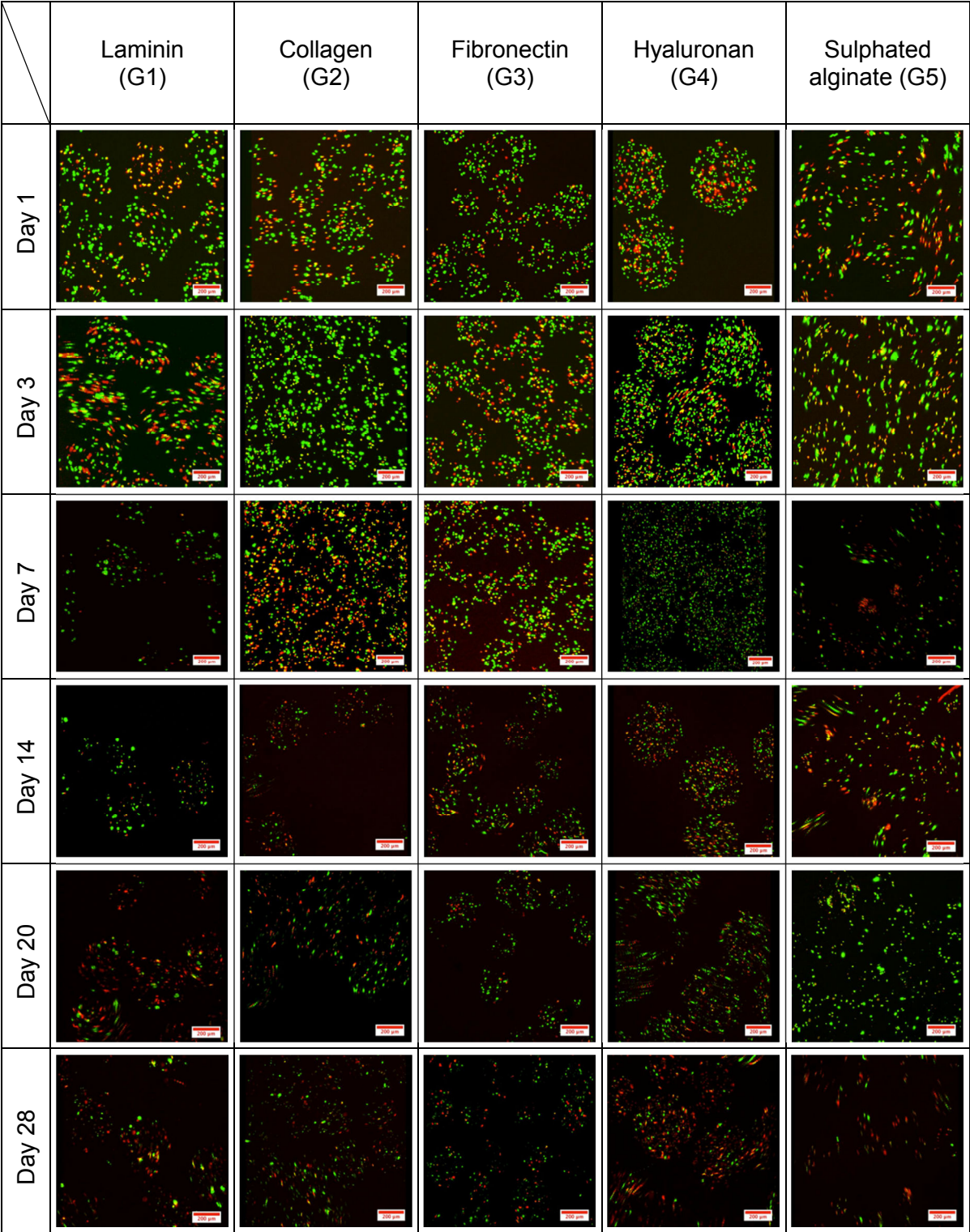


Figure 3.22: Live/dead assay. CLSM Z stacks 3D projections of 1.5 mil/mL OECs encapsulated in 1.0% UP-LVG Ca²⁺/Ba²⁺ alginate mixed with 1mg/mL different ECM molecules, and 1mg/mL sulphated alginate. Green fluorescence indicates live cells as opposed to red fluorescence, which indicates dead cells. Several capsules are shown in each picture. A 10x objective was used for image acquisition and the size bar is 200µm.

The settings of the CLSM were changed after day 7 to obtain higher resolution. This caused reduced intensity in pictures taken subsequently compared to the pictures taken before day 7 and may give a wrong impression of the Live/Dead ratio. G5 capsules moved during image acquisition at day 3, which led to that the green live cell clusters seem larger than they were in reality.

At day 1 all samples displayed viable cell percentage ≥ 75%.

The cells residing in capsules containing collagen and hyaluronic acid displayed increased viability on day 3 and 7 after encapsulation, respectively. All the other batches displayed gradually decreasing viabilities after encapsulation, with the exception of cells encapsulated in sulphated alginate that showed improved viability on day 20 before it decreased again at day 28.

The viability of all batches were estimated as lower than the viability of 1.5 mil/mL OECs encapsulated in 1.0% UP-LVG alginate, solely by comparing to previous experiments (3.3 and 3.4).

Figure 3.23 shows that capsules containing hyaluronic acid and sulphated alginate displayed highest viability throughout the project, while collagen, fibronectin and laminin displayed approximately similar patterns of viability decline.

An estimate of live cell percentage in all batches is presented in figure 3.23.

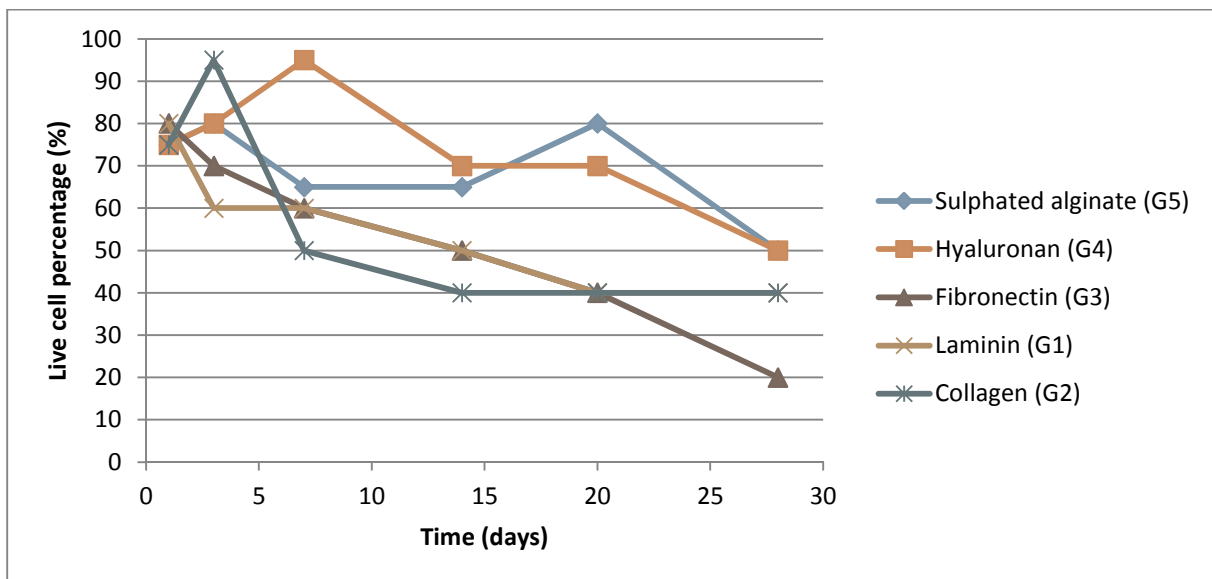


Figure 3.23: An estimated percentage of live OECs encapsulated in 1.0% UP-LVG Ca²⁺/Ba²⁺ alginate mixed with 1mg/mL different ECM molecules, and 1mg/mL sulphated alginate, based on figure 3.22.

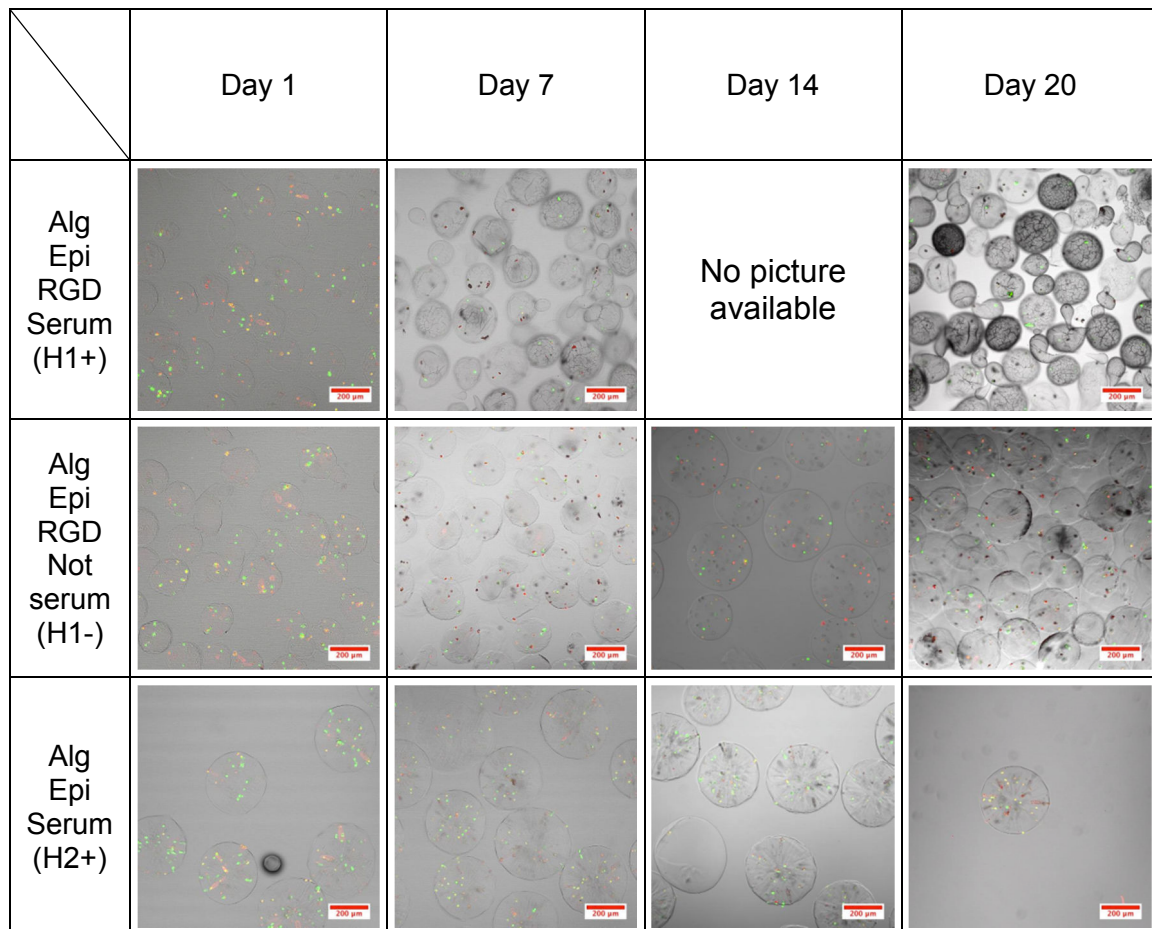
3.8. Encapsulation of OECs in 1.0% LG alginate grafted with 0,1-0.4% RGD peptide

Experiment 3.2 was repeated with a different 1.0% epimerised Ca^{2+} alginate grafted with 0,1-0.4% RGD peptide, produced by Birgitte McDonagh during her master thesis. 1.5 mil/mL OECs were encapsulated in 1.0% peptide grafted epimerized alginate, 1.0% non-peptide grafted epimerized alginate and 1.0% UP-LVG alginate.

Each batch was split in two and cultured in OECs growth media with, and without serum, giving a total of six batches. The cell culture in serum-free media was relevant for the collection of supernatant to protein analysis and was performed to see if the change in culture conditions was affecting cell viability. The purpose of this encapsulation was to see if an increased concentration of RGD peptide compared to the previous experiment (3.2) would elicit any response in the cells, in terms of cell viability and morphology.

The cells viability was monitored by Live/Dead assay.

Figure 3.24 displays cross sections through the equator of capsules overlaid with transmitted light obtained by CLSM.



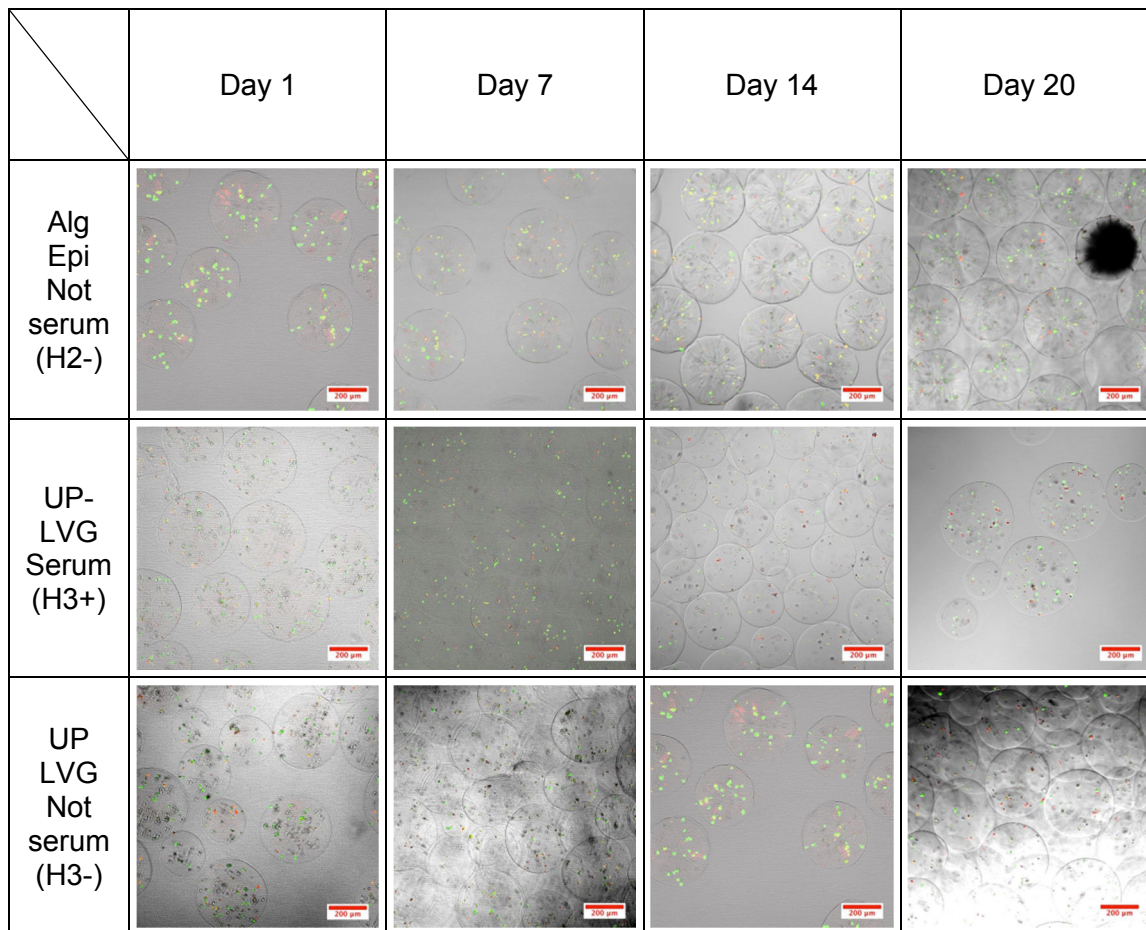


Figure 3.24: CLSM cross-sections through the equator of 1.0% epimerised Ca^{2+} capsules grafted with 0,1-0.4% RGD peptide, non-peptide grafted and 1.0% UP-LVG alginate containing 1.5 mil/mL OECs overlaid with transmitted light. A 10x objective was used for image acquisition and the size bar is 200 μm .

At day 1 the capsules made with RGD peptide grafted epimerized LG alginate displayed a very small diameter ($< 250\mu\text{m}$), compared to the other two batches and their shape was more irregular.

The non-peptide grafted epimerized LG alginate capsules and the UP-LVG capsules displayed roughly the same diameter ($< 400\text{-}500\mu\text{m}$) and they were almost circular with a narrow size distribution.

Most capsules were stable throughout the experiment with a few randomly distributed broken capsules. Very few capsules of batch H2+ was observed during Live/Dead assay at day 20, which may have indicated that these capsules had dissolved and were less stable.

The capsules made with alginate epimerized with AlgE4 and AlgE6 displayed the characteristic star shaped channels, which were also observed in experiment 3.2. In addition, the RGD grafted alginate capsules developed an unidentified white precipitation on the capsule surface, which increased during the experiment until the capsules were perceived as opaque and white when examined without a microscope.

When inspected with cross sections through the equator of capsules overlaid with transmitted light by the CLSM, the surface appeared wrinkled and cracked. It looked like the capsules had shrivelled over time, but no apparent reduction of size was detected when the experiment was terminated at day 20. The wrinkled surface of an RGD peptide grafted alginate capsule can be observed in figure 3.25.A. This effect was more pronounced in the RGD peptide grafted alginate capsules cultured in OEC growth media with serum, than those cultured in OEC growth media without serum.

Some precipitation could be detected in the epimerized alginate without RGD graft as well, but this was not observed in approximately 1 out of 30 capsules, and the precipitation seemed to be located within the capsule. The surface of these capsules did not appear wrinkled and cracked when examined by cross sections through the equator of capsules overlaid with transmitted light, either. Epimerized alginate without RGD graft capsules can be observed in figure 3.25.B. The precipitate occurred independently of serum in the OEC growth medium or not.

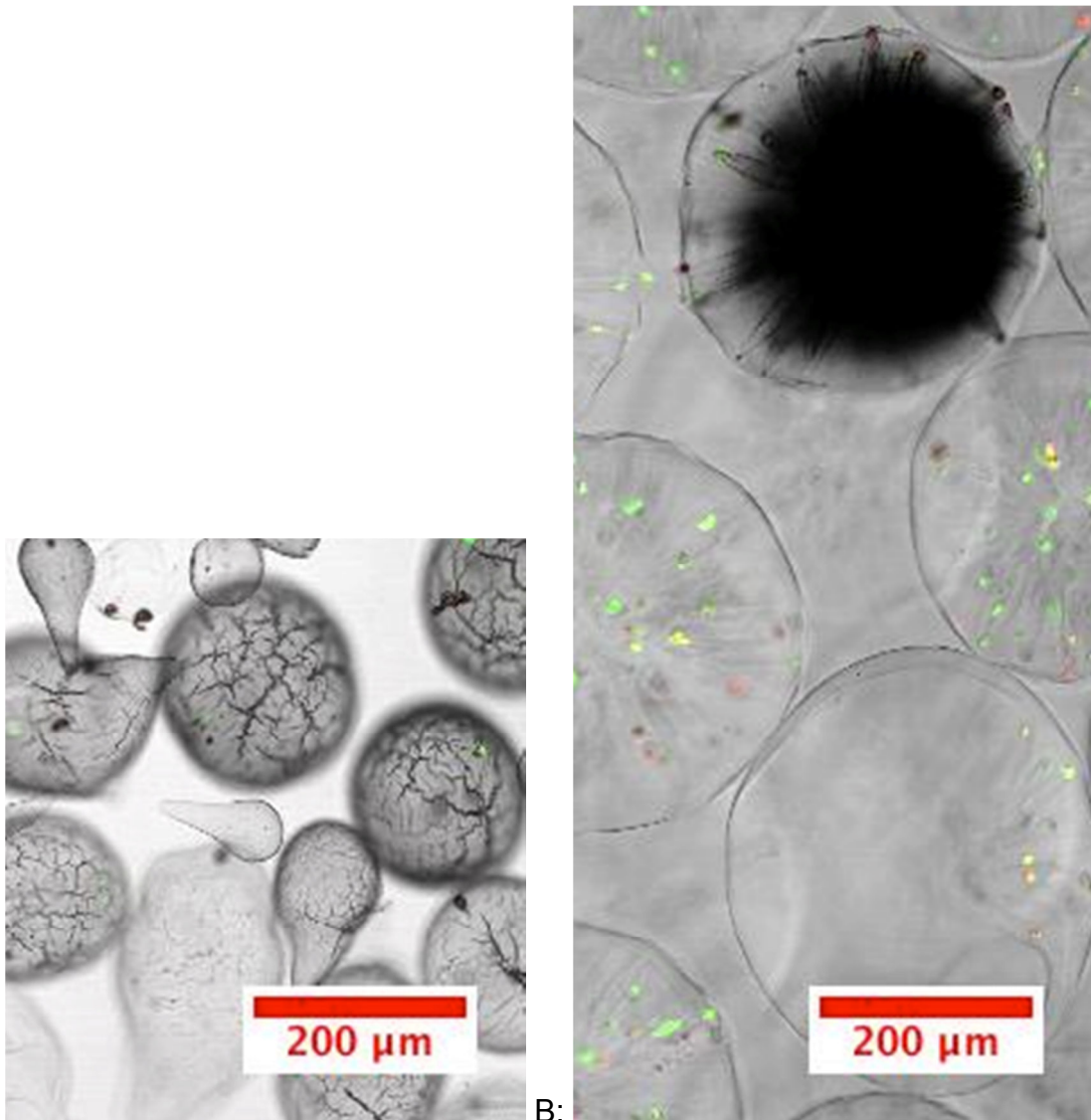
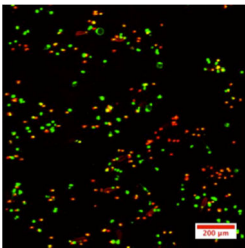
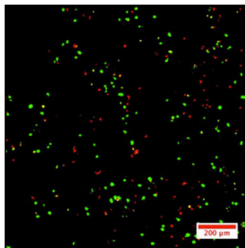
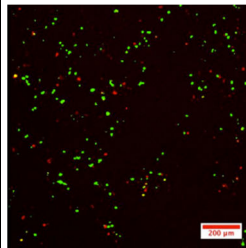
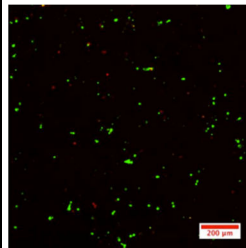


Figure 3.25: Section of CLSM pictures of: **A:** 0,1-0.4% RGD peptide grafted epimerized alginate with 1.5 mil/mL OEC concentration cultured in OEC growth media with serum, taken at day 20. **B:** epimerized LG alginate with 1.5 mil/mL OEC concentration cultured in OEC growth media without serum, taken at day 20.

The distribution of live and dead cells was visualized by 3D Z stack projections by CLSM and is shown in figure 3.26.

	Day 1	Day 7	Day 14	Day 20
Alg Epi RGD Serum (H1+)				

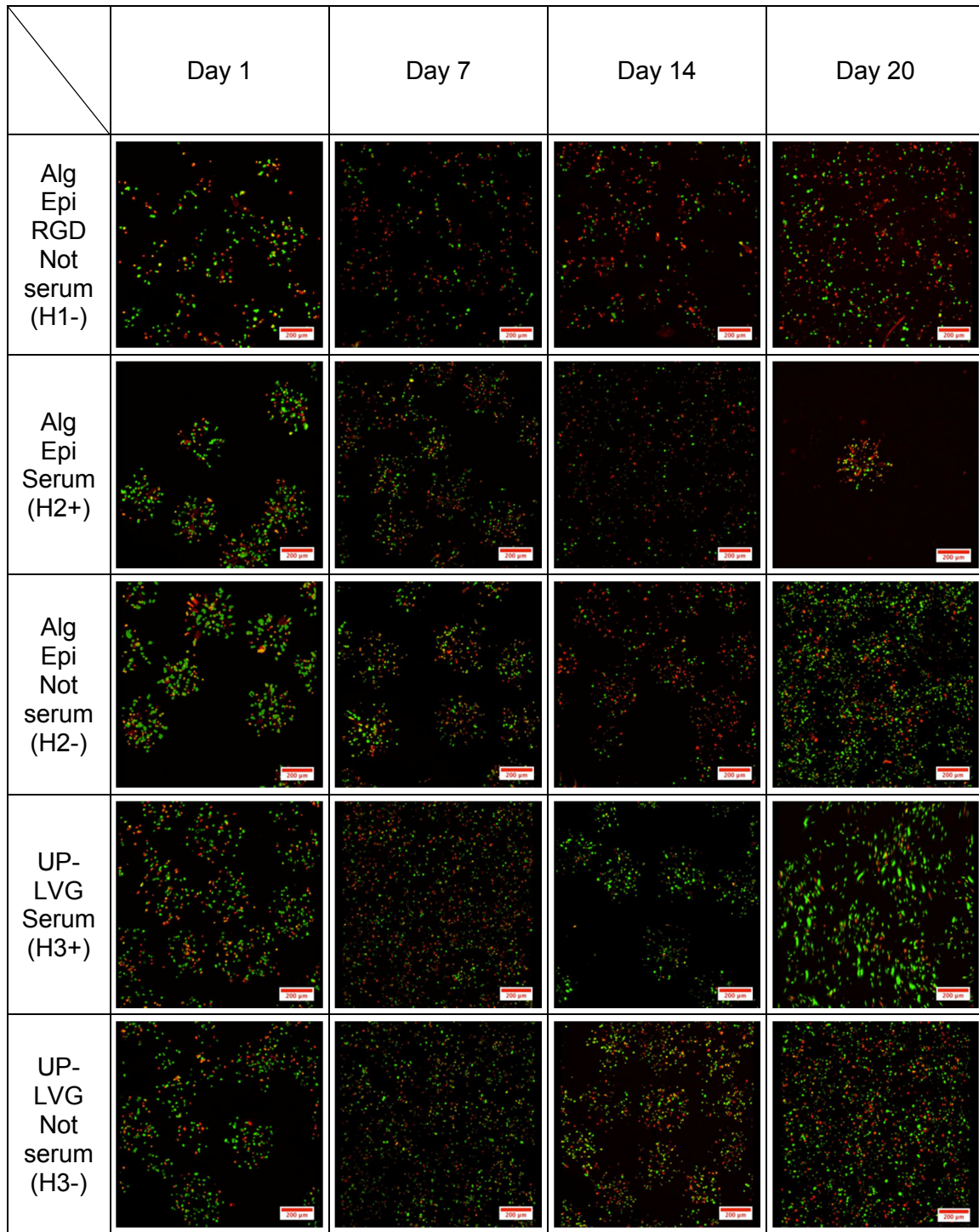


Figure 3.26: Live/dead assay. CLSM Z stacks 3D projections of 1.5 mil/mL OECs encapsulated in 0,1-0.4% RGD peptide grafted epimerized 1.0% Ca²⁺ alginate, non-peptide grafted epimerized 1.0% Ca²⁺ alginate and 1.0% UP-LVG Ca²⁺ alginate. Green fluorescence indicates live cells as opposed to red fluorescence, which indicates dead cells. Several capsules are shown in each picture. A 10x objective was used for image acquisition and the size bar is 200μm. In the picture of UP-LVG capsules with serum at day 28 the capsules are moving during picture acquisition, which caused the cell clusters to appear larger than they really were.

At day 1 batch H3+ and H3- (capsules made with 1.0% UP-LVG) displayed the lowest viability of 70% and 60% live cells respectively. The other batches with capsules made of epimerized alginate all displayed viabilities >70%.

No apparent improvement in cell viability could be observed in the epimerized alginate capsules cultured in media containing serum, in fact, the lowest viability of all batches was displayed by the cells encapsulated in epimerized non-peptide grafted alginate cultured in OEC media with serum.

There may have been a small difference in viability of the cells encapsulated in UP-LVG alginate, with and without media as the estimated percentage of live cells were 80% and 65% when the experiment was terminated, respectively.

An estimate of live cell percentage in all batches is presented in figure 3.27.

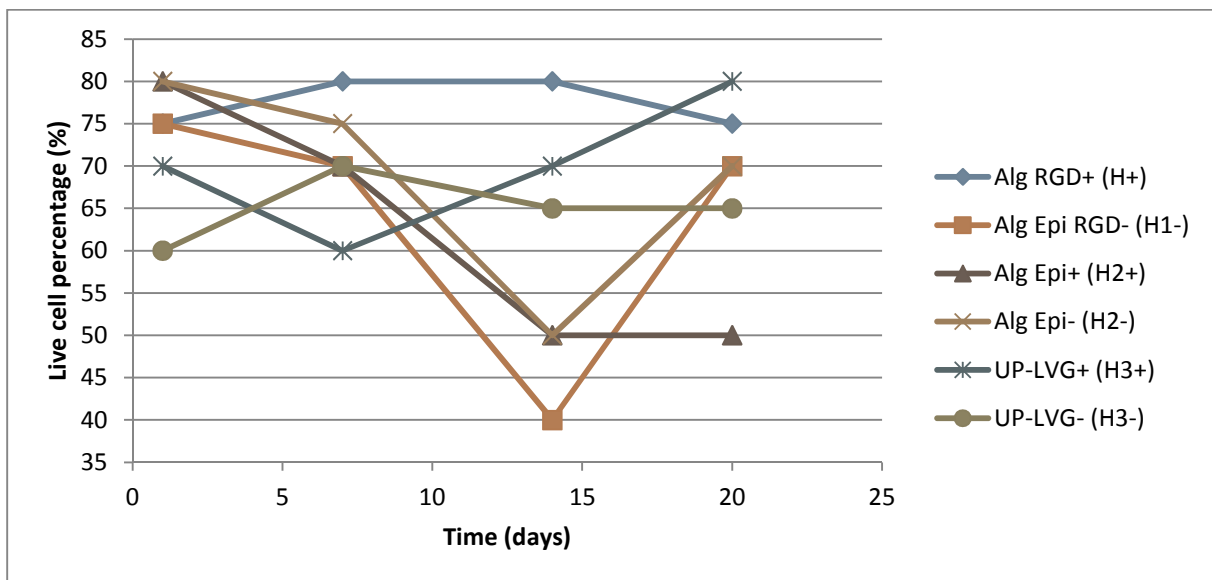


Figure 3.27: An estimated percentage of live OECs encapsulated in in 0,1-0.4% RGD peptide grafted 1.0% epimerized Ca^{2+} alginate, non-peptide grafted 1.0% epimerized Ca^{2+} alginate and 1.0% UP-LVG Ca^{2+} alginate, based on figure 3.26. The + and - designates whether the cells were cultured in serum with or without serum, respectively.

3.9. Actin filament and nucleus staining

Alexa Fluor 488® phalloidin and DRAQ5™ was used to stain F-actin and nuclear DNA, respectively. The fluorescent staining was examined by CLSM. The purpose of this staining was to detect eventual morphological changes in OECs due to encapsulation in RGD peptide grafted alginate (batch H1+ and H1-), and cells encapsulated in alginate mixed with ECM molecules and sulphated alginate (batch G1, G2, G3, G4 AND G5). No consistent morphological changes were observed in any sample. Most cells displayed a circular morphology and one example is given in figure 3.28. Some cells were of irregular shape, but these were not limited to any specific environment and were randomly distributed between the batches, both G and H.

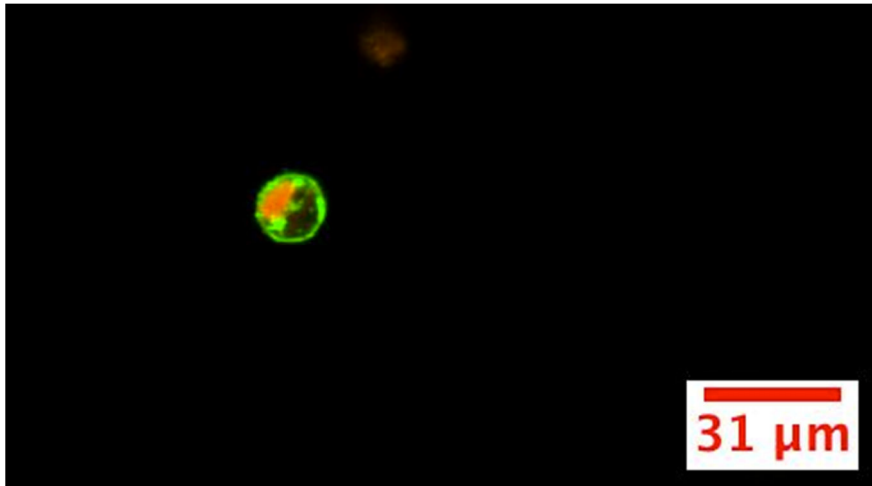


Figure 3.28: Actin filament (Phalloidin, green) and nucleus staining (DRAQ5, red) of OEC in 1.0% UP-LVG alginate mixed with 1mg/mL laminin capsule at day 28. The picture was obtained by CLSM cross-sections through the equator of the capsule. A 40x objective was used for image acquisition and the size bar is 31μm.

Most cells appeared in clusters, as can be seen in figure 3.30. In some cells DNA seemed to be located outside the actin perimeter, these were believed to be dead cells in various states of degradation. Overlap between green and red colour can be observed.

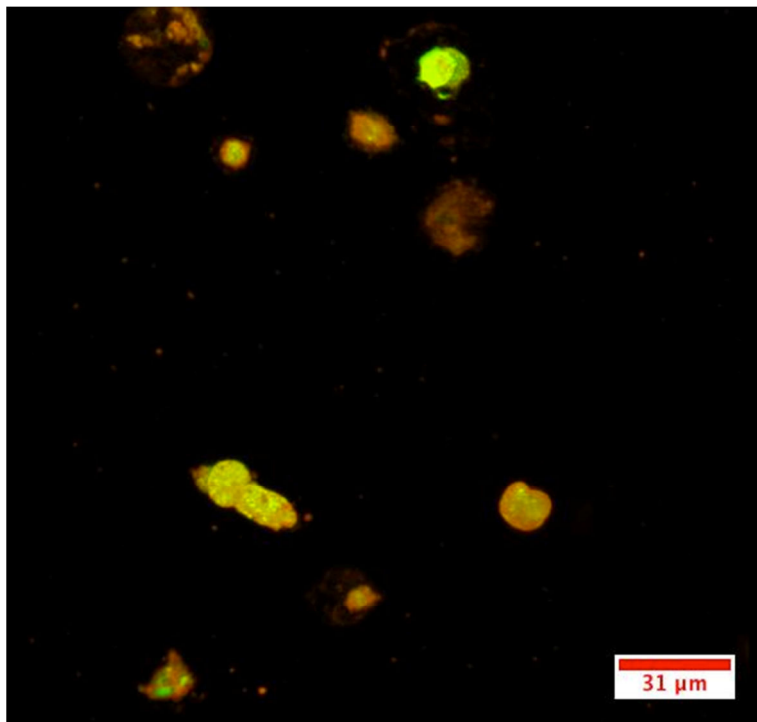


Figure 3.30: Actin filament (Phalloidin, green) and nucleus staining (DRAQ5, red) of OEC clusters encapsulated in 1.0% UP-LVG mixed with 1.0 mg/mL collagen (batch G4). The picture was obtained by CLSM cross-sections through the equator of the capsule at day 15. A 40x objective was used for image acquisition and the size bar is 31μm.

3.10. Bubble formation around cell clusters

In several capsules a bubble shape around the encapsulated cells similar to that shown in figure 3.31 appeared. This could be caused by excretion of some substance from the cells that dissolve the alginate gel around them, creating a softer environment, or it may be caused by shrinking cells.



Figure 3.31: Picture of OEC cultured in 1.0% UP-LVG capsule in media without serum, obtained at day 20. Around the cell a bubble shape can be observed. The picture was obtained by CLSM cross-sections through the equator of capsules overlaid with transmitted light. A 40x objective was used for image acquisition and the size bar is 35μm.

3.11. alamarBlue® and MTT assay

The alamar Blue assay® was performed on the cells encapsulated in the experiments described in section 3.1, 3.2, 3.3, 3.4 and 3.5 with the aim of quantitatively assess the cells viability and metabolic activity. It was decided to omit this assay in further encapsulations (3.6, 2.7 and 3.8) because the fluorescence values often turned out negative for samples from the lowest cell concentrations (1.5 mil/mL) when the control sample of pure media from the corresponding culture flask were subtracted. Method 1 described in Materials and Methods section 2.51 was applied on the cells encapsulated in experiment 3.1 and 3.2, which are described below. The method is elaborated in appendix A1, and the fluorescence values and calculations are shown in A2. The graph is shown in appendix A3.

In experiment 3.1 different concentrations of OECs were encapsulated in 1.8% UP-LVG capsules, and their viability was tested with both Live/Dead assay and alamar Blue assay®. The protocol described as Method 1 was applied on these batches.

It can be observed from figure 3.31 that the levels of fluorescence were rapidly declining during the period of 14 days, and higher signals in these samples compared to control resulted in positive values throughout the experiment.

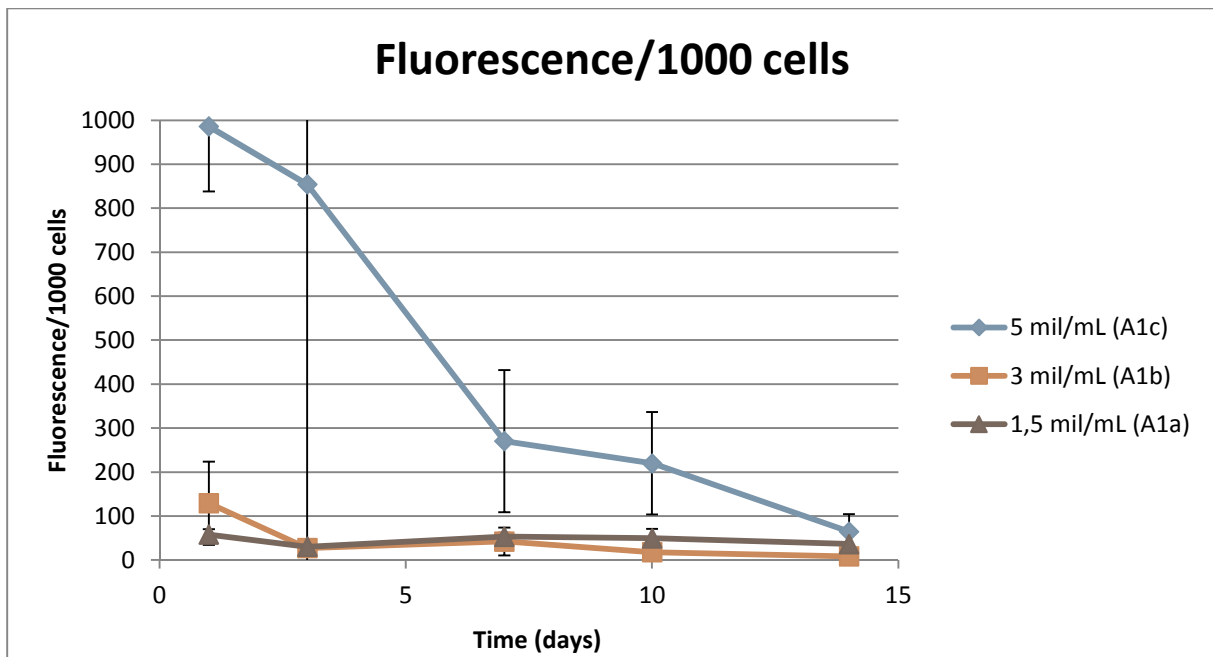


Figure 3.31. Graph showing fluorescence values/1000 cells from alamarBlue® assay performed on cells from encapsulation A1a, A1b and A1c (different OEC concentration encapsulated in 1.8% UP-LVG alginate.)

The results coincided with the results obtained in the Live/Dead assay, which was performed simultaneously in terms of reduced viability over time and the very rapid decline in viability of batch A1c, as can be observed in figure 3.2. The alamarBlue® assay might not illustrate the correct relationship between the cell concentration in the different batches as batch A1b were so close to A1a in fluorescence value, and should display values in the middle of A1a and A1c in terms of cell concentration. This may be due to low viability of the cells in batch A1b, and there were indications of low viability of cells in this batch in the Live/Dead assay. On day 7 in figure 3.2, batch A1b display low viability compared to the other two batches.

In contrast to the alamarBlue® assays performed on later batches, all sample fluorescence values in this experiment were larger than the control sample, giving positive results when the control sample was subtracted.

In the next experiments (3.2, 3.3, 3.4 and 3.5) problems with background values higher than the signals from cell containing samples were experienced, as well as low correlation with the results from the Live/Dead assay were experienced. The problems that were faced in experiment 3.2 is further elaborated in appendix A4. The calculations and fluorescence values are found in appendix A5, while a graph depicting the fluorescence values over time can be found in appendix A6.

The difficulties that were experienced with the alamarBlue® assay during experiment 3.2 spurred a test round, in which OECs encapsulated in 1.0% UP-LVG with a concentration of 1.5 mil/mL were utilized as a test subject. Four different protocols were tested, in addition to the regular protocol described as method 1 in section 2.51 the Materials and Methods chapter.

Briefly explained, method 1 involved withdrawal of five parallels of media (180µl) with capsules from each culture flask, as well as control samples from the corresponding culture flask (180µL of only media). The samples were transferred to a 96 well plate and added 10% of alamarBlue® reagent (18µL) before incubation in RT for four hours.

Method 2 was identical with method 1 in all but one detail, incubation in RT for six hours instead of four. This increased fluorescence values in both samples containing capsules and control samples, resulting in negative results still.

Method 3 was also similar with method 1, except that the incubation was done in an incubator at 37°C and 7% CO₂, which is the culture settings for OECs.

Method 4 included a volume of media and capsules corresponding to 50 000 cells were taken out from each culture flask and placed in a 6-well plate. Media from the corresponding culture flask was added to a total volume of 5,1 mL in each well. 0.51 mL of alamarBlue® reagent were added to each well in the 6-well plate. Five parallels of control samples with a volume of 180 µl were withdrawn from each culture flask and placed in a 96 well plate. The control samples were each added 18 µl alamarBlue® reagent and both the 6-well plate containing capsules and media and the 96-well plate containing controls were incubated in an incubator with 37°C and 7% CO₂. Five samples of 180 µl from each batch in the 6-well plate were withdrawn and placed in a 96-well plate at three time points; 2, 4 and 6 hours after incubation and their fluorescence was measured.

Method 5 After withdrawal of control samples (5 x 180µL with 5 x 18µL alamarBlue reagent added in a 96 well plate), 1 mL of alamarBlue® reagent were added directly to the culture flasks (total volume in flask: 10mL). The control samples and the culture flasks were incubated in an incubator with 37°C and 7% CO₂.

Five parallels of 180 µl were withdrawn from the flasks at three time points; 2, 4 and 6 hours and the samples were placed in a 96-well plate and the fluorescence intensity was measured.

The disadvantages and advantages with method 3, 4 and 5 are presented in table 9.

Table 9: Advantages and disadvantages of the three methods.

	Method 3	Method 4	Method 5
Advantages	High sensitivity. Low contamination risk.	No counting of capsules, less time-consuming than Method 3.	No counting of capsules, less time-consuming than Method 3. Positive fluorescence values after two hours, because of the large cell number.
Disadvantages	Time-consuming. Occasionally background signals higher than signals from samples. Counting of capsules, difficult when the capsule number exceeds 100.	Loss of many capsules every time the assay is performed. Lack of sensitivity, due to ten times higher cell number the recommended by Invitrogen. Low fluorescence per cell compared to Method 3.	Potential contamination of the whole batch. Potential harmful effects of the alamarBlue® reagent on the cultured cells. Total media exchange every time the assay is performed, expensive and time-consuming. Lack of sensitivity, due to very high cell numbers compared to the number recommended by Invitrogen (5000 cells). Low fluorescence per cell compared to Method 3. Potential saturation of the reagent due to high cell numbers.

It was decided to use method 3 when taking all considerations in account, and thus accept that some fluorescent values would become negative. In the next experiments (3.4 and 3.5) negative values were experienced to such a degree that the results of these alamarBlue® assays can be found in appendix A7, A8, A9 and A10 as they were discarded due lack of relevance.

As one last test of the alamarBlue® assay, it was decided to compare it with another viability assay, the MTT assay. The fluorescence values and calculations that led to figure 3.32 can be found in appendix B3 and B4. Figure 3.32 clearly shows the negative fluorescence values for the alamarBlue® assay, while figure 3.33 displays positive absorbance values for the MTT assay, even though the numbers were low. The values are also increasing with time, which appears illogical as the viability of OECs have been shown to decrease over time when encapsulated.

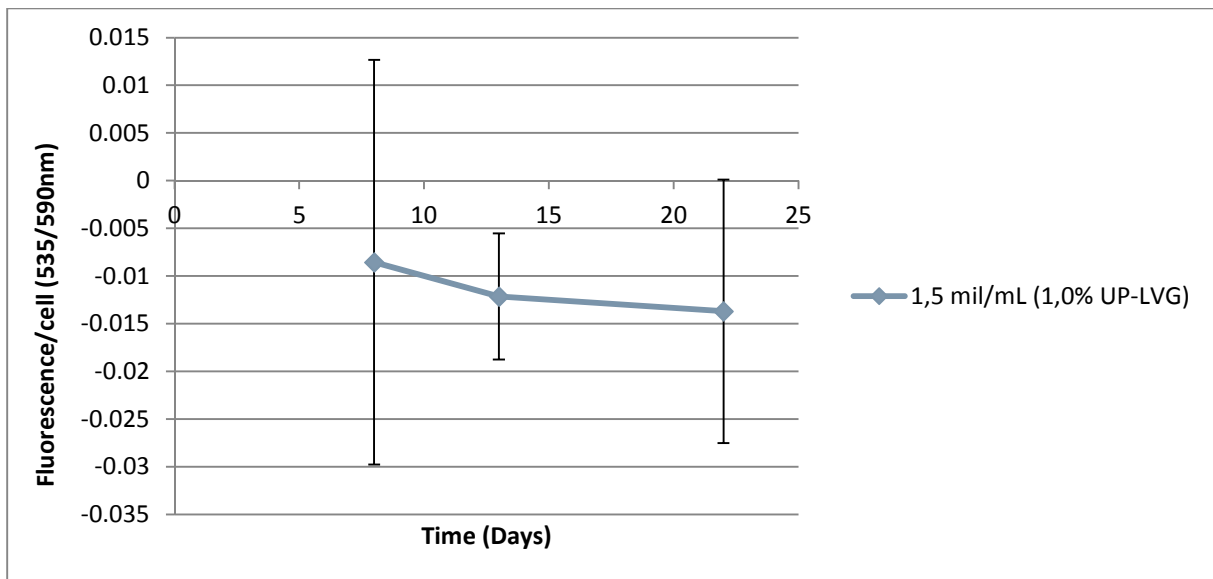


Figure 3.32: alamarBlue® fluorescence values from 1.5 mil/mL OECs encapsulated in 1.0% UP-LVG alginate obtained at day 8, 13 and 22.

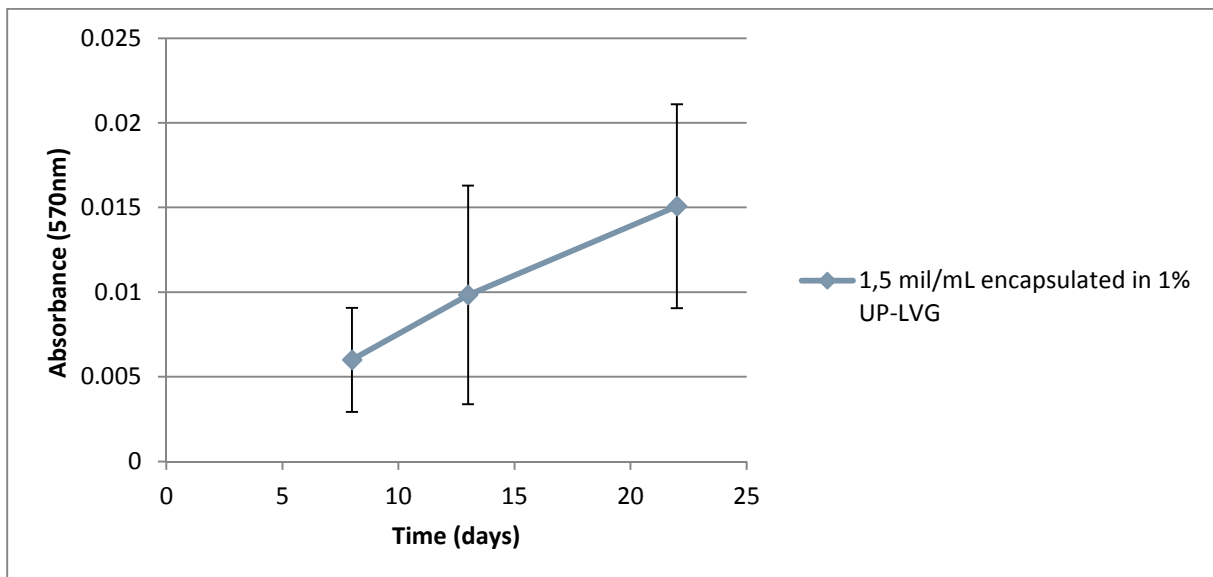


Figure 3.33: MTT absorbance values from on average 40 capsules. 1.5 mil/mL OECs encapsulated in 1.0% UP-LVG alginate obtained at day 8, 13 and 22.

The absorbance values and calculations that led to figure 3.33 can be viewed in appendix B1 and B2 shows the graph. Figure 3.34 shows the Live/Dead assay that was performed simultaneously with the alamarBlue assay and MTT assay. The Live/DEAD assay shows good viability on day 8, very few cell clusters, but few dead cells at day 13 and then again, good viability at day 22. The small amount of clusters at day 13 may be due to a smaller capsule number in the picture. The results support the MTT assay in that the viability is good, but shows no sign of increasing, which is not expected when culturing OECs in 3D capsules.

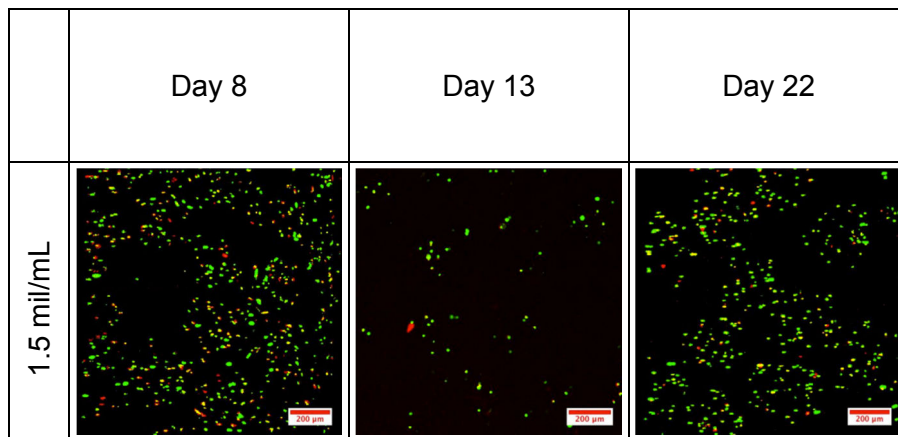


Figure 3.34: The Live/Dead assay performed on 1.5 mil/mL OECs encapsulated in 1.0% UP-LVG $\text{Ca}^{2+}/\text{Ba}^{2+}$ alginate, concurrent with the MTT and alamarBlue® assay. Green fluorescence indicates live cells as opposed to red fluorescence, which indicates dead cells. Several capsules are shown in each picture. A 10x objective was used for image acquisition and the size bar is 200µm.

3.12. Capsule stability

The stability of the capsules was tested in different solutions; pure water, 0,9 % NaCl, MG lyase, citrate and EDTA. The goal was to assess the gel strength and also to find a gentle capsule dissolver that did not harm the cells, in case the cells needed to be extracted from capsules.

Pure water

OECs encapsulated in 1.0% epimerised Ca^{2+} alginate capsules were placed in sterile water in room temperature for 1.5 hours, and checked in a light microscope every 10 minutes. No changes in capsule stability was observed after 1.5 hours.

0.9% NaCl

OECs encapsulated in 1.0% epimerised Ca^{2+} alginate capsules were placed in sterile 0.9% NaCl in room temperature and the capsule stability was checked in a light microscope at 10x magnification every 10 minutes. After 30 minutes, all capsules had dissolved.

The capsules tested with sterile water and NaCl were both made with gelling solution containing only Ca^{2+} ions.

MG lyase

MG lyase enzyme (8 units/mL) solved in 1 mL PBS was added to 0.5 mL batch C1a capsules (1.0 mil/mL OECs encapsulated in 1.0% UP-LVG $\text{Ca}^{2+}/\text{Ba}^{2+}$ alginate) suspended in 4 mL OEC growth media, and incubated in an incubator with 37°C and 7% CO_2 for three days. No effect on the capsules was observed on capsule stability in a light microscope at 10x magnification.

Citrate

1 mL 50 mM citrate solution was added to 200 μ L suspension of batch C1a (1.0 mil/mL OECs encapsulated in 1.0% UP-LVG $\text{Ca}^{2+}/\text{Ba}^{2+}$ alginate) capsules in 1mL HBSS. The capsules were monitored in a light microscope at 10x magnification every 5 minutes for 25 minutes. For every 5 minutes without any dissolving capsules, another 1 mL of citrate solution was added to the capsules. After 25 minutes and a total of 5 mL citrate solution, no effect on capsule stability could be observed.

EDTA

600 μ L of 50 mM EDTA was added to 100 μ L of batch C1a capsules suspended in 1 mL OEC growth media, and were monitored in a light microscope at 10x magnification after 1 minute, because after 1 minute all capsules had dissolved.

4. Discussion

4.1. Cell viability

One of the major aims of the study was to investigate whether encapsulation of OECs in different types of alginate would improve cell viability over time. Viability of OECs up to 14 days in 1.8% UP-LVG Ca^{2+} alginate capsules have been reported by Kristin Karstensen (Karstensen, 2010), and similar results were achieved in this study. At day 14 very few cells inside the 1.8% UP-LVG $\text{Ca}^{2+}/\text{Ba}^{2+}$ alginate gel capsules were viable in any of the three batches with different cell concentration, although 1.5 mil/mL displayed better viability during the 14 days than 3.0 mil/mL and 5.0 mil/mL (figure 3.2 and 3.3).

Two concentrations of OECs (1.5 mil/mL and 5.0 mil/mL) were further encapsulated in 1.0% epimerized Ca^{2+} alginate gel (figure 3.5 and 3.6), with (B2) and without (B1) 0.2 % RGD peptide graft. The viability of the cells was extended with one week compared to cells encapsulated in 1.8% UP-LVG $\text{Ca}^{2+}/\text{Ba}^{2+}$ alginate gel, and the experiment was terminated after 22 days. In this experiment the viability as a result of cell concentration was less pronounced as both 1.5 mil/mL batches displayed 70% and 30% viability after 22 days in culture, respectively. The two batches with 5.0 mil/mL cell concentration displayed an average live cell percentage of 45%, after 22 days in culture. This experiment was therefore inconclusive in terms of improved viability connected to cell concentration, but indicated that a lower alginate concentration had a beneficial impact on cell viability. The experiment did not show a clear significance of the RGD peptide on cell viability.

Star shaped channels were observed inside all capsules in this experiment, and a large fraction of dead cells were found to be located inside these channels. This was also found by Kristin Karstensen in her study (Karstensen, 2010). This experiment was later repeated in experiment 3.8 with another source of epimerized alginate grafted with $\approx 0.4\%$ RGD peptide, which will be discussed below.

It was thus decided to conduct an encapsulation of 1.5 mil/mL and 5.0 mil/mL OEC concentration in 1.0% UP-LVG alginate (figure 3.9 and 3.10), with the aim of examining whether it was the reduced alginate concentration that improved cell viability, or if viability depended on the composition of the epimerized alginate. As most of the dead cells observed in the experiment with OECs encapsulated in 1.0% epimerized Ca^{2+} alginate gel were located inside the aforementioned channels, it was also of interest to examine cell viability without the channel formation that was observed in the epimerized alginate, but with similar alginate concentration, as channel formation did not occur in the UP-LVG $\text{Ca}^{2+}/\text{Ba}^{2+}$ alginate capsules. The results were promising, with a stable live cell percentage of 60% in the C1a batch after 51 days. Batch C1b was discarded after 22 days with estimated 30% live cells. This result strengthened the hypothesis that lower cell concentration enhanced cell viability, and confirmed that lower alginate concentration improved cell viability

notably. Experiment 3.3 (figure 3.9 and 3.10), and 3.4 (figure 3.12 and 3.12) both supported this hypothesis.

The viable cell percentage on day 1 provides an indication of how well the cells have tolerated the encapsulation process. A factor that can influence the cell viability during encapsulation is shear forces in the cell-alginate mix during mixing, as the shear forces may damage the plasma membrane. The shear forces will vary in terms of molecular weight of the alginate as well as the alginate concentration, as the shear forces increase proportionally with the solution's viscosity (Lee and Mooney, 2012). Another factor may be the swiftness of execution of the encapsulation procedure; if the cells are kept in room temperature too long or stored in solutions other than OEC growth media for long periods, it may reduce cell viability.

The live cell percentage varied from 70% to 90% in the 1.8% UP-LVG capsules, and from 50% to 60% in the 1.0% UP-LVG alginate capsules at day 1 post encapsulation. This did not coincide with theory in terms of lower shear rates expected with lower alginate concentration, but in the 1.0% UP-LVG alginate capsules the viability increased during the project. The cell viability only decreased over time for the cells in the 1.8% UP-LVG alginate capsules.

The cells in the 1.0% epimerized alginate capsules (3.2 and 3.8) displayed overall high live cell percentages of $\geq 80\%$. The high cell viability in these two experiments may be caused by lower viscosity or be due to a more effective encapsulation process. The capsules mixed with gelatin (3.5 and 3.6) displayed 60% and on average 65% live cell percentage after encapsulation, respectively, and the relatively low cell viability might have been caused by the heating of the solutions, implemented to avoid gelling of the gelatin during the encapsulation process, at least in experiment 3.6 where both the gelling solution and gelatin alginate mix was kept at 40°C for as long as possible.

The cells in the 0.9% UP-LVG alginate capsules mixed with ECM molecules displayed an overall high viability, and the same held true for the 0.9% UP-LVG alginate mixed with sulphated alginate. These mixes displayed higher cell viabilities than pure 1.0% UP-LVG alginate capsules at day 1, and this might be explained by less viscosity in the solution before encapsulation, due to lower alginate concentration.

The cell concentration appeared to be varying from experiment to experiment. This may be caused by insufficient centrifugation of cells before encapsulation.

It must be noted that all analysis of viability data are rough qualitative estimates of Live/Dead ratios from CLSM pictures with varying numbers of capsules present. It could have been beneficial to utilize software for these estimates, but this was not implemented during this study. The estimate tables are given in appendix C. The

alamarBlue® assay meant to provide a quantitative measurement of metabolic activity did not work satisfactorily during this project, and this is discussed below.

4.1.1. Alginate concentration

The elastic moduli of a gel has been shown to increase proportionally with the square of the alginate concentration (Smidsrød, 1972), and thus also the gel stiffness (Martinsen et al., 1989a) and gel strength (personal communication from Dr. Ing. Berit Strand, 05.05.2012). This is illustrated in figure 4.1.

The UP-LVG alginate used in this study had an average G – block length of $N_{G>1} = 12$ and a G monomer fraction of 0.67. The two epimerized alginates utilized in experiment B has an average G block length of $N_{G>1} = 4,5$ and a G monomer fraction of 0.54. Referring to figure 4.1 it is therefore likely that the stiffness of the gel increases more prominently for UP-LVG gel when increasing the alginate concentration, than for the epimerized alginate gel. This is explained by the fact that more junctions will be created between the alginate chains in the high G gel, creating a more rigid and open network structure with larger pores. The epimerized alginate is composed of MG and G blocks with a few M blocks interspersed, and will create a more elastic and compact gel (Morch et al., 2007, Morch et al., 2008).

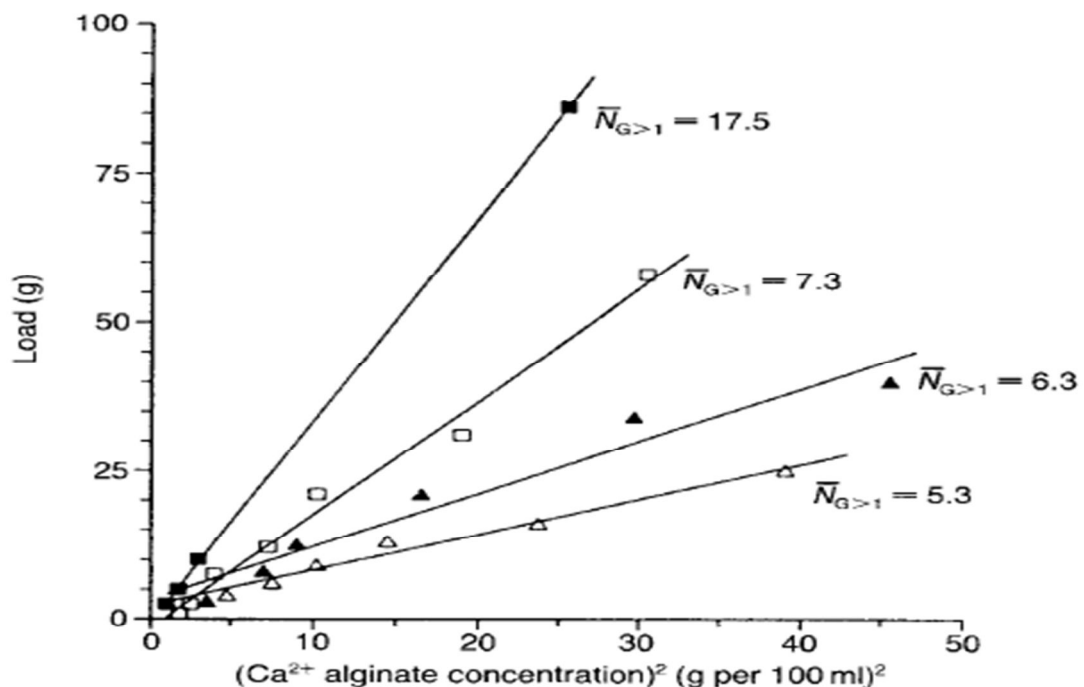


Figure 4.1: Graph showing the increase in rigidity (load (g) needed to compress the alginate gel with 1 mm), versus the square of the alginate concentration (directly reproduced from (Smidsrod and Skjak-Braek, 1990)).

The elasticity of the epimerized alginate gel is described by experiments where the elastic moduli have been investigated. These experiments show that while the high G gel is stiff (e.g. has a high elastic moduli), it is also brittle and will rupture under

pressure. Gels containing MG-blocks will have lower elastic moduli, but higher rupture strength (Mitchell and Blanshard, 1976) (Mitchell, 1980). The rupture strength increases proportionally with the molecular weight of the polymer (Moe, 1995).

It is therefore hypothesized that a gel made from 1.0% epimerized alginate is softer, more compact and elastic than a gel made of 1.0% UP-LVG alginate and the latter will possess a more rigid and open chain network with larger pores (Smidsrod and Skjak-Braek, 1990).

The gel strength is also dependent on the molecular weight of the polymer, but only to a certain extent. When the M_w is large enough to produce an intrinsic viscosity of 550-600 mL/g the gel strength becomes constant and independent of M_w (Martinsen et al., 1989a). This holds true as long as the gel is Ca^{2+} saturated (Draget et al., 1993). All alginates used in this experiment are of high molecular weight, and were gelled in gelling solution containing an abundance of crosslinking ions. The gel strength, and thus, stiffness was therefore thought to be independent of molecular weight, and only related to alginate concentration and composition.

The OECs displayed highest viability in capsules with low cell concentration made from 1.0% UP-LVG alginate. It is therefore assumed that OECs demonstrate a preference for gels with an open network structure, which is soft due to low alginate concentration, than in a more compact but elastic gel. This suggests that less rigid biopolymer network structures might be utilized for OEC encapsulation for transplantation *in vivo*.

4.1.2. Alginate gel porosity

The cells displayed lower viability in the more compact epimerized alginate gel. This could in part perhaps be explained by lower diffusion rates due to less porosity and thus lower permeability of proteins required by the cells.

High G alginates have been reported to have the highest porosity and therefore the highest permeability. This is due to their open and rigid network, caused by many junctions between the polymer chains. Small molecules such as glucose and ethanol have diffusion rates up to 90% of the rates observed in pure water. Larger molecules such as proteins will experience diffusional resistance, depending on their charge, radius of gyration (R_G), molecular weight and shape (Smidsrod and Skjak-Braek, 1990). Most proteins are negatively charged at physiological pH, and will be repelled by the polyanionic alginate chains and this will decrease their diffusion rate in and out of alginate capsules (Smidsrod and Skjak-Braek, 1990). However, proteins with $M_w > 3 \cdot 10^5$ kDa have been shown to diffuse through high G gels, with a diffusion rate depending on their size, shape and pH of the solution (Martinsen et al., 1989b). Epimerized alginate has shown reduced permeability for immunoglobulin with molecular weight of 150 kDa (Morch et al., 2007).

It could be argued that the capsules in this study were so small (diameter ranging from approximately 250 μ m to 600 μ m) that the diffusional pathway for solutes was

short enough to secure satisfactory waste disposal and nutrition delivery (Colton, 1996).

Cell concentration was also shown to influence viability of the OECs, especially in UP-LVG capsules. Westrin and Axelsson reported that encapsulation of cells in gels hinders diffusion and that the diffusion rate decreases with increasing cell load (Westrin and Axelsson, 1991). This might partly explain the decreasing viability of cells in capsules containing higher cell concentrations, as the access to nutrition, oxygen and disposal of waste products is hindered by the decreased diffusion rates and the increase in competitors. Also, dead cells may have a negative effect on live cells in the capsule, as increased amounts of cellular waste accumulates in the restricted microenvironment in the capsule. Thus, a vicious cycle of cell death in capsules with large cell concentration occurs due to lower diffusion rates of nutrition, oxygen and waste products. The remains of the dead cells may create a toxic environment for the live cells in the capsule and low diffusion rate hinders the clearance of the cell remains, causing more cells to die.

Increased cell concentration did not affect cell viability as clearly in epimerized alginate capsules, and one explanation could be the elasticity of the material. The alginate chain network may give in for pressure created by larger amounts of cells and permit them to spread out and shape their environment, in a way the rigid UP-LVG gel may not permit. In the rigid high G gel high cell concentration may have created a limited and crowded environment. In contrast, increasing the alginate concentration and/or the cell concentration in UP-LVG alginate capsules will both result in lower viability as shown in figure 3.12, as the outcome is the same; a crowded and rigid limited living space where the cells are trapped in the chain network.

4.1.3. Structural differences between UP-LVG capsules and epimerized alginate capsules

Certain structural differences between the capsules made of UP-LVG and epimerized alginate I and II was observed. The latter displayed channels arranged in a star-like formation around the center of the capsule. These channels were presumed to be hollow, as dead cells appeared to fill the channels progressively through experiment 3.2 and to some extent, 3.8. An example can be viewed in figure 3.25.A. The channels appeared to push the surface of the capsule outwards, as can be observed in figure 3.22. This led to the hypothesis that the alginate gel forming the surface of channels was stiffer than the rest of the capsule.

Whether the cells were randomly trapped inside these channels or migrated there is not known. Some indications to that most cell clusters are located inside such channels were noted, and an example is shown in figure 3.22. This led to the hypothesis that the channels appear filled with dead cells because the clusters have disintegrated and their remains are trapped inside the channels. As the interior environment inside the channels is unknown, the reasons for the cells presence there

cannot be determined. It might be that the interior were perceived as less compact than the rest of the capsule, causing the cells to migrate there (as they have been shown to prefer softer gels) but the diffusion rate of nutrition and waste into the channels might be lower due to the assumed stiff surface of the channel. This would also explain the build-up of dead cell debris inside the channels.

It has been suggested that the channels are formed by a viscous drag that may have occurred during gelling, and the channels are assumed to contain lower gel concentration (personal communication from Dr. Ing. Berit Strand and unpublished results from Kristin Karstensens research).

4.1.4. RGD peptide grafted alginate I and II

In experiment 3.2, high and low cell concentrations (1.5 mil/mL and 5.0 mil/mL) were encapsulated in 1.0% epimerized Ca^{2+} alginate grafted with 0.2% RGD peptide and epimerised with AlgE4 and AlgE6, creating an alginate consisting of MG and G blocks interspersed with M-blocks. A similar alginate without RGD peptide was included as control samples. The experiment was repeated (experiment 3.8), with a similar alginate from a different source and with only 1.5 mil/mL cell concentration with an added control sample of 1.0% UP-LVG capsules and a probable RGD peptide graft percentage of 0.4%.

All cells displayed high viability with live cell percentage > 80% up until day 10 in experiment 3.2, regardless of batch. After day 10 the viability of the cells in the 1.5 mil/mL cells concentration encapsulated in epimerized alginate without RGD peptide and the 5.0 mil/ mL cell concentration encapsulated in epimerized alginate with RGD peptide decreased quite suddenly from $\approx 80\%$ to 40% and 30% at day 14, respectively, compared to the other two batches in which the viability decreased more gradually (figure 3.5 and 3.6).

In this experiment no evident differences in cell viability was observed, in terms of either RGD peptide or cell concentration. The reason for the sudden decrease in cell viability in two of the batches at day 10 is not known.

The cells in experiment 3.2 displayed a more uniform high viability with a live cell percentage $\geq 80\%$, up until day 10 than the cells in experiment 3.8 (figure 3.6 and 3.27). However, after day 10 the viability decreased to $\leq 50\%$ at day 22 for all samples, except the epimerized 1.0% Ca^{2+} alginate gel capsules containing 1.5 mil/mL, which displayed 70% viable cells at day 22. In experiment 3.8 the epimerised 1.0% Ca^{2+} alginate gel capsules with $\approx 0.4\%$ RGD peptide graft cultured in serum-containing media displayed $\geq 70\%$ viable cells throughout the 20 days of the experiment, with the exception of day 14 when the live cell percentage was estimated to 50%. The epimerised 1.0% Ca^{2+} alginate gel capsules without RGD peptide cultured in serum-containing media displayed 80% live cells at day 1, and gradually decreased to 50% live cells at day 14 and this percentage was constant until termination at day 20. The increased viability in the RGD peptide grafted alginate gel capsules may be due to higher concentration of RGD peptide in the alginate utilized

in experiment 3.8. It must however be noted that no such effect was observed in the corresponding batches cultured in media without serum. Also, only one capsule were shown in the picture of epimerized 1.0% Ca^{2+} alginate gel capsules without RGD peptide cultured in serum-containing media at day 20, giving a poor estimate of viability in these capsules.

It has been reported that cell ligand density must exceed a cell specific density threshold before they are able to elicit any reaction from the cells (Lee and Mooney, 2012). As the RGD peptide fraction of the alginate was 0.2%, and $\approx 0.4\%$ the ligands may have been placed too far from each other on the alginate chain network to reach this threshold, and consequently unable to impact the viability of the cells. In addition, the length of the spacer arm between the RGD peptide and the alginate chain is a key parameter for integrin attachment and at least four glycine residues is regarded as an appropriate number to promote a proper binding between integrin receptors and RGD peptides in fibroblasts in both 2D and 3D culture (Lee and Mooney, 2012). In this project the number of glycine residues in the spacer arm was only one glycine, and the short spacer length may be a part of the explanation for not observing any interaction between the OEC integrins and RGD peptides, and no impact on viability of the OECs.

Kristin Karstensen (Karstensen, 2010) observed OEC attachment to RGD peptide alginates in 2D culture in her master thesis, using the same alginate (1.8% epimerized Ca^{2+} alginate with RGD peptide) as in this experiment. The OECs displayed a round morphology with bipolar protrusions attached to the substrate. The attachment decreased after 72 hours. Karstensen encapsulated OECs in the same alginate with 1.8% alginate concentration and did not observe any improved cell viability as a result of OEC interaction with the RGD peptide coupled alginates. Viable cells were found in the capsules up to approximately day 16, which correlates to the viability of cells in 1.8% UP-LVG alginate observed in this experiment. This may indicate that the alginate concentration is more important than the alginate composition.

The alginate concentration that was used in experiment 3.2 and 3.8 was lower than the concentration Karstensen utilized (1.0% versus 1.8%) and it is therefore plausible that the RGD peptide had even lower density in the gel in these experiments than they displayed in Karstensen's experiment.

The only difference between this study and Kristin Karstensen's study was that the cells showed an increased viability over time and thus, resided longer in the capsules. As no interaction was detected, the extended stay did not seem to improve the chance of interaction. It is also believed that cell-matrix interactions happen quite quickly (personal communication, Dr. Ing. Berit Strand 07.05.12) and Karstensen observed attachment of cells to RGD peptide after 24 hours (Karstensen, 2010).

4.2. Alginate mixed with ECM molecules

4.2.1. 1.0% UP-LVG alginate mixed with gelatin

Two experiments (3.5 and 3.6) with three different concentrations of gelatin (0.5%, 1.0% and 2.0%) mixed with 1.0% UP-LVG was conducted. It was hypothesized that gelatin would resemble collagen, which is the most abundant protein in the connective tissue. OECs were encapsulated with a concentration of 1.5 mil/mL alginate and kept in culture for 22 days in experiment 3.5. Experiment 3.6 focused mostly on improving the encapsulation process, and the cells were kept in culture for 16 days. In both experiments the cells displayed high viability regardless of gelatin concentration, comparable to the viability of 1.5 mil/mL encapsulated in 1.0% UP-LVG alginate gel.

The cells were cultured at 37°C, which is above the melting point for gelatin. It was therefore hypothesized that the gelatin did not contribute to gel formation, but were found dispersed as α -chains in the alginate gel (Babel, 1996) unlike collagen that is comprised of three different polypeptide α -chains intertwined in a triple helix conformation (Bruce Alberts, 2002). It was also hypothesized that gelatin α -chains might retain some of the RGD peptide domains present in collagen that integrins bind to. Integrin-mediated cell adhesion to these domains might have induced morphological change, but no morphological changes were observed in this experiment. As the gelatin was mixed with the alginate and not linked directly to it in any way, it might be proposed that if binding of integrins to RGD peptides occurred it would not lead to morphological changes as the gelatin chains were dispersed freely in the mixture. The cells might pull them along, instead of changing shape as they might have done if the gelatin had been fixed in the lattice.

Gelatine is thought to have a net positive charge at physiological pH, and this would probably lead to interaction with the polyanionic alginate chains (personal communication, Magnus Hattrem, 10.05.2012), perhaps rendering the RGD domains sterically unavailable for the OECs.

Assuming that less junctions between the alginate chains were formed, it would lead to an even softer gel than pure 1.0% UP-LVG alginate, and this may explain the relatively high cell viability observed in these experiments. In the alamarBlue® assay that was performed on these cells at the same time points as the Live/Dead assay the viability and metabolic activity seemed to be proportional with gelatin concentration as seen appendix A10. This could be explained by the auto-fluorescence of gelatin observed in both experiment 3.5 and 3.6, as alamarBlue® also utilizes fluorescence, or it could reflect the viability of the cells. A drawback with this assay is background signals higher than signals from samples registered for the lowest gelatin concentration, which casts doubt on the assays accuracy. The high background signals are further discussed below. No obvious differences in viability between the batches could be observed in the Live/Dead assay (figures 3.54 and 3.53).

The cell clusters in all samples in experiment 3.5 were larger than observed in any of the other experiments. This may be due to inadequate mixing of the cells with the alginate-gelatin solution before encapsulation, as the process had to be done rapidly to prevent the gelatin from gelling. This was taken into account when encapsulating in experiment 3.6, where mixing was done more thoroughly. This resulted in smaller cell clusters, but the cell clusters still appeared larger than the cell clusters observed in previous experiments. This might have been due to increased elasticity in the gel, enabling the clusters to spread out.

4.2.2. 1.0% UP-LVG mixed with different ECM molecules, and sulphated MG alginate

In experiment 3.7, four batches of 1.5 mil/mL OECs were encapsulated in 1.0% UP-LVG alginate gel with one ECM molecule mixed with the gel per batch. Sulphated MG alginate with an average of 1.5 sulphate groups per monomer (personal communication, Øystein Arlov) was included in the experiment. The sulphated alginate resemble the ECM protein heparin and to a lesser degree, HSPGs.

The experiment was terminated at day 28, with varying cell viabilities in the different samples. Common for all was an overall lower cell viability compared with the viability observed for cells with similar concentration encapsulated in pure 1.0% UP-LVG, but as no control sample with pure 1.0% UP-LVG alginate was cultured simultaneously, the samples cannot be directly compared.

The reason for the reduced viability is not known. All of the proteins mixed with the alginate are quite large, as all of them have a molecular weight over $3 \cdot 10^5$ Da, while hyaluronic acid ranges from $5 \cdot 10^3$ - $2 \cdot 10^6$ Da (Deister et al., 2007). A hypothesis could be that the large molecules block the pores in the alginate and decrease the diffusion rate of solutes as mentioned above. The drawback of this theory is that the gelatin-alginate mix displayed rather good viabilities, despite the fact that gelatin has a molecular weight of $9,5 \cdot 10^5$. Perhaps gelatin interrupts junction formation, and thus creates a softer elastic gel or interacts with the alginate in a different way due to its net positive charge, while the ECM molecules do not interrupt junction formation and just block the pores. Also, the concentration of gelatin was much higher, 0.5-2 % per 1.0% alginate and is therefore not directly comparable. High concentrations of heparin has been shown to kill cancer cells (personal communication, Øystein Arlov, 14.05.2012), but these concentrations are believed to be much higher than the sulphate concentrations utilized in this project.

As most proteins have a net negative charge at neutral pH (Smidsrod and Skjak-Braek, 1990) it is assumed that collagen, fibronectin and laminin will not interact with the polyanionic alginate chains. This might support that the proteins do not interfere with junction formation and merely clogs the pores, obstructing diffusion. As hyaluronic acid is highly negatively charged (Picart et al., 2001), the same hypothesis applies to hyaluronic acid.

Laminin has been reported to destabilize Ca^{2+} crosslinked alginate chains, as laminin has high affinity for calcium ions (Tisay and Key, 1999). This was not observed during the 28 days of the experiment, as the alginate beads stayed relatively intact compared to the other batches for the duration of the experiment.

The cell clusters in the sulphated alginate capsules appear larger than in the capsules without sulphate. This may be due to insufficient mixing of cells and alginate before encapsulation. Another hypothesis is that the MG composition of the sulphated alginate creates a more elastic gel, allowing the cells to form their environment and spread out in a way that was not possible in the rigid pure UP-LVG alginate gel. The cells displayed good viability up until day 20, where the estimated percentage of live cells was 80%. At day 28 this had dropped to 50%. The reason for this is not known, but it can be hypothesized that the high sulphate content compared to heparin is decrease cell viability.

4.3. Morphology

It is of interest to acquire knowledge of which matrices that induces change from circular cell morphology to stellate- or spindle-like morphology. The different morphologies are associated with different protein expression and secretion, and therefore the type of morphology will indicate the type of benefits to be derived from OEC transplantation after encapsulation and transplantation into CNS.

Several different approaches were attempted with the main aim of improving OEC viability. It was also attempted to observe cell-matrix interactions by CLSM. The cells were encapsulated in alginate with RGD peptide graft (experiment 3.2 and 3.8), alginate mixed with gelatin (experiment 3.5 and 3.6) and alginate mixed with one ECM molecule per batch, and sulphated MG alginate (experiment 3.7). None of these alginate compositions induced detectable changes in cell morphology. The cells were examined with CLSM with Live/Dead assay at both 10 x magnification and 40 x magnification. The actin and nucleus of the cells in experiment 3.7 and 3.8 were stained and examined and most of the cells were found to either gather in clusters, making it difficult to assess their morphology, or to be spherical. Some cells with non-circular shapes that were not associated with any known morphology were randomly distributed between the different experiments, but none was distinctly linked to one specific alginate variety.

As mentioned before, all ligands require a certain ligand density to elicit a cell reaction, and this density may not have been reached in these experiments. The gelatin and ECM molecules that were only mixed with alginate may not have provided a firm enough anchorage even if the cell may have attached to them; the attachment could cause the cell to drag the ligand along with it instead of changing morphology. Another explanation may be that the conformation of the ligands is different in the negatively charged alginate gel, and this might make the binding domains less sterically available for the cells.

4.4. Capsule stability

The capsules made from 1.8% UP-LVG $\text{Ca}^{2+}/\text{Ba}^{2+}$ alginate gel capsules were stable throughout the experiment (3.1) period of 14 days, with no observable swelling or syneresis. 1.0% UP-LVG capsules (3.3) were shown to be stable after 51 days in culture and no swelling or syneresis was observed. The diameter of 1.0% UP-LVG capsules proved to be smaller than the 1.8 % capsules, because of decreased viscosity in the alginate solution before gelling. The capsules with high cell concentration displayed a notably larger diameter than capsules with less cell concentration. This may be caused by reduced number of junctions between alginate chains due to high cell numbers (personal communication, Dr. Ing. Berit Strand, 14.05.2012).

High G gels have been shown to be stable over time, especially when crosslinked with Ba^{2+} ions in addition to Ca^{2+} ions. G-blocks have high affinity for Ba^{2+} ions that counteracts the exchange of crosslinking ions with other non-crosslinking ions, such as Na^+ . This hinders swelling and dissolution of capsules.

The epimerized Ca^{2+} alginate gel capsules utilized in experiment 3.2 was stable in culture for 22 days, with no observed swelling. This alginate was engineered to be crosslinked with Ca^+ without the need for Ba^{2+} ions to keep it stable. The alginate contains a large fraction of MG blocks ($F_{\text{MG}} = 0.35$), compared with UP-LVG alginate, which contains a MG fraction of 0.12. The high MG content counteracts swelling without the need of Ba^{2+} in the gelling solution (Morch et al., 2006). The epimerized alginate produced smaller capsules than the capsules observed in experiment 3.1. This might be caused by the epimerized alginates tendency to create smaller and more compact gels. It was also observed that the capsules containing high cell concentration appeared larger than the low cell concentration capsules, but to a lesser degree than the diameter difference observed in experiment 3.3. The star shaped channels described earlier was observed in all batches, and the mechanisms leading to these formations are not known. This is discussed more thoroughly earlier in the discussion part (4.1.3.). The channels did not appear to affect the capsule stability.

In experiment 3.5 and 3.6 different concentrations of gelatin (0.5%, 1.0% and 2.0%) was mixed with 1.0% UP-LVG alginate and gelled in the presence of Ca^{2+} and Ba^{2+} ions. The capsules from experiment 3.5 displayed increased instability and irregular shapes proportionally with increased gelatin concentration. However, in experiment 3.6 the alginate mixed with the middle gelatin concentration displayed the most circular and stable capsules. This may be due to better encapsulation routines, as the gelatin-alginate mix and gelling solution was kept at $\approx 40^\circ\text{C}$ as long as possible up until encapsulation.

In the capsules containing ECM molecules it was observed that the capsule diameter varied between the different samples. Capsules containing laminin and hyaluronic acid displayed the largest relative diameter, capsules containing fibronectin and

collagen were middle sized and sulphated alginate capsules were by far the smallest. The capsules containing fibronectin were the only batch that displayed a tail formation (figure 3.21). The reason for the variation in capsule size in the samples is not known.

White precipitation that increased over time was observed on the surface of the capsules made of 1.0% epimerized Ca^{2+} with $\approx 0.4\%$ RGD peptide graft in experiment 3.8. The precipitation occurred on the capsules cultured in OEC media containing serum, and the surface of these capsules appeared dark, wrinkled and cracked when observed by transmitted light in the CLSM. As the cells in these capsules displayed the highest viability throughout the period of the experiment, it is not believed that the precipitation affected cell viability negatively.

Precipitation was observed in the 1.0% epimerized Ca^{2+} capsules grown in media without serum as well, but to a much lesser degree. No surface precipitation was observed in capsules made of 1.0% epimerized Ca^{2+} alginate. It is therefore hypothesized that the precipitation is linked to protein content in the media, and RGD peptide grafted alginate. As no precipitation was observed with 0.2% RGD peptide content, it is proposed that the $\approx 0.4\%$ RGD peptide content led to precipitation when the capsules was cultured with protein-containing media. Some internal precipitation in roughly 1 out of 30 of the epimerized alginate capsules without RGD peptide was also observed (figure 3.25 B). This has been reported before and has been suggested to be linked with dead cells in the capsules (personal communication, Dr. Ing. Berit L. Strand). The internal precipitation was not observed until day 14 of the experiment and exclusively in capsules cultured in media without serum. The cells in both samples of epimerized alginate displayed decreasing viabilities from day 7 to day 10, independent of serum-containing media or not.

It could be proposed that the wrinkled and cracked surface of the epimerized alginate capsuled with RGD graft was caused by syneresis. The alginate did have $N_{G>1} = 3$, which was lower than the corresponding alginate in experiment 3.2, but the MG-block content was roughly similar (table 2.1) and no unambiguous sign of shrinking was observed during experiment 3.8. A similar local collapse of the gel upon binding of protein has been observed in beads coated with poly-L-lysine (Strand et al., 2002b).

It was attempted to dissolve 1.0% $\text{Ca}^{2+}/\text{Ba}^{2+}$ UP-LVG alginate capsules with MG lyase, citrate and EDTA. Only EDTA led to capsule dissolution, which is unfortunate in terms of cell extraction as EDTA is toxic for cells. 1.0% Ca^{2+} epimerized alginate capsules were attempted dissolved in pure water and 0.9% NaCl. The capsules did not dissolve in pure water, but did dissolve in 0.9% NaCl. The 1.0% $\text{Ca}^{2+}/\text{Ba}^{2+}$ UP-LVG alginate capsules are not believed to dissolve in 0.9% NaCl as the capsules were stored in this solution for weeks during the MTT assay, with no sign of effect on the capsules. It is proposed that Ba^{2+} crosslinking prevents disintegration caused by NaCl, and this is supported by literature (Morch et al., 2006, Morch et al., 2007)

4.5. alamarBlue®

The alamar Blue assay® was performed on the cells encapsulated in the experiments described in section 3.1, 3.2, 3.3, 3.4 and 3.5 with the aim of quantitatively assessing the cells metabolic activity. It was later decided to omit this assay in further encapsulations (3.6, 2.7 and 3.8) because the fluorescence values often turned out negative for samples from the lowest cell concentrations (1.5 mil/mL) when the control sample of pure media from the corresponding culture flask were subtracted from the fluorescence value of the sample.

Several different alamarBlue® protocols were tested during the project, but the assay did only work satisfactorily in experiment 3.1. In all other experiments the lowest cell concentrations produced background signals higher than signals from samples containing cells. The reason for this is not known, but it is hypothesized that the cells have a very low metabolic activity and do not proliferate when encapsulated. Why the OEC media produced such high fluorescence signals it not known, but contamination cannot be ruled out. Another source of error may be the alginate itself, it may bind the reagent and hinder its conversion to a fluorescent molecule.

The MTT assay showed increasing mitochondrial activity throughout the experiment, which implies that the cells either proliferated inside the capsules or increased their metabolomics activity. This is not expected when culturing OECs in 3D capsules, and has not been observed in previous experiments. The concurrent Live/Dead assay showed good overall viability of the cells, but it did not seem to increase. As the experience with MTT was limited to this test round it is not possible to assess its accuracy when assaying viability and metabolic activity of OECs, but the absorbance values were at least positive, however, the increasing viability and metabolic activity is not probable. It may be that the alginate displays some inherent absorbance, and one approach if this is the case is to include capsules without cells as a control sample.

Rokstad *et al* encapsulated endo cells in 1.8% Ca²⁺ UP-LVG alginate and used the MTT assay to measure survival and proliferation of the encapsulated cells, with good results. These cells proliferate when cultured in capsules, and this may explain why the MTT assay provides reliable results, as the cells display higher mitochondrial activity (Rokstad et al., 2003). Karstensen used the MTT assay on myoblasts encapsulated in 1.8% epimerized alginate with 0.2% RGD graft. The cells were expected to divide 1-2 times during encapsulation. The MTT values obtained during the experiment correlated generally well with Live/Dead staining observed by CLSM (Karstensen, 2010). Again, these were proliferating cells, but not to the same extent as in Rokstad's experiment.

4.6. Future perspectives

The percentage of RGD peptide graft coupled to the alginate chains should be increased, with the aim of gaining higher ligand density, and thus eliciting effects on the cell *via* integrin binding. It should also be attempted to increase the glycine

residue spacer length to at least four monomers in accordance to the findings of Mooney *et al* (Lee and Mooney, 2012).

It would also be interesting to observe whether the surface precipitation experienced in this project will occur on capsules with higher RGD peptide graft percentage. If so, the mechanisms behind the formation of precipitate should be investigated. As the capsule surface might collapse from protein adhesion on the surface due to low F_G fraction in the alginate, it could be beneficial to couple the RGD peptide to an alginate with higher $N_{G>1}$ number. This may also be beneficial for the OEC viability as they displayed higher viability in UP-LVG alginate gel, which has $N_{G>1} = 12$, in contrast to the epimerised alginate with $\approx 0.4\%$ RGD peptide that has $N_{G>1} = 3$.

The channel formation inside epimerized alginate capsules should be avoided, as increasing amounts of dead cells are observed inside these channels over time. It would also be interesting to examine the structure of these channels by using fluorescent alginate, which would indicate alginate concentration gradients throughout the capsule and reveal if the channels are hollow, as it has been suggested.

It would be interesting to observe whether the bubble formation described in section 3.10 was present from the beginning of encapsulations or formed over time. It would also be interesting to investigate whether the bubble formation occurred in both RGD peptide coupled gels and non-coupled gels.

The actin filament and nuclear DNA staining that was performed at day 20 and day 28 in this project should have been done earlier to ensure that the cells in the pictures were live cells, as the concurrent Live/Dead assay displayed many dead cells at the time. In addition, many of the cells with stained actin filament and nuclear DNA displayed stained DNA outside the actin boundaries of the cells, and thus they were perceived as dead, disintegrating cells.

As it is difficult to assess and quantify cell-matrix interaction in a 3D environment only with the aid of actin filament/nuclear DNA staining and Live/Dead assays perhaps another approach could be more effective. Mooney *et al* has proposed a FRET method where a fluorophore is be coupled to the cell adhesion peptides conjugated to the polymer chains and the cell membrane is be pre-stained with a another fluorophore. The cell receptor ligands can thus be quantified (Lee and Mooney, 2012).

The Live/Dead assay performed in this study aimed at a rough qualitative assessment of cell viabilities. It would be beneficial to utilize a software programme to assess the distribution of red and green cells in the CLSM 3D projections, as it would be more accurate and provide less variation in the assessment. The MTT and alamarBlue® assay should also be optimized for encapsulated OEC cells, to provide a quantitative measurement of the metabolic activity and cell viability.

The settings of the electrostatic bead generator should be optimized for lower alginate concentrations to ensure narrow size distribution of capsules and obtain capsules with a suitable diameter.

If encapsulation of cells in gelatin-alginate mix is attempted it would be interesting to investigate the capsules with scanning electron microscope (SEM) to assess whether the gelatin resembles collagen triple helices in the capsule.

If morphology changes of the OECs are observed, protein analysis should be performed to elucidate what proteins the cells are expressing. The different morphologies are associated with different protein expression and knowledge of the protein production of encapsulated OECs is important in terms of capsule design with the aim of cell-mediated repair of CNS lesions.

5. Conclusion

Alginate concentration was found to be the key parameter for the OECs viability in this project, as viable cells were observed for as long as 51 days in capsules with 1.0 mil/mL cell concentration in capsules made from 1.0% UP-LVG $\text{Ca}^{2+}/\text{Ba}^{2+}$ alginate. In 1.8% UP-LVG $\text{Ca}^{2+}/\text{Ba}^{2+}$ alginate capsules, viable cells were only observed for 14 days. In all subsequent experiments the 1.0% alginate concentration was utilized, and the capsules displayed viable cells for longer periods than 14 days. The beneficial effect of lower alginate concentration is assumed to be related to the resulting lower rigidity of the gel, and possible increased gel porosity and thus higher diffusion rates of nutrients, waste and oxygen. High cell concentration in the alginate capsules also proved to have an impact on cell viability, but this effect was most evident in the UP-LVG alginate gels. The negative effect on cell viability related to high cell concentration was not as profound in the epimerized Ca^{2+} alginate gels.

RGD peptide grafted onto alginate did not show any unambiguous effect on cell viability, regardless of 0.2 % peptide graft or $\approx 0.4\%$ peptide graft. The cell viability in capsules made of 1.0% UP-LVG $\text{Ca}^{2+}/\text{Ba}^{2+}$ alginate mixed with gelatin was overall high, and the major reason for cell death in these samples was capsule instability and consequently capsule breakage. The samples of capsules made of 0.9% UP-LVG alginate mixed with one ECM molecule, and 0.9% UP-LVG alginate mixed with sulphated alginate displayed overall lower cell viabilities than previous experiments performed with pure 1.0% UP-LVG alginate capsules.

No changes of morphology induced by the different types of alginate matrices were detected during this project. The RGD peptide grafted alginate may have failed to induce morphological changes due to low ligand density, short spacer arm or sterical hindrance, preventing the OECs integrins to attach to the RGD peptide. The gelatin-alginate mix also failed to induce morphology change in the OECs, and neither did any of the ECM molecule-alginate mixes or the sulphated alginate-alginate mix. This may have been due to sterical hindrance or unfortunate conformation of the gelatin.

All capsule varieties displayed generally good stability in culture, with the exception of the gelatin-alginate mix capsules that progressively dissolved. Precipitation that increased over time in culture occurred on the surface $\approx 0.4\%$ RGD peptide grafted epimerized alginate capsules. It is suggested that this precipitation is linked to the presence of protein in the culture media, and the increased RGD peptide content in relation the 0.2% RGD peptide grafted epimerized alginate capsules, where no such precipitation was observed. The binding of protein to the surface may have induced local collapse of the gel due to lower F_G fraction in the $\approx 0.4\%$ RGD peptide grafted epimerized alginate capsules compared to the 0.2% RGD peptide grafted epimerized alginate capsules, causing the observed wrinkled and cracked capsule surface.

The Live/Dead assay was found to perform satisfactorily throughout the project, giving reliable, yet rough estimates of cell viability. To provide a quantitative measurement of viability and metabolic activity the alamarBlue® assay was included

in the project. The alamarBlue® assay did not work satisfactorily as it produced background signals higher than signals from samples containing cells, especially for lower cell concentrations. The MTT assay was performed simultaneously as the alamarBlue® assay with the aim of comparing their results, and the results turned out to be opposite of each other. None of the metabolic assays seemed to correspond to the results obtained by the Live/Dead assay.

Literature

- A. ALOVSKAYA, T. A., J.B. PHILLIPS, V. KING, R.BROWN 2007. Fibronectin, Collagen, Fibrin -Components of Extracellular Matrix for Nerve regeneration. *Topics in Tissue Engineering*.
- ALBERT L. LEHNINGER, D. L. N., MICHAEL M. COX 2008. *Lehninger Principles of Biochemistry*, W.H. Freeman.
- AUGST, A. D., KONG, H. J. & MOONEY, D. J. 2006. Alginate hydrogels as biomaterials. *Macromol Biosci*, 6, 623-33.
- BABEL, W. 1996. Gelatine – A versatile Biopolymer. *Chemie in unserer Zeit*, 30, 86-95.
- BARNETT, S. C. & CHANG, L. 2004. Olfactory ensheathing cells and CNS repair: going solo or in need of a friend? *Trends in Neurosciences*, 27, 54-60.
- BJERKAN, T. M., LILLEHOV, B. E., STRAND, W. I., SKJAK-BRAEK, G., VALLA, S. & ERTESVAG, H. 2004. Construction and analyses of hybrid *Azotobacter vinelandii* mannuronan C-5 epimerases with new epimerization pattern characteristics. *Biochem J*, 381, 813-21.
- BRACCINI, I. & PEREZ, S. 2001. Molecular basis of C(2+)-induced gelation in alginates and pectins: the egg-box model revisited. *Biomacromolecules*, 2, 1089-96.
- BRUCE ALBERTS, A. J., JULIAN LEWIS, MARTIN RAFF, KEITH ROBERTS, AND PETER WALTER 2002. *Molecular Biology of the Cell* New York, Garland Science. Page 1131-1205.
- CAMPA, C., HOLTAN, S., NILSEN, N., BJERKAN, T. M., STOKKE, B. T. & SKJAK-BRAEK, G. 2004. Biochemical analysis of the processive mechanism for epimerization of alginate by mannuronan C-5 epimerase AlgE4. *Biochem J*, 381, 155-64.
- COLTON, C. K. 1995. Implantable biohybrid artificial organs. *Cell Transplant*, 4, 415-36.
- COLTON, C. K. 1996. Engineering challenges in cell-encapsulation technology. *Trends Biotechnol*, 14, 158-162.
- DAVID, S. & AGUAYO, A. J. 1985. Axonal regeneration after crush injury of rat central nervous system fibres innervating peripheral nerve grafts. *Journal of Neurocytology*, 14, 1-12.
- DE VOS, P., HAMEL, A. F. & TATARKIEWICZ, K. 2002. Considerations for successful transplantation of encapsulated pancreatic islets. *Diabetologia*, 45, 159-173.

- DEISTER, C., ALJABARI, S. & SCHMIDT, C. E. 2007. Effects of collagen 1, fibronectin, laminin and hyaluronic acid concentration in multi-component gels on neurite extension. *J Biomater Sci Polym Ed*, 18, 983-97.
- DHOOT, N. O., TOBIAS, C. A., FISCHER, I. & WHEATLEY, M. A. 2004. Peptide-modified alginate surfaces as a growth permissive substrate for neurite outgrowth. *J Biomed Mater Res A*, 71, 191-200.
- DONATI, I., HOLTAN, S., MORCH, Y. A., BORGOGNA, M., DENTINI, M. & SKJAK-BRÆK, G. 2005. New hypothesis on the role of alternating sequences in calcium-alginate gels. *Biomacromolecules*, 6, 1031-40.
- DRAGET, K. I., SIMENSEN, M. K., ONSØYEN, E. & SMIDSRØD, O. 1993. Gel strength of Ca-limited alginate gels made in situ. *Hydrobiologia*, 260-261, 563-565.
- DRAGET, K. I., SKJÅK-BRÆK, G. & STOKKE, B. T. 2006. Similarities and differences between alginic acid gels and ionically crosslinked alginate gels. *Food Hydrocolloids*, 20, 170-175.
- DRAGET, K. I., SKJÅK-BRÆK, G., SMIDSRØD, O. 2006a. *Alginates*. In *Food Polysaccharides and Their Applications*, Boca Raton, CRC Press.
- DRAGET, K. I., SMIDSRØD, O., SKJÅK-BRÆK G. 2002. *Alginates from Algae.*, Wiley-VCH Verlag GmbH.
- DRAGET, K. I., SMIDSRØD, O., SKJÅK-BRÆK G. 2005. *Alginates from Algae*. In *Polysaccharides and Polyamides in the Food Industry*, Wiley-VCH Verlag GmbH & Co, Weinheim.
- DRAGET, K. I. A. S., O. 2006b. *Modification of gelling kinetics and elastic properties by nano structuring of alginate gels exploiting the properties of poly-guluronate.*, Cambridge, RSCPublishing.
- EDUCATION, N. 2011. *Cell Adhesion and Cell Communication* [Online]. Nature.com Available: <http://www.nature.com/scitable/topicpage/cell-adhesion-and-cell-communication-14050486> [Accessed 15.03. 2012].
- FLORY, P. J. 1953. *Principles of polymer chemistry*, Ithaca, Oxford University.
- FOUNDATION, C. 1989. The biology of Hyaluronan. *Ciba Foundation Symposium*. London.
- FREEMAN, I., KEDEM, A. & COHEN, S. 2008. The effect of sulfation of alginate hydrogels on the specific binding and controlled release of heparin-binding proteins. *Biomaterials*, 29, 3260-3268.
- FRIESS, W. 1998. Collagen--biomaterial for drug delivery. *Eur J Pharm Biopharm*, 45, 113-36.

- GORIN, P. A. J. A. S., J. F. T. 1966. Exocellular Alginic Acid from *Azotobacter Vinelandii*. *Canadian Journal of Chemistry*, 44, 993-&.
- HERSEL, U., DAHMEN, C. & KESSLER, H. 2003. RGD modified polymers: biomaterials for stimulated cell adhesion and beyond. *Biomaterials*, 24, 4385-4415.
- HIGGINSON, J. R. & BARNETT, S. C. 2011. The culture of olfactory ensheathing cells (OECs)--a distinct glial cell type. *Exp Neurol*, 229, 2-9.
- HUEBSCH, N., ARANY, P. R., MAO, A. S., SHVARTSMAN, D., ALI, O. A., BENCHERIF, S. A., RIVERA-FELICIANO, J. & MOONEY, D. J. 2010. Harnessing traction-mediated manipulation of the cell/matrix interface to control stem-cell fate. *Nat Mater*, 9, 518-26.
- INVITROGEN 2005. Live/Dead Viability/Cytotoxicity Kit *for mammalian cells*. *TECHNOLOGIES, I.D.*: Eugene, Oregon: Invitrogen.
- KARSTENSEN, K. 2010. *Novel alginate matrix for tissue engineering*. Master, NTNU.
- KEY, B., TRELOAR, H. B., WANGEREK, L., FORD, M. D. & NURCOMBE, V. 1996. Expression and localization of FGF-1 in the developing rat olfactory system. *J Comp Neurol*, 366, 197-206.
- KOHN, R. & LARSEN, B. 1972. Preparation of water-soluble polyuronic acids and their calcium salts, and the determination of calcium ion activity in relation to the degree of polymerization. *Acta Chem Scand*, 26, 2455-68.
- KONG, H. J., SMITH, M. K. & MOONEY, D. J. 2003. Designing alginate hydrogels to maintain viability of immobilized cells. *Biomaterials*, 24, 4023-9.
- LEE, K. Y. & MOONEY, D. J. 2012. Alginate: properties and biomedical applications. *Prog Polym Sci*, 37, 106-126.
- LEITINGER, B. & HOHENESTER, E. 2007. Mammalian collagen receptors. *Matrix Biol*, 26, 146-55.
- LI, R. H. 1998. Materials for immunisolated cell transplantation. *Advanced Drug Delivery Reviews*, 33, 87-109.
- LINDSAY, S. L., RIDDELL, J. S. & BARNETT, S. C. 2010. Olfactory mucosa for transplant-mediated repair: a complex tissue for a complex injury? *Glia*, 58, 125-34.
- LOWELL, C. A. & MAYADAS, T. N. 2012. Overview: studying integrins in vivo. *Methods Mol Biol*, 757, 369-97.

- MARTINSEN, A., SKJAK-BRAEK, G. & SMIDSRØD, O. 1989a. Alginate as immobilization material: I. Correlation between chemical and physical properties of alginate gel beads. *Biotechnol Bioeng*, 33, 79-89.
- MARTINSEN, A., SKJÅK-BRÆK, G. & SMIDSRØD, O. 1989b. Alginate as immobilization material: I. Correlation between chemical and physical properties of alginate gel beads. *Biotechnol Bioeng*, 33, 79-89.
- MCCREEDY, D. A. & SAKIYAMA-ELBERT, S. E. 2012. Combination therapies in the CNS: Engineering the environment. *Neurosci Lett*.
- MITCHELL, J. R. 1980. THE RHEOLOGY OF GELS. *Journal of Texture Studies*, 11, 315-337.
- MITCHELL, J. R. & BLANSHARD, J. M. V. 1976. RHEOLOGICAL PROPERTIES OF ALGINATE GELS. *Journal of Texture Studies*, 7, 219-234.
- MOE, S. T., DRAGET, K. I., SKJÅK-BRÆK, G. AND SMIDSRØD, O. 1995. *Alginates. In Food polysaccharides and their*, New York, Marcel Decker Inc.,.
- MORCH, Y. A., DONATI, I., STRAND, B. L. & SKJAK-BRAEK, G. 2006. Effect of Ca²⁺, Ba²⁺, and Sr²⁺ on alginate microbeads. *Biomacromolecules*, 7, 1471-80.
- MORCH, Y. A., DONATI, I., STRAND, B. L. & SKJAK-BRAEK, G. 2007. Molecular engineering as an approach to design new functional properties of alginate. *Biomacromolecules*, 8, 2809-14.
- MORCH, Y. A., HOLTAN, S., DONATI, I., STRAND, B. L. & SKJAK-BRAEK, G. 2008. Mechanical properties of C-5 epimerized alginates. *Biomacromolecules*, 9, 2360-8.
- MOSMANN, T. 1983. Rapid colorimetric assay for cellular growth and survival: application to proliferation and cytotoxicity assays. *J Immunol Methods*, 65, 55-63.
- MØRCH, Y. A. 2008. *Novel Alginate Microcapsules for Cell Therapy*. Doktor ingeniør Doctoral Thesis, NTNU.
- OMER, A., DUVIVIER-KALI, V., FERNANDES, J., TCHIPASHVILI, V., COLTON, C. K. & WEIR, G. C. 2005. Long-term normoglycemia in rats receiving transplants with encapsulated islets. *Transplantation*, 79, 52-8.
- ORIVE, G., HERNANDEZ, R. M., RODRIGUEZ GASCON, A., CALAFIORE, R., CHANG, T. M., DE VOS, P., HORTELANO, G., HUNKELER, D., LACIK, I. & PEDRAZ, J. L. 2004. History, challenges and perspectives of cell microencapsulation. *Trends Biotechnol*, 22, 87-92.

- OYAAS, J., STORRO, I., SVENDSEN, H. & LEVINE, D. W. 1995. The effective diffusion coefficient and the distribution constant for small molecules in calcium-alginate gel beads. *Biotechnol Bioeng*, 47, 492-500.
- PAGE, B., PAGE, M. & NOEL, C. 1993. A new fluorometric assay for cytotoxicity measurements in-vitro. *Int J Oncol*, 3, 473-6.
- PAINTER T.J. 1983. *In The polysaccharides*, Academic Press, London.
- PARTAP, S., MUTHUTANTRI, A., REHMAN, I., DAVIS, G. & DARR, J. 2007. Preparation and characterisation of controlled porosity alginate hydrogels made via a simultaneous micelle templating and internal gelation process. *Journal of Materials Science*, 42, 3502-3507.
- PAWAR, S. N. & EDGAR, K. J. 2012. Alginate derivatization: a review of chemistry, properties and applications. *Biomaterials*, 33, 3279-305.
- PICART, C., LAVALLE, P., HUBERT, P., CUISINIER, F. J. G., DECHER, G., SCHAAF, P. & VOEGEL, J. C. 2001. Buildup Mechanism for Poly(l-lysine)/Hyaluronic Acid Films onto a Solid Surface. *Langmuir*, 17, 7414-7424.
- ROKSTAD, A. M., KULSENG, B., STRAND, B. L., SKJÅK-BRÆK, G. & ESPEVIK, T. 2001. Transplantation of Alginate Microcapsules with Proliferating Cells in Mice. *Annals of the New York Academy of Sciences*, 944, 216-225.
- ROKSTAD, A. M., STRAND, B., RIAN, K., STEINKJER, B., KULSENG, B., SKJAK-BRAEK, G. & ESPEVIK, T. 2003. Evaluation of different types of alginate microcapsules as bioreactors for producing endostatin. *Cell Transplant*, 12, 351-64.
- ROWLEY, J. A., MADLAMBAYAN, G. & MOONEY, D. J. 1999. Alginate hydrogels as synthetic extracellular matrix materials. *Biomaterials*, 20, 45-53.
- SANDVIG, I. 2011. *The role of olfactory ensheathing cells, MRI, and biomaterials in transplant mediated CNS repair*. Philosophiae Doctor Doctoral Thesis, Ntnu.
- SHAY, E. L., GREER, C. A. & TRELOAR, H. B. 2008. Dynamic expression patterns of ECM molecules in the developing mouse olfactory pathway. *Developmental Dynamics*, 237, 1837-1850.
- SITTERLEY, G. 2008. *Laminin* [Online]. <http://www.sigmaaldrich.com>: Sigma-Aldrich. Available: <http://www.sigmaaldrich.com/technical-documents/articles/biofiles/laminin.html> [Accessed 15.03. 2012].
- SMIDSRØD, O. & SKJAK-BRAEK, G. 1990. Alginate as immobilization matrix for cells. *Trends Biotechnol*, 8, 71-8.

- SMIDSRØD, O. 1974. Molecular basis for some physical properties of alginates in the gel state. *Faraday Discussions of the Chemical Society*, 57, 263.
- SMIDSRØD, O., HAUG, A. 1972. Properties of Poly(1,4-hexauronates) in the Gel State. *Acta Chemica Scandinavia*, 26, 79-88.
- SMIDSRØD O., M. T. M. 1995. Biopolymerkjemi 2. utgave. *In: NTNU (ed.)*.
- SMITH, P. J., WILTSHIRE, M. & ERRINGTON, R. J. 2004. DRAQ5 labeling of nuclear DNA in live and fixed cells. *Curr Protoc Cytom*, Chapter 7, Unit 7 25.
- STEIGEDAL, M., SLETTA, H., MORENO, S., MAERK, M., CHRISTENSEN, B. E., BJERKAN, T., ELLINGSEN, T. E., ESPIN, G., ERTESVAG, H. & VALLA, S. 2008. The *Azotobacter vinelandii* AlgE mannuronan C-5-epimerase family is essential for the in vivo control of alginate monomer composition and for functional cyst formation. *Environ Microbiol*, 10, 1760-70.
- STOKKE, B. T., DRAGET, K.I., SMIDSRØD, O., YUGUCHI, Y., URAKAWA, H. AND KAJIWARA, K. 2000. Small-angle X-ray scattering and rheological characterization of alginate gels. 1. Ca-alginate gels. *Macromolecules*, 33, 1853-1863.
- STOKKE, B. T., SMIDSRØD, O., ZANETTI, F., STRAND, W. & SKJÅK-BRÆK, G. 1993. Distribution of uronate residues in alginate chains in relation to alginate gelling properties — 2: Enrichment of β -d-mannuronic acid and depletion of α -l-guluronic acid in sol fraction. *Carbohydrate Polymers*, 21, 39-46.
- STOKKE, B. T., SMIDSRØD, O., ZANETTI, F., STRAND, W. AND SKJÅK-BRÆK, G. 1993. Distribution of uronate residues in alginate chains in relation to alginate gelling properties .2. Enrichment of beta-d-mannuronic acid and depletion of alpha-l-guluronic acid in sol fraction. *Carbohydr. Polym.*, 21.
- STRAND, B. L., GASEROD, O., KULSENG, B., ESPEVIK, T. & SKJAK-BAEK, G. 2002a. Alginate-polylysine-alginate microcapsules: effect of size reduction on capsule properties. *J Microencapsul*, 19, 615-30.
- STRAND, B. L., GÅSERØD, O., KULSENG, B., ESPEVIK, T. & SKJÅK-BRÆK, G. 2002b. Alginate-polylysine-alginate microcapsules: effect of size reduction on capsule properties. *J Microencapsul*, 19, 615-630.
- STRAND, B. L., MORCH, Y. A., ESPEVIK, T. & SKJAK-BRAEK, G. 2003. Visualization of alginate-poly-L-lysine-alginate microcapsules by confocal laser scanning microscopy. *Biotechnol Bioeng*, 82, 386-94.
- STRAND, B. L., RYAN, L., VELD, P. I., KULSENG, B., ROKSTAD, A. M., SKJ, ARING, K-BRAEK, G. & ESPEVIK, T. 2001. Poly-L-Lysine Induces Fibrosis on Alginate Microcapsules via the Induction of Cytokines. *Cell Transplantation*, 10, 263-275.

- SVANEM, B. I., STRAND, W. I., ERTESVAG, H., SKJAK-BRAEK, G., HARTMANN, M., BARBEYRON, T. & VALLA, S. 2001. The catalytic activities of the bifunctional *Azotobacter vinelandii* mannuronan C-5-epimerase and alginate lyase AlgE7 probably originate from the same active site in the enzyme. *J Biol Chem*, 276, 31542-50.
- SYSTEMS, N. U. B. 2012. *Safety and Toxicology of PRONOVA UP Sodium alginates* [Online]. <http://www.novamatrix.biz/Quality/SafetyandToxicologyAlginate.aspx>: FMC Corporation. [Accessed 11.05.12 2012].
- TANAKA, H., MATSUMURA, M. & VELIKY, I. A. 1984. Diffusion characteristics of substrates in Ca-alginate gel beads. *Biotechnol Bioeng*, 26, 53-8.
- THU, B., BRUHEIM, P., ESPEVIK, T., SMIDSROD, O., SOON-SHIONG, P. & SKJAK-BRAEK, G. 1996. Alginate polycation microcapsules. II. Some functional properties. *Biomaterials*, 17, 1069-79.
- TISAY, K. T. & KEY, B. 1999. The extracellular matrix modulates olfactory neurite outgrowth on ensheathing cells. *J Neurosci*, 19, 9890-9.
- ULUDAG, H., DE VOS, P. & TRESKO, P. A. 2000. Technology of mammalian cell encapsulation. *Advanced Drug Delivery Reviews*, 42, 29-64.
- VOLD, I. M., KRISTIANSEN, K. A. & CHRISTENSEN, B. E. 2006. A study of the chain stiffness and extension of alginates, in vitro epimerized alginates, and periodate-oxidized alginates using size-exclusion chromatography combined with light scattering and viscosity detectors. *Biomacromolecules*, 7, 2136-46.
- WESTRIN, B. A. & AXELSSON, A. 1991. Diffusion in gels containing immobilized cells: a critical review. *Biotechnol Bioeng*, 38, 439-46.
- WULF, E., DEBOBEN, A., BAUTZ, F. A., FAULSTICH, H. & WIELAND, T. 1979. Fluorescent phallotoxin, a tool for the visualization of cellular actin. *Proc Natl Acad Sci U S A*, 76, 4498-502.
- ZIMMERMANN, D. R. & DOURS-ZIMMERMANN, M. T. 2008. Extracellular matrix of the central nervous system: from neglect to challenge. *Histochem Cell Biol*, 130, 635-53.

Appendix A: alamarBlue® assay

The procedure of the different alamarBlue® assays are elaborated below, as the assay did not work satisfactorily, and is therefore not included in the main part of the report.

A1: Procedure of the alamarBlue assay performed in experiment 3.1

Three different cell concentrations were encapsulated in 1.8% UP-LVG alginate in the experiment:

$$A1a: 1.5 \cdot 10^6 \text{ cells/ mL}$$

$$A1b: 3 \cdot 10^6 \text{ cells/ mL}$$

$$A1c: 5 \cdot 10^6 \text{ cells/ mL}$$

The alamarBlue® assay was performed at day 1, 3, 7, 10 and 14 during the experiment. The amount of media and capsules used in the assay was computed by the following calculations:

$$V = \frac{4}{3}\pi r^3 = \frac{4}{3}\pi (0.250\mu m)^3$$

$$V = 0,654\mu m^3/\text{capsule} = 0,0654 \mu L$$

The following calculation gives the number of cells per capsule:

$$A1: 1.5 \cdot 10^3 \text{ cells/ } \mu L \cdot 0,0654 \mu L = 98,1 \text{ cells/capsule}$$

$$B1: 3 \cdot 10^3 \text{ cells/ } \mu L \cdot 0,0654 \mu L = 196,2 \text{ cells/capsule}$$

$$C1: 5 \cdot 10^3 \text{ cells/ } \mu L \cdot 0,0654 \mu L = 327 \text{ cells/capsule}$$

The appropriate number of cells per sample tested with alamarBlue® assay is 5000 cells, according to the manual designed by the manufacturer, Invitrogen. The following calculation shows how many capsules that were required to meet this requisition.

$$A1a: \frac{5000 \text{ cells}}{98,1 \text{ cells/capsule}} = 51 \text{ capsules}$$

$$A1b: \frac{5000 \text{ cells}}{196,2 \text{ cells/capsule}} = 25 \text{ capsules}$$

$$A1c: \frac{5000 \text{ cells}}{327 \text{ cells/capsule}} = 15 \text{ capsules}$$

$$1 \text{ mL capsules/ } 10 \text{ mL media gives: } \frac{1000\mu L}{0,0654\mu L/\text{capsule}} = 15290 \text{ capsules in } 10 \text{ mL media.}$$

Subsequently, this gives 1529 capsules/mL media, and the calculations that led to sample volume are shown below:

$$A1: \frac{51 \text{ capsules}}{1529 \text{ capsules/mL}} = 0,033\text{m} = 33\mu\text{L}$$

$$B1: \frac{25 \text{ capsules}}{1529 \text{ capsules/mL}} = 0,016\text{mL} = 16\mu\text{L}$$

$$C1: \frac{15 \text{ capsules}}{1529 \text{ capsules/mL}} = 0,0098\text{mL} \approx 10\mu\text{L}$$

The setup protocol is shown in table 1.

Batch	Work solution	Sample withdrawal	Desired number of capsules	Media from culture flask	alamarBlue® reagent
1.5mil/mL	1 mL	5 × 33μL	51	147 μL	18μL
3.0 mil/mL	1 mL	5 × 16μL	25	164 μL	18μL
5.0 mil/mL	1 mL	5 × 10 μL	15	170 μL	18μL
Media from culture flask					
1.5mil/mL	1 mL			5 × 180μL	18μL
3.0 mil/mL	1 mL			5 × 180μL	18μL
5.0 mil/mL	1			5 × 180μL	18μL
Clean media	900μL			5 × 180μL	18μL

Table A1: The protocol for the alamarBlue® assay used in experiment 1

The amount of media used in the assay was replaced after every alamarBlue® assay.

The sample was left in room temperature with an incubation time of 4 hours with the 96 well plate with opaque walls and see-through bottom covered by aluminium foil, and fluorescence was measured at 535nm and 590nm on a Victor platelet reader. At day three the incubation time were only 3 hours.

A2: Fluorescence values and calculations from experiment 3.1

Batch	Day	Fluorescence for parallels 1-5					Fluorescence for control parallels 1-5				
		1	2	3	4	5	1	2	3	4	5
A1c	1	469	221		367	829	63	87	63	87	63
	3	295	269	262	257	238	196	188	203	190	190
	7	327	344	316	380	338	252	226	274	221	226
	10	244	262	228		284	194	207	205		205
	14	207	255	212	208	256	186	192	180	210	192
A1b	1	225	237	130	146	373	76	76	89	76	89
	3	200	233	295	231		191	194	191	206	
	7	275	286	247	278	255	223	230	196	237	223
	10	206	182	246		226	172	165	165	172	165
	14	180	202	226	196		166	164	166	173	166
A1a	1	179	181	244	191	252	97	97	94	94	94
	3	189	167	193	226	190	140	146	148	148	140
	7	236	289	230	252	216	165	162	192	187	187
	10	192	173	211	217	274	146	166	164	159	159
	14	186	192	180	210	278	161	193	186	177	177

Average	Fluorescence per well-average blank					Number of capsules in each well				
control	1	2	3	4	5	1	2	3	4	5
72,6	396,4	148,4		294,4	756,4	11	4		11	25
193,4	101,6	75,6	68,6	63,6	44,6	3	1	4	8	7
239,8	87,2	104,2	76,2	140,2	98,2	5	21	7	27	16
202,75	41,25	59,25	25,25	-202,75	81,25	5	5	4		31
192	15	63	20	16	64	18	17	6	10	55
81,2	143,8	155,8	48,8	64,8	291,8	5	17	10	7	21
195,5	4,5	37,5	99,5	35,5		6	8	29	10	
221,8	53,2	64,2	25,2	56,2	33,2	17	6	6	30	10
168	38,2	14,2	78,2		58,2	20	6	34		44
167	13	35	59	29		18	54	38	39	
95,2	83,8	85,8	148,8	95,8	156,8	45	53	70	65	63
144,4	44,6	22,6	48,6	81,6	45,6	42	35	37	83	47
178,6	57,4	110,4	51,4	73,4	37,4	30	42	38	37	21
159	33,2	14,2	52,2	58,2	115,2	12	15	32	35	102
179	7,2	13,2	1,2	31,2	99,2	14	10	35	11	77

Standard deviation:	A1c	148,0422051	868,7411434	161,6012336	116,6654413	39,59007484
	A1b	94,38516454	18,42182967	31,68668209	4,355777003	3,872335399
	A1a	12,29832179	7,24557439	8,570218225	21,48413641	32,24450915

Average	Standard deviation
fluor/cell *1000	*1000
986,030	148,042
854,170	868,741
270,410	161,601
219,951	116,665
64,462	39,590
129,074	94,385
27,235	18,422
42,223	31,687
17,953	4,356
8,333	3,872
57,997	12,298
30,148	7,246
53,263	8,570
49,314	21,484
36,323	32,245

A3: Graph of fluorescence/1000 cells from experiment 3.1

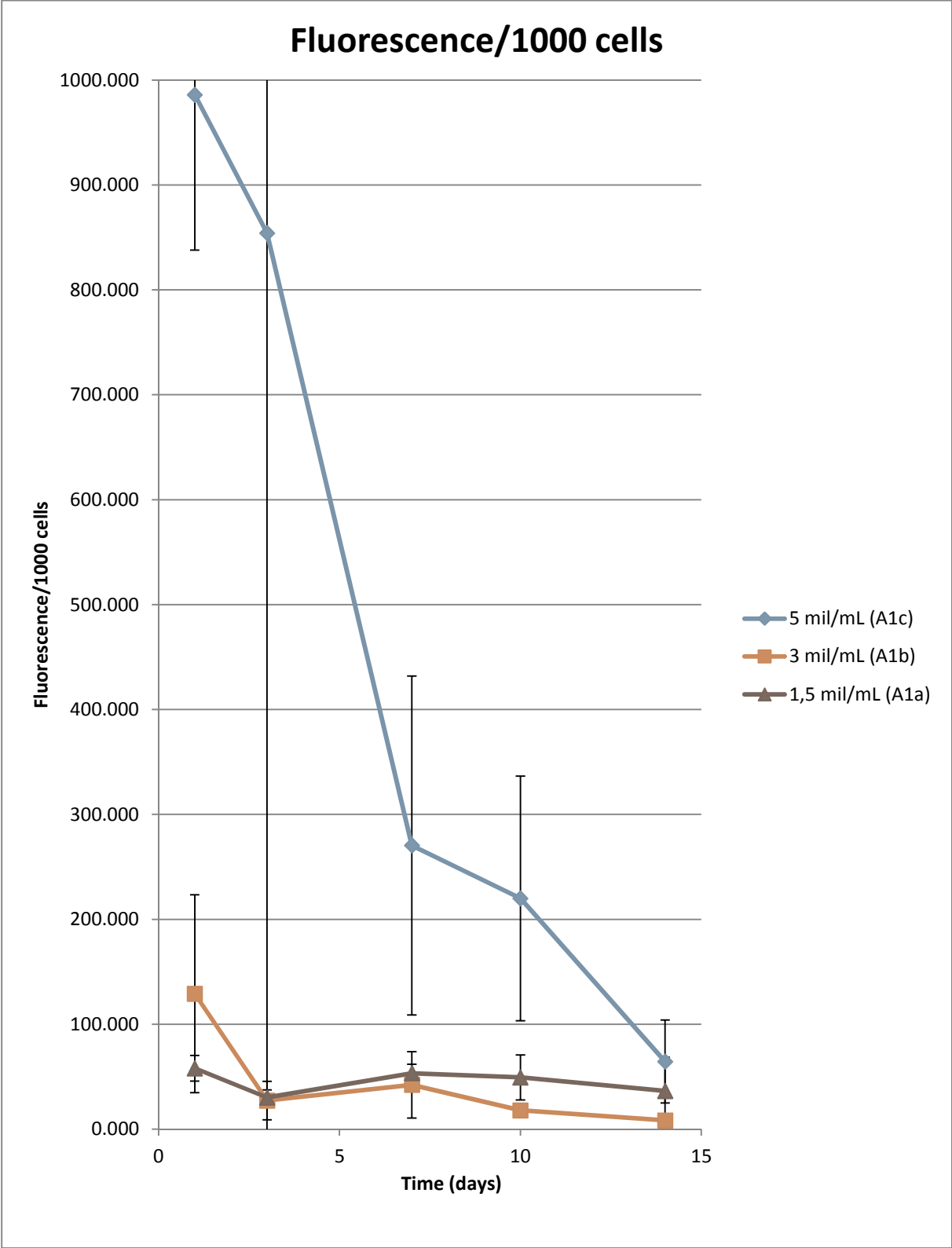


Figure A3: Graph showing fluorescence values from alamarBlue assay performed on batch A1a, A1b and A1c.

A4: Second experiment: The alamarBlue procedure for experiment 3.2

Two different cell concentrations were used: 1.5 mil/mL and 5.0 mil/mL and both were encapsulated in 1.0% LG alginate with and without RGD peptide grafted onto it. In total this setup included four batches.

It was assumed that the size of the capsules was the same as in the previous experiment, and hence the same setup as described above was applied in this assay. However, it was discovered during day 1 Live/Dead assay that the average diameter was noticeably smaller, thus giving the capsules only 1/3 of the assumed volume. This difference could have been caused by less viscosity of the alginate and led to a new calculation of sample amount:

Average radius: 0,174 μ m

$$V = \frac{4}{3}\pi r^3 = \frac{4}{3}\pi (0,174\mu\text{m})^3$$

$$V = 0,654\mu\text{m}^3/\text{capsule} = 0,022\ \mu\text{L}$$

$$\text{A2: } 1.5 \cdot 10^3 \text{ cells}/\mu\text{L} \cdot 0,022\ \mu\text{L} = 33 \text{ cells}/\text{capsule}$$

$$\text{B2: } 5 \cdot 10^3 \text{ cells}/\mu\text{L} \cdot 0,022\ \mu\text{L} = 110 \text{ cells}/\text{capsule}$$

Number of capsules required to obtain 5000 cells/well:

$$\text{B1: } \frac{5000 \text{ cells}}{33 \text{ cells}/\text{capsule}} = 152 \text{ capsules}$$

$$\text{B2: } \frac{5000 \text{ cells}}{110 \text{ cells}/\text{capsule}} = 45 \text{ capsules}$$

$$1 \text{ mL capsules}/ 10 \text{ mL media gives: } \frac{1000\mu\text{L}}{0,022\mu\text{L}/\text{capsule}} = 45454,5 \text{ capsules in } 10 \text{ mL media.}$$

Subsequently, this gives 4545,5 capsules/mL media, and the calculations that led to sample volume are shown below:

$$\text{B1: } \frac{152 \text{ capsules}}{4545,5 \text{ capsules}/\text{mL}} = 0,033\text{mL} = 33\mu\text{L}$$

$$\text{B2: } \frac{45 \text{ capsules}}{4545,4 \text{ capsules}/\text{mL}} = 0,009,8\text{mL} = 9,8\mu\text{L} \approx 10\mu\text{L}$$

The capsules with 5.0 mil/mL cell concentration were slightly larger than the capsules containing 1.5 mil/mL cell concentration. This may have caused the cell number in the higher cell concentration sample to be larger than intended (5000 cells/well).

On day 1 the same setup was used as in the previous experiment, but after encountering the same problem with contaminating of the controls by capsules, it

was decided to increase work solution of media from the culture flask from 1 mL to 1.5 mL.

This improved the quality of the controls considerably and combined with the new calculations it led to the revised protocol setup shown in table 2.

Batch	Work solution	Sample withdrawal	Desired number of capsules	Media from culture flask	alamarBlue® reagent
1.5mil/mL Alg	1 mL	5 × 33µL	152	147 µL	18µL
5.0 mil/mL Alg	1 mL	5 × 10 µL	45	170 µL	18µL
1.5mil/mL Alg+RGD	1 mL	5 × 33µL	152	147 µL	18µL
5.0 mil/mL Alg+RGD	1 mL	5 × 10 µL	45	170 µL	18µL
Media from culture flask					
1.5mil/mL	1.5 mL			5 × 180µL	18µL
5mil/mL Alg	1.5 mL			5 × 180µL	18µL
1.5mil/mL Alg+RGD	1.5 mL			5 × 180µL	18µL
5mil/mL Alg+RGD	1.5 mL			5 × 180µL	18µL
Clean media	900 µL			5 × 180µL	18µL

Table A4: The revised alamarBlue® protocol for the second experiment

A 96 well plate with opaque walls and see-through bottom was used as in experiment A1.

A5: Fluorescence values and calculations from experiment 3.2

Batch	Day	Fluorescence for samples 1-5					Fluorescence for control samples 1-5				
		1	2	3	4	5	1	2	3	4	5
B1a	3	102	102		113	103	182	180		161	153
	7	133	143	148	138	147	187	187	204	201	182
	10	128	138	144	135	140	181	170	183	203	173
	14	103	99	107	153	154	153	153	154	167	
	22	228	170	204	213	203		192	158	143	165
B1b	3	223	187	195	261	314	226	243	235	203	227
	7	324	420	353	430	358	274	222	282	259	265
	10	190	194	215	185	205	187	203	198	184	190
	14	157	183	142	148	154	152	143	165		153
	22	172	152	135	165	155	161	132	148	133	167
B2a	3	193	194	180	188	231	179	164	187	187	161
	7	226	284	294	245		221	212	226	214	213
	10	247	360	248	244	209	163	162	184	184	212
	14	208	180	187	182	154	143	135	157	151	157
	22	204	177	168	204	217	154	149	156	164	151
B2b	3	268	306	334	253	341	183	227	219	202	198
	7	313	563	337	385	367	248	245	262	305	246
	10	266	218	244	246	206	216	186	230	205	209
	14	151	177	154	132	156	149		165		175
	22	131	152	175	152	136	130	147	140	149	134

Standard deviation *1000	B1a	10,04341055	3,666255497	2,71729441	11,42586666	12,30036243
	B1b	8,471598628	2,139323012	4,119897508	2,556270847	4,329189768
	B2a	6,471612501	36,38200568	5,860664808	7,955146768	6,086870158
	B2b	6,516363884	6,850913585	7,796310555	24,8159889	5,219767535

		Average	Fluorescens per well - average control					Number of capsules per well					
Batch	Day	control	1	2	3	4	5	1	2	3	4	5	
B1a	3	169	-67	-67	-169	-56	-66	68	161	134	91	95	
	7	192,2	-59,2	-49,2	-44,2	-54,2	-45,2	84	70	93	74	57	
	10	182	-54	-44	-38	-47	-42	78	75	61	63	52	
	14	157	-54	-58	-50	-4	-3	66	82	84	129	87	
	22	165	64	6	40	49	39	86	56	58	45	35	
B1b	3	226,8	-3,8	-39,8	-31,8	34,2	87,2	62		23	80	120	
	7	260,4	63,6	159,6	92,6	169,6	97,6	65	129		132	125	
	10	192,4	-2,4	1,6	22,6	-7,4	12,6	21	13	27	21	40	
	14	153	4	30	-11	-5	1	59	62	40	54	31	
	22	148	24	4	-13	17	7	71	25	36	19	11	
B2a	3	175,6	17,4	18,4	4,4	12,4	55,4	61	49	54	45	83	
	7	217,2	8,8	66,8	76,8	27,8	-217,2	35	74	102	36	111	
	10	181	66	179	67	63	28	90		75	75	61	
	14	149	59,4	31,4	38,4	33,4	5,4	104	42	48	72	38	
	22	155	49,2	22,2	13,2	49,2	62,2	76	112	51	157	9	
B2b	3	205,8	62,2	100,2	128,2	47,2	135,2	20	48	79	37	55	
	7	261,2	51,8	301,8	75,8	123,8	105,8		99	21	52	56	
	10	209,2	56,8	8,8	34,8	36,8	-3,2	36	16	20	23	14	
	14	163	-12	14	-9	-31	-7	11	24	50	5	25	
	22	140	-9	12	35	12	-4	30	56	29	36	66	

Batch	Day	Fluorescence per capsule					Cells per capsule
		1	2	3	4	5	
B1a	3	-0,985	-0,416	-1,261	-0,615	-0,695	33
	7	-0,705	-0,703	-0,475	-0,732	-0,793	33
	10	-0,692	-0,587	-0,623	-0,746	-0,808	33
	14	-0,814	-0,704	-0,592	-0,029	-0,032	33
	22	0,738	0,098	0,681	1,078	1,100	33
B1b	3	-0,061		-1,383	0,428	0,727	110
	7	0,978	1,237		1,285	0,781	110
	10	-0,114	0,123	0,837	-0,352	0,315	110
	14	0,064	0,480	-0,281	-0,097	0,024	110
	22	0,335	0,152	-0,367	0,884	0,618	110
B2a	3	0,285	0,376	0,081	0,276	0,667	33
	7	0,251	0,903	0,753	0,772	-1,957	33
	10	0,733		0,893	0,840	0,459	33
	14	0,571	0,748	0,800	0,464	0,142	33
	22	0,647	0,198	0,259	0,313	6,911	33
B2b	3	3,110	2,088	1,623	1,276	2,458	110
	7		3,048	3,610	2,381	1,889	110
	10	1,578	0,550	1,740	1,600	-0,229	110
	14	-1,091	0,583	-0,180	-6,200	-0,280	110
	22	-0,300	0,214	1,207	0,333	-0,061	110

Batch	Day	Fluorescence per cell					Average	St.dev.
							fluor/cell	
B1a	3	-0,030	-0,013	-0,038	-0,019	-0,021	-24,077	10,043
	7	-0,021	-0,021	-0,014	-0,022	-0,024	-20,656	3,666
	10	-0,021	-0,018	-0,019	-0,023	-0,024	-20,943	2,717
	14	-0,025	-0,021	-0,018	-0,001	-0,001	-13,161	11,426
	22	0,022	0,003	0,021	0,033	0,033	22,396	12,300
B1b	3	-0,001		-0,013	0,004	0,007	-0,658	8,472
	7	0,009	0,011		0,012	0,007	9,730	2,139
	10	-0,001	0,001	0,008	-0,003	0,003	1,470	4,120
	14	0,001	0,004	-0,003	-0,001	0,000	0,344	2,556
	22	0,003	0,001	-0,003	0,008	0,006	2,951	4,329
B2a	3	0,009	0,011	0,002	0,008	0,020	10,214	6,472
	7	0,008	0,027	0,023	0,023	-0,059	4,379	36,382
	10	0,022		0,027	0,025	0,014	22,164	5,861
	14	0,017	0,023	0,024	0,014	0,004	16,514	7,955
	22	0,020	0,006	0,008	0,009		10,741	6,087
B2b	3	0,028	0,019	0,015	0,012	0,022	19,189	6,516
	7		0,028	0,033	0,022	0,017	24,837	6,851
	10	0,014	0,005	0,016	0,015	-0,002	9,526	7,796
	14	-0,010	0,005	-0,002	-0,056	-0,003	-13,032	24,816
	22	-0,003	0,002	0,011	0,003	-0,001	2,534	5,220

A6: Graph of fluorescence value/1000 cells from experiment 3.2

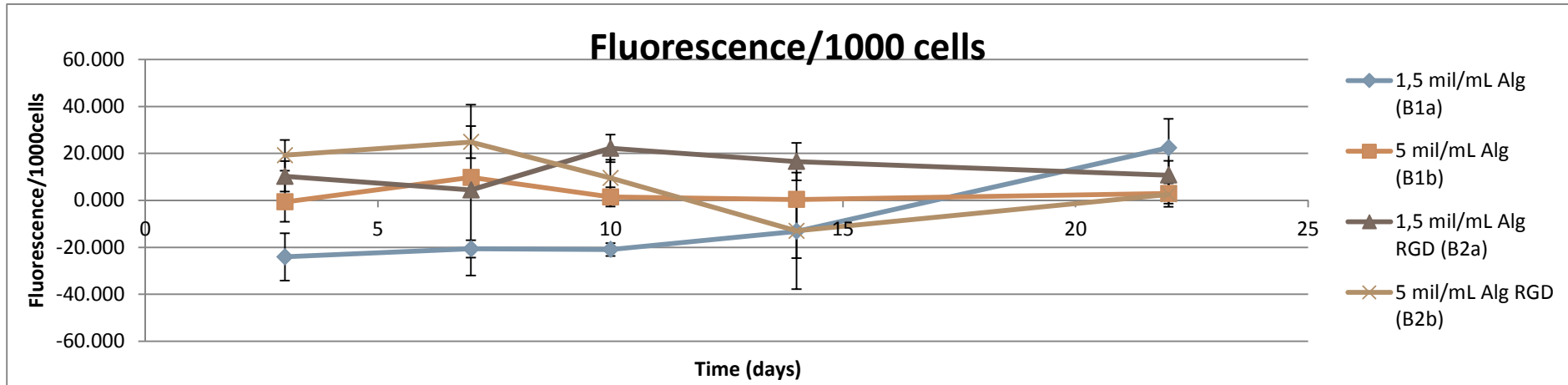


Figure A6: Graph showing fluorescence values/1000 cells from alamarBlue® assay performed on cells from encapsulation B1a, B1b, B2a and B2b (encapsulation of high and low cell concentration in alginate with and without RGD-grafted onto it)

In experiment 3.2 two different OEC concentrations (1.5 mil/mL and 5.0 mil/mL) were encapsulated in LG 0.2% RGD grafted alginate and a similar alginate without RGD graft, resulting in four different batches (B1a, B1b, B2a and B2b) as seen in figure 1 below. Batch B2a displayed fluorescence values above zero throughout the experiment, whilst the B2b batch had positive fluorescence values up until day 12 approximately. At day 14 the fluorescence values from batch B2b were negative, but the cells in the batch appeared to redeem themselves from day 14 to day 22, when the values turned positive again. The B1a batch displayed negative fluorescence values up until the last day of the experiment. The cells may have adjusted to the environment inside the capsules, but the results from the concurrent Live/Dead assay did not support this theory. Batch B1b displayed low viability throughout the experiment with fluorescence values slightly larger than zero, according to the alamarBlue® assay. These results can be observed in figure 1. The concurrent Live/Dead assay did not correlate well with this result as the viability of cells in all batches in the experiment were estimated as almost similar up until day 10 (Figure 3.6.)

A7: Fluorescence values and calculations for experiment 3.4

Batch	Day	Fluorescence for samples, parallels 1-5					Fluorescence for control samples, parallels 1-5				
		1	2	3	4	5	1	2	3	4	5
D1a	2	944	939	1140	982	1041	358	327	326	347	
	3	623	517	563	557	605	650	619	650	613	654
	7	1208	1491	1298	722	926	688	939	1072	1121	1074
	10	363	345	362	404	389	558	542	569	526	532
	14	226	202	214	182	232	191	198	218	215	221
	16	184	255	167	188	224	210	206	216	206	232
	20	184	180	162	177	190	280	250	254	242	246
	24	119	149	138	151	144	191	198	222	196	
	27	146	199	213	233	193	256	252	277	255	289
	29	132	119	130	143	129	238	206	229	210	214
D1b	2	1144	1650	1598	1274	1828	834	873	798		
	3	1870	1626	1389	1482	1661	1374	1290	1450	1329	
	7	1143	1471	1833	1900	1700	1511	1319	1308	1465	1439
	10	805	1164	814	795	766	729	780	759	749	799
	14	252	423	434	456	357	198	211	207	224	262

Batch	Day	Average controls	Fluorescence/well - average control					Number of capsules in each well				
			1	2	3	4	5	1	2	3	4	5
D1a	2	339,5	605	600	801	643	702	85	54	120	92	119
	3	637,2	-14,2	-120,2	-74,2	-80,2	-32,2	96	51	47	63	45
	7	978,8	229,2	512,2	319,2	-256,8	-52,8	28	55	51	106	53
	10	545,4	-182	-200,4	-183,4	-141,4	-156,4	74	42	39	59	33
	14	209	17	-7	5	-27	23	92	27	62	29	77
	16	214	-30	41	-47	-26	10	150	27	33	88	
	20	254	-70	-74	-92	-77	-64	86	59	40	16	72
	24	202	-83	-53	-64	-51	-58	33	45	49	79	58
	27	266	-120	-67	-53	-33	-73	43	95	44	30	30
	29	219	-87	-100	-89	-76	-90	200	54	6	17	12
D1b	2	835	309	815	763	439	993	7	41	35	20	42
	3	1360,75	509,25	265,25	28,25	121,25	300,25	52	32	22	25	46
	7	1408,4	-265,4	62,6	424,6	491,6	291,6	15	28	32	18	8
	10	763,2	41,8	400,8	50,8	31,8	2,8	37	112	45	14	28
	14	220	32	203	214	236	137	16	50	63	55	31

Batch	Day	Fluorescence per capsule					No. of cells per capsule
		1	2	3	4	5	
D1a	2	7,111764706	11,10185185	6,670833333	6,983695652	5,894957983	33
	3	-0,147916667	-2,356862745	-1,578723404	-1,273015873	-0,715555556	33
	7	8,185714286	9,312727273	6,258823529	-2,422641509	-0,996226415	33
	10	-2,464864865	-4,771428571	-4,702564103	-2,396610169	-4,739393939	33
	14	0,189130435	-0,244444444	0,087096774	-0,917241379	0,303896104	33
	16	-0,2	1,518518519	-1,424242424	-0,295454545		33
	20	-0,818604651	-1,261016949	-2,31	-4,8375	-0,894444444	33
	24	-2,507575758	-1,172222222	-1,301020408	-0,642405063	-0,995689655	33
	27	-2,786046512	-0,703157895	-1,2	-1,093333333	-2,426666667	33
	29	-0,437	-1,859259259	-14,9	-4,494117647	-7,533333333	33
D1b	2	44,14285714	19,87804878	21,8	21,95	23,64285714	110
	3	9,793269231	8,2890625	1,284090909	4,85	6,527173913	110
	7	-17,69333333	2,235714286	13,26875	27,31111111	36,45	110
	10	1,12972973	3,578571429	1,128888889	2,271428571	0,1	110
	14	1,975	4,052	3,39047619	4,283636364	4,406451613	110

Standard deviation	D1a	61,807	25,478	163,915	38,306	14,916	36,79	50,952	21,41	27,53	174
	D1b	91,570	29,930	193,403	12,069	9,096					

Batch	Day	Fluorescence per cell					Average fluor./1000 cells	St. dev. *1000
		1	2	3	4	5		
D1a	2	0,215508021	0,336419753	0,202146465	0,211627141	0,17863509	228,8672941	61,80716281
	3	-0,004482323	-0,071420083	-0,047840103	-0,038576239	-0,021683502	-36,80044997	25,4780779
	7	0,248051948	0,282203857	0,189661319	-0,073413379	-0,030188679	123,2630131	163,9147875
	10	-0,074692875	-0,144588745	-0,142501943	-0,072624551	-0,143617998	-115,6052221	38,30584832
	14	0,005731225	-0,007407407	0,002639296	-0,027795193	0,009208973	-3,524621278	14,91597875
	16	-0,006060606	0,046015713	-0,043158861	-0,008953168		-3,039230691	36,78802159
	20	-0,024806202	-0,038212635	-0,07	-0,146590909	-0,027104377	-61,34282451	50,95189983
	24	-0,075987144	-0,035521886	-0,039424861	-0,01946682	-0,030172414	-40,11462489	21,41019659
	27	-0,084425652	-0,021307815	-0,036363636	-0,033131313	-0,073535354	-49,75275398	27,53396634
	29	-0,013242424	-0,05634119	-0,451515152	-0,136185383	-0,228282828	-177,1133954	173,9463694
D1b	2	0,401298701	0,180709534	0,198181818	0,199545455	0,214935065	238,9341147	91,57037095
	3	0,08902972	0,075355114	0,011673554	0,044090909	0,059337945	55,89744828	29,93047119
	7	-0,160848485	0,020324675	0,120625	0,248282828	0,331363636	111,949531	193,4027229
	10	0,01027027	0,032532468	0,010262626	0,020649351	0,000909091	14,92476112	12,06897933
	14	0,017954545	0,036836364	0,030822511	0,038942149	0,040058651	32,92284394	9,095723837

A8: Graph of fluorescence values per 1000 cells for experiment 3.4

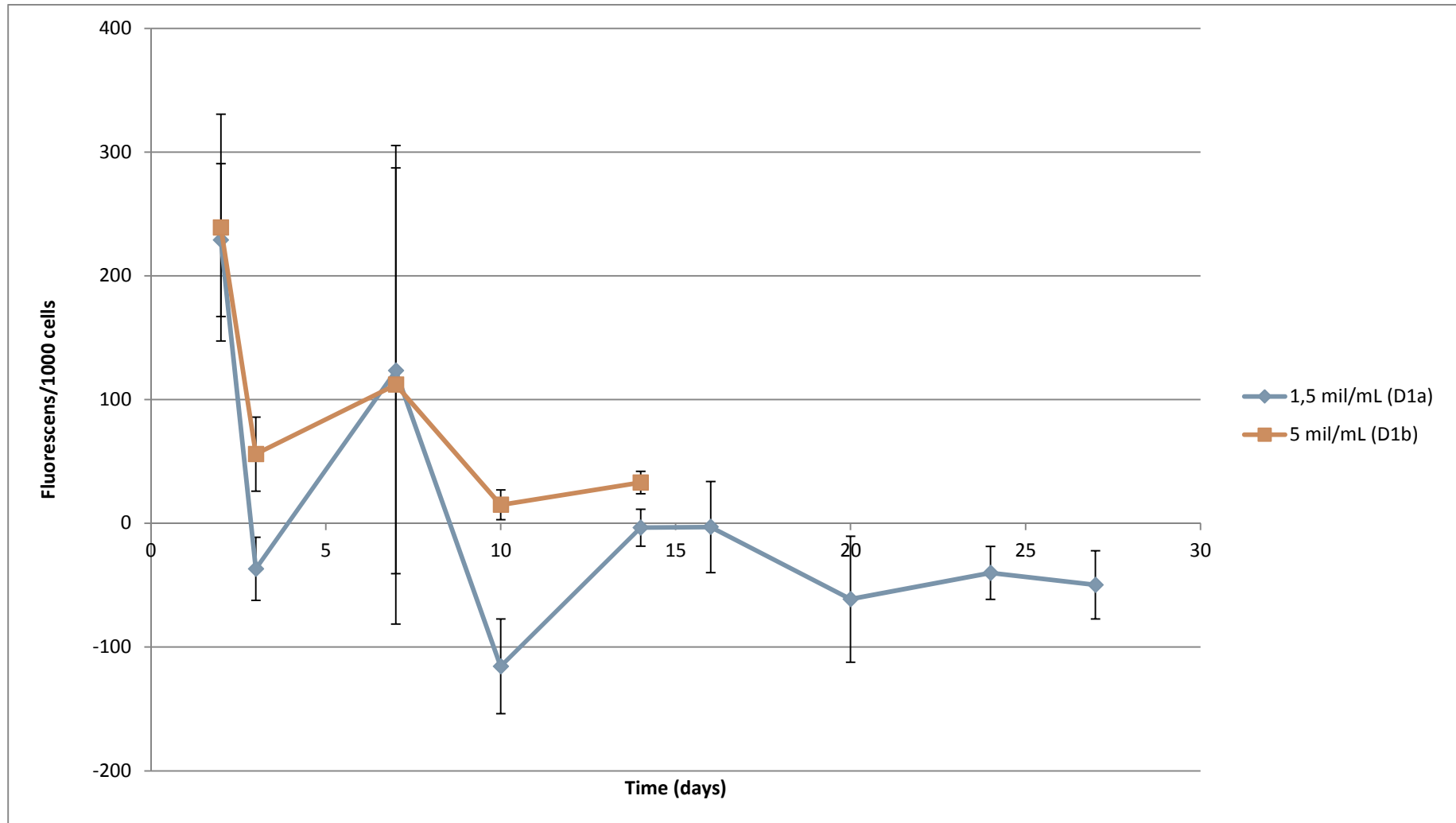


Figure A8: Graph showing fluorescence values/1000 cells from alamarBlue® assay performed on cells from encapsulation D1a and D1b

A9: Fluorescence values and calculations for experiment 3.5

Batch	Day	Fluorescence for samples, parallels 1-5					Fluorescence for control samples, parallels 1-5				
		1	2	3	4	5	1	2	3	4	5
E1	1	199	211	188	242	210	160	150	164	178	172
	3	64	77	101	90	141	163	139	187	138	155
	6	141	145	173	180	175	156	190	152	151	147
	9	113	128	163	144	168	166	172	176	155	131
	13	147	150	182	164	145	180	151	159	186	
	15	134	120	118	140	112	163	163	163	192	188
E2	1	201	514	227	212	236	171	164	170	150	169
	3	149	169	157	154	139	162	169	155	165	175
	6	142	274	154	185	182	149	150	159	161	151
	9	131	154	192	180	163	133	186	176	166	157
	13	133	177	205	205	204	146	174	168	180	137
	15	211	170	142	177	156	173	206	145	151	159
E2	1	545	398	330	298	338	159	180	160	164	185
	3	216	208	268	209	178	165	135	160	168	159
	6	174	305	257	221	263	125	152	163	166	139
	9	208	244	273	172	162	143	156	160	172	
	13	194	317	235	196	207	155	160	166	191	184
	15	311	186	161	143	164	164	153	137	149	136
Blank media controls		Day	Fluorescence values of blank media								
			1	2	3	4	5				
		1	168	161	173	169	177				
		3	144	154	154	144	157				
		6	125	152	163	166	139				
		9	173	144	169	142					
	13	155	214	158							

Batch	Day	Average control	Fluorescence per well- average control					Number of capsules in each well				
			1	2	3	4	5	1	2	3	4	5
E1	1	164,8	34,2	46,2	23,2	77,2	45,2	40	46	45	52	63
	3	156,4	-92,4	-79,4	-55,4	-66,4	-15,4	11	45	34	20	75
	6	159,2	-18,2	-14,2	13,8	20,8	15,8	79	35	62	73	53
	9	160	-47,0	-32,0	3,0	-16,0	8,0	13	20	33	41	36
	13	169	-22,0	-19,0	13,0	-5,0	-24,0	26	71	43	52	45
	15	173,8	-39,8	-53,8	-55,8	-33,8	-61,8	65	35	29	35	46
E2	1	164,8000	36,2	349,2	62,2	47,2	71,2	6	38	29	26	15
	3	165,2	-16,2	3,8	-8,2	-11,2	-26,2	18	48	17	14	8
	6	154	-12,0	120,0	0,0	31,0	28,0		52		20	8
	9	163,6	-32,6	-9,6	28,4	16,4	-0,6			13	10	11
	13	161	-28,0	16,0	44,0	44,0	43,0	7	16	33	13	29
	15	166,8	44,2	3,2	-24,8	10,2	-10,8	33	36	16		
E2	1	169,6	375,4	228,4	160,4	128,4	168,4	45	54	51	18	32
	3	157,4	58,6	50,6	110,6	51,6	20,6	18	27	36	33	35
	6	149	25,0	156,0	108,0	72,0	114,0		36	38	24	30
	9	157,75	50,3	86,3	115,3	14,3	4,3	31	27	49	13	6
	13	171,2	22,8	145,8	63,8	24,8	35,8	16	41	14	8	10
	15	147,8	163,2	38,2	13,2	-4,8	16,2	108	28	7		

Batch	Day	Fluorescence per capsule					No. of cells per capsule
		1	2	3	4	5	
E1	1	0,855	1,004347826	0,515555556	1,484615385	0,717460317	33
	3	-8,4	-1,764444444	-1,629411765	-3,32	-0,205333333	33
	6	-0,230379747	-0,405714286	0,222580645	0,284931507	0,298113208	33
	9	-3,615384615	-1,6	0,090909091	-0,390243902	0,222222222	33
	13	-0,846153846	-0,267605634	0,302325581	-0,096153846	-0,533333333	33
	15	-0,612307692	-1,537142857	-1,924137931	-0,965714286	-1,343478261	33
E2	1	6,033333333	9,189473684	2,144827586	1,815384615	4,746666667	33
	3	-0,9	0,079166667	-0,482352941	-0,8	-3,275	33
	6		2,307692308		1,55	3,5	33
	9			2,184615385	1,64	-0,054545455	33
	13	-4	1	1,333333333	3,384615385	1,482758621	33
	15	1,339393939	0,088888889	-1,55			33
E2	1	8,342222222	4,22962963	3,145098039	7,133333333	5,2625	33
	3	3,255555556	1,874074074	3,072222222	1,563636364	0,588571429	33
	6		4,333333333	2,842105263	3	3,8	33
	9	1,620967742	3,194444444	2,352040816	1,096153846	0,708333333	33
	13	1,425	3,556097561	4,557142857	3,1	3,58	33
	15	1,511111111	1,364285714	1,885714286			33

		Fluorescence/cell					Average	St. Dev*1000
Batch	Day						fluor/1000cells	
E1	1	0,025909091	0,030434783	0,015622896	0,044988345	0,021741222	27,73926717	11,07845931
	3	-0,254545455	-0,053468013	-0,049376114	-0,100606061	-0,006222222	-92,84357298	96,37280191
	6	-0,006981204	-0,012294372	0,006744868	0,008634288	0,009033734	1,027462588	9,953176961
	9	-0,10955711	-0,048484848	0,002754821	-0,011825573	0,006734007	-32,07574063	48,48209762
	13	-0,025641026	-0,008109262	0,009161381	-0,002913753	-0,016161616	-8,732855018	13,18642518
	15	-0,018554779	-0,046580087	-0,05830721	-0,029264069	-0,040711462	-38,68352138	15,37408379
E2	1	0,182828283	0,2784689	0,064994775	0,055011655	0,143838384	145,0283993	91,84907409
	3	-0,027272727	0,00239899	-0,014616756	-0,024242424	-0,099242424	-32,59506833	39,01207461
	6		0,06993007	0	0,046969697	0,106060606	55,74009324	44,41241303
	9		0	0,066200466	0,04969697	-0,001652893	28,56113583	34,60283541
	13	-0,121212121	0,03030303	0,04040404	0,102564103	0,044932079	19,39822629	83,51641969
	15	0,040587695	0,002693603	-0,046969697			-1,229466381	43,91033001
E2	1	0,252794613	0,128170595	0,095306001	0,216161616	0,159469697	170,3805044	64,07983043
	3	0,098653199	0,056790123	0,093097643	0,04738292	0,017835498	62,75187663	33,53728848
	6		0,131313131	0,086124402	0,090909091	0,115151515	105,8745348	21,1913254
	9	0,049120235	0,096801347	0,071273964	0,033216783	0,021464646	54,37539504	30,18254445
	13	0,043181818	0,107760532	0,138095238	0,093939394	0,108484848	98,29236617	34,76320736
	15	0,045791246	0,041341991	0,057142857			48,09203143	8,147824919

A10: Fluorescence values/1000 cells from experiment 3.5

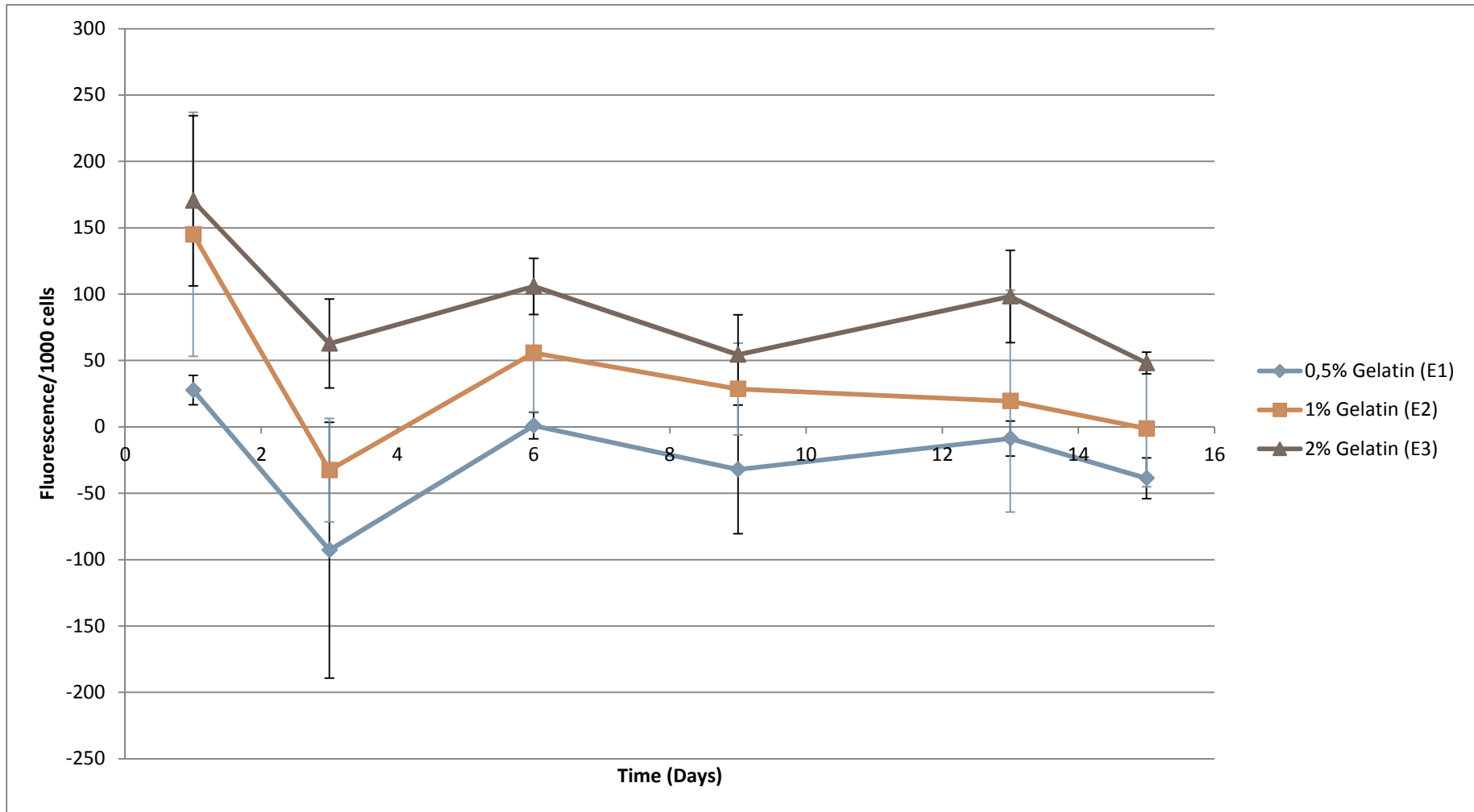


Figure A10: Graph showing fluorescence values/1000 cells from alamarBlue® assay performed on cells from encapsulation E1,E2 and E3

Appendix B: MTT assay performed in comparison with the alamarBlue® assay

As the alamarBlue® assay did not work satisfactorily during the project, it was decided to compare its results with the MTT assay to see if both assays showed similar results. The Live/Dead assay was utilized as control on both assays. The assays were performed on 1.5 mil/mL OECs encapsulated in 1.0% UP-LVG alginate, at day 8, 13 and 22.

B1: Absorbance values and calculations from the MTT assay.

Raw Data Wavelength:570.0								
Day	1	2	3	4	5	6	Average absorbance	St.dev
8	0,055	0,052	0,058	0,052	0,049	0,054	0,053333333	0,003076795
13	0,049	0,062	0,061	0,049	0,059	0,063	0,057166667	0,006462714
22	0,056	0,066	0,065	0,056	0,069		0,0624	0,006024948
							Average absorbance blank samples	
Blank samples (DMSO)	0,052	0,046	0,048	0,045	0,048	0,045	0,047333333	

Day	Average absorbance - average absorbance blank samples
8	0,006
13	0,009833333
22	0,015066667

Standard deviation	0,003077	0,006463	0,006025

B2: Graph showing the MTT absorbance values for 1.5 mil/mL encapsulated in 1.0% UP-LVG

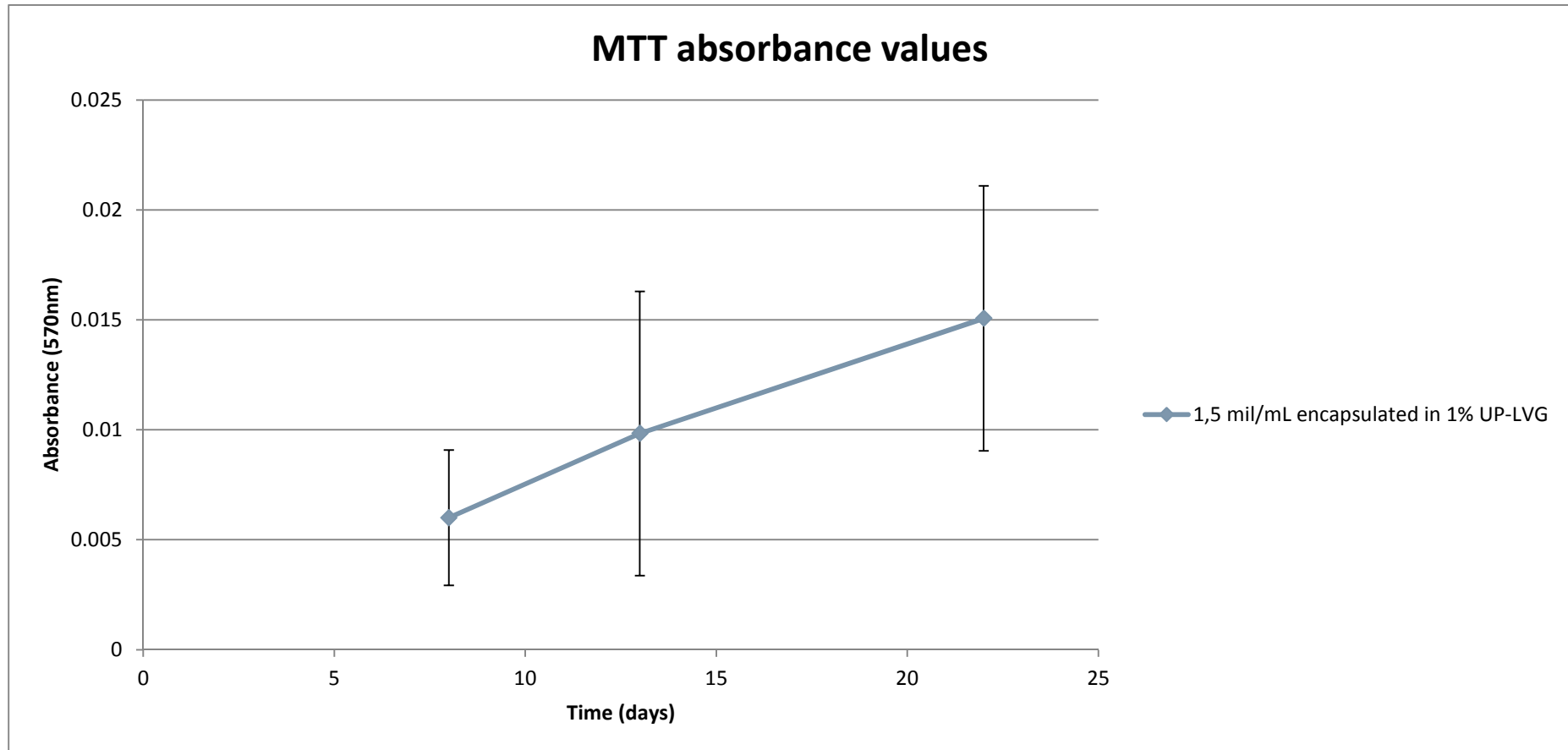


Figure B1: Graph showing absorbance values, shown as an average value of two parallels of 40 capsules. MTT assay performed cell concentration 1.5 mil/mL

B3: Fluorescence values from the alamarBlue® assay performed on comparison with the MTT assay

Fluorescence values for samples, parallels 1-5					
Day	1	2	3	4	5
8	574	616	749	532	546
13	103	121	143	132	151
22	119	135	123	122	147

Blank samples , media without capsules						Average
Day	1	2	3	4	5	controls
8	579	624	567	615	620	601
13	130	143	144	158	247	164
22	141	140	154	177	165	155

Fluorescence per well - mean, blank.					
Day	1	2	3	4	5
8	-27	15	148	-69	-55
13	-61	-43	-21	-32	-13
22	-36	-20	-32	-33	-8

Number of capsules in each well					
Day	1	2	3	4	5
8	227	250	250	92	46
13	120	63	100	75	85
22	98	120	85	27	83

	Fluorescence per capsule				
Day	1	2	3	4	5
8	-0,118942731	0,06	0,592	-0,75	1,195652174
13	-0,511666667	0,688888889	-0,214	-0,432	0,157647059
22	-0,371428571	-0,17	0,381176471	1,237037037	0,101204819

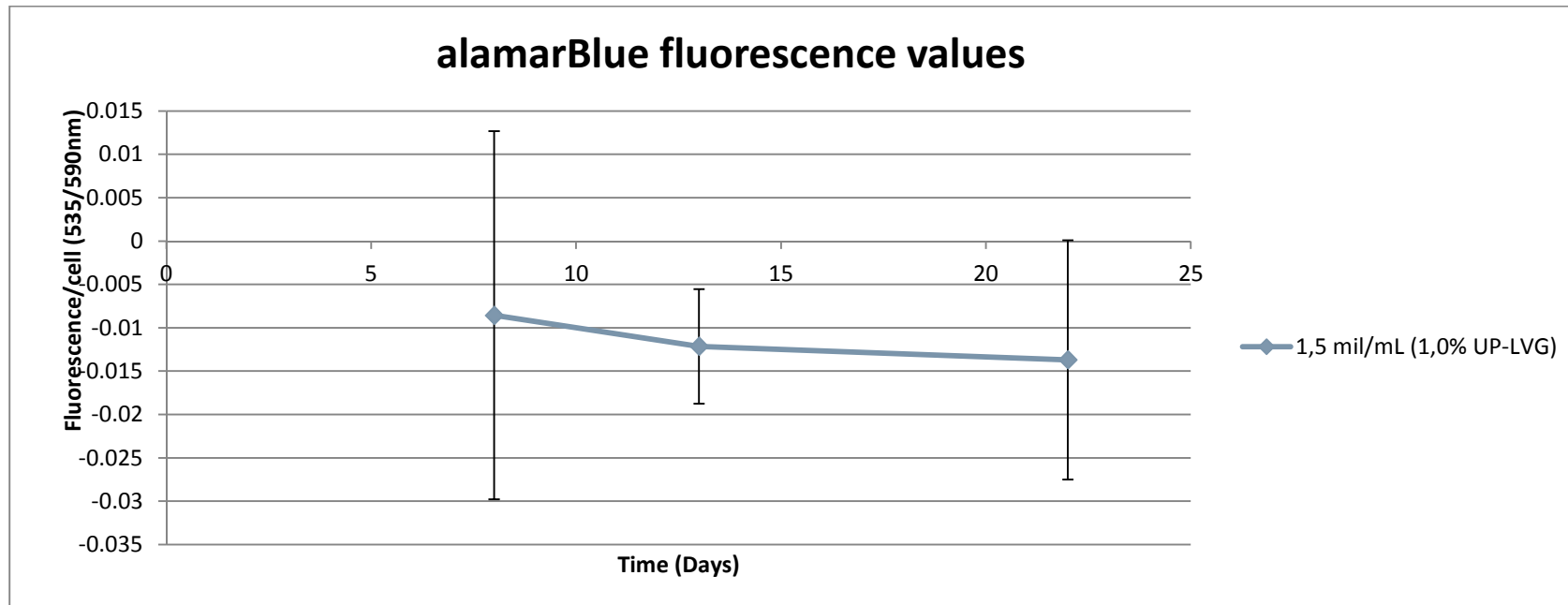
	Cells	(Fluorescence/capsule)/(Cells/capsule)				
Day	per capsule.					
8	33	0,003604325	0,001818182	0,017939394	0,022727273	0,036231884
13	33	0,015505051	0,020875421	0,006484848	0,013090909	0,004777184
22	33	0,011255411	0,005151515	0,011550802	0,037485971	0,003066813

	Average	Normalised	Standard
Day	fluor/1000 cells		deviation
8	-0,008561181	1	0,021218671
13	-0,012146683	1,418809177	0,006609216
22	-0,013702102	1,600492038	0,01380678

		1	2	3	4	5	Average
Blank	Day 8	149	147	164	179	138	155
samples:	Day 13	153	168	162	165	160	162
						Average	159

Standard deviation:		0,021218671	0,006609216	0,01380678
---------------------	--	-------------	-------------	------------

B4: Graph showing fluorescence per cell from alamarBlue® assay performed in comparison with MTT assay



Appendix C: Excel tables for the estimated live cell percentages in chapter 3

The Live/Dead assay that was performed on all experiments during the project was analyzed with estimated live cell percentage based on 3D projections obtained by CLSM. The estimated live cells percentages from all experiments are shown below.

Experiment 3.1	Day				
Cell conc.	1	3	7	10	14
1.5 mil/mL (A1a)	90	90	85	30	10
3.0 mil/mL (A1b)	70	80	30	30	30
5.0 mil/mL (A1c)	80	80	40	50	15

	Day					
Experiment 3.2	1	3	7	10	14	22
Cell conc.						
1.5 mil/mL (B1a)	95	95	95	95	80	70
1.5 mil/mL (B2a)	90	90	90	90	30	30
5.0 mil/ML (B1b)	90	90	90	85	40	40
5.0 mil/ML (B2b)	95	95	95	80	60	50

	Cell conc.	
Experiment 3.3	1.0 mil/mL (C1a)	4.0 mil/mL (C1b)
Day		
1	50	50
2	70	80
9	80	80
10	80	50
14	80	40
17	80	
22	75	
24	75	
29	75	
32	75	
36	70	
44	60	
51	50	

Experiment 3.4	Cell conc.	
	1.5 mil/mL	5.0 mil/mL
Day		
2	60	60
3	75	50
7	75	50
10	75	60
14	80	30
16	40	
21	75	
24	60	
27	60	
36	60	

Experiment 3.5	Percentage of gelatin		
	0.5%	1.0%	2.0%
Day			
1	60	60	60
3	70	70	80
6	80	80	70
9	70	80	75
13	70	70	80
22	60	80	70

Experiment 3.6	Percentage of gelatin		
	0.5%	1.0%	2.0%
Day			
1		70	60
9	80	85	85
16	75	75	75

Experiment 3.7	Day					
	1	3	7	14	20	28
Additive						
Sulphated Alg	75	80	65	65	80	50
Hyaluronan	75	80	95	70	70	50
Fibronectin	80	70	60	50	40	20
Laminin	80	60	60	50	40	40
Collagen	75	95	50	40	40	40
Experiment 3.8	Alginate type					
	RGD +	RGD-	Epi+	Epi-	UP-LVG+	UP-LVG-
Day						
1	75	75	80	80	70	60
7	80	70	70	75	60	70
14	80	40	50	50	70	65
20	75	70	50	70	80	65